DYNAMICS AND SOCIAL CLUSTERING ON COEVOLVING NETWORKS

Hsuan-Wei Lee

A dissertation submitted to the faculty at the University of North Carolina at Chapel Hill in partial fulfillment of the requirements for the degree of Doctor of Philosophy in the Department of Mathematics in the College of Arts and Sciences.

Chapel Hill
2016

Approved by:

Peter J. Mucha

David Adalsteinsson

Shankar Bhamidi

Greg Forest

Jingfang Huang

ABSTRACT

Hsuan-Wei Lee: Dynamics and Social Clustering on
Coevolving Networks
(Under the direction of Peter J. Mucha)

Complex networks offer a powerful conceptual framework for the description and analysis of many real world systems. Many processes have been formed into networks in the area of random graphs, and the dynamics of networks have been studied. These two mechanisms combined creates an adaptive or coevolving network – a network whose edges change adaptively with respect to its states, bringing a dynamical interaction between the state of nodes and the topology of the network.

We study three binary-state dynamics in the context of opinion formation, disease propagation and evolutionary games of networks. We try to understand how the network structure affects the status of individuals, and how the behavior of individuals, in turn, affects the overall network structure. We focus our investigation on social clustering, since this is one of the central properties of social networks, arising due to the ubiquitous tendency among individuals to connect to friends of a friend, and can significantly impact a coevolving network system. Introducing rewiring models with transitivity reinforcement, we investigate how the mechanism affects network dynamics and the clustering structure of the networks.

We perform Monte Carlo simulations to explore the parameter space of each model. By applying improved compartmental formalism methods, including approximate master equations, our semi-analytical approximation generally provide accurate predictions of the final states of the networks, degree distributions, and evolution of fundamental quantities. Different levels of semi-analytical estimation are compared.

To my parents Ming and Sherry and my brother Victor
for their unconditional love and support.

ACKNOWLEDGEMENTS

I would like to express my sincere gratitude to my advisor Peter J. Mucha for his support, encouragement, and patience. His guidance helped me in all the time of research and writing of this thesis. He gave me time to learn and the freedom to choose the topics I love and is always very helpful when I need his help and advice. I could not have imagined having a better advisor and mentor for my Ph.D. study.

Besides my advisor, I would like to thank my collaborator and mentor Nishant Malik greatly. Nishant was a postdoc fellow with Peter, so again I want to thank Peter for steering our efforts in this direction. Nishant had helped me through the toughest time of my early research, spent a lot of time on discussing mathematical ideas and helping me writing better codes. My sincere thanks also go to my collaborators Feng (Bill) Shi and Huan-Kai Tseng. Bill was also a graduate student of Peter's, and we collaborated on the work provided in Chapter 2 and Chapter 3. He always gives me great insights and is always very kind and supportive. Huan-Kai is my good friend and also a political scientist. Although I didn't put our work in my thesis, his help of applying for the work in Chapter 4 to world trade broadens the scope of my research to the real world. I thank my fellow Mucha group-mates Dane Taylor, Saray Shai, Clara Granell, Simi Wang, Natalie Stanley and Samuel Heroy for all the fun we have had in the last few years. They gave me great feedbacks to my work and talks, and also from them, I learned a lot in the different fields of Complex Systems.

Final thanks to the members of my thesis committee David Adalsteinsson, Shankar Bhamidi, Greg Forest, and Jingfang Huang for their insightful comments, useful discussions, and encouragement in the preparation of this thesis.

Research reported in this thesis was supported by the Eunice Kennedy Shriver National Institute of Child Health & Human Development of the National Institutes of Health under Award Number R01HD075712, and by the James S. McDonnell Foundation under 21st Century Science Initiative – Complex Systems Scholar Award #220020315. The content is solely the responsibility of the authors and does not necessarily represent the official views of the funding organizations.

TABLE OF CONTENTS

LIST OF FIGURES

CHAPTER 1

Introduction

1.1 Networks Overview

We are surrounded by systems that are extremely complicated. The emergence of network science is a brilliant demonstration that interdisciplinary science can take up the challenge of studying such systems [9, 110]. These systems are collectively called complex systems, capturing the fact that it is difficult to derive their collective behavior from a knowledge of the system's components. Network science deals with complexity by summarizing complex systems as components and capturing the interplay between them. Despite or even perhaps because of such simplifications, informative discoveries can and have been made. A network based mathematical and statistical approach is extremely desirable for such endeavors as it is a formalism allowing one to couple microscopic and macroscopic dynamics. The following is a sample of some of the applications in which network science are becoming increasingly significant.

Biological processes are often represented in the form of graphs or networks, and a biological network is any network that applies to biological systems [3, 12, 78]. A biological system could be represented in a framework of networks consisting of a set of nodes representing biological entries and edges denoting relationships between pairs of nodes. Biological networks provide a mathematical model of connections found in ecological, evolutionary, and physiological studies, such as protein-protein interaction networks, metabolic pathways, gene regulatory networks, cell signaling networks, neural networks, and food webs. The study of biological networks, their construction, mathematical and statistical analysis, and visualization are significant tasks in life science today.

The fabric of our environments and societies is held together by physical systems of various kinds, such as power grid systems, water supply, sewage disposal, telecommunications and transportation systems [2, 6, 17]. A transportation network is a realization of a spatial network, referring to a structure which allows either vehicular movement or flow of some commodity, with a set of nodes

and links that represent the infrastructure or supply side of the transportation. Perhaps the most historically famous problem at the beginning of this field is the Seven Bridges of Königsberg; its negative resolution by Leonhard Euler in 1736 laid the foundations of graph theory and prefigured the idea of topology and network structure. Examples of transport networks are roads and streets, railways, aqueducts, pipes, and power lines.

Social network analysis examines the structure of relationships and interactions between social entities, such as individuals and organizations [36, 76]. The analysis of social networks is an inherently interdisciplinary academic field which emerged from sociology, political science, social psychology, business and economics, statistics, and graph theory. Within the social sciences, network theory has had an unprecedented impact. Social network analysis is now one of the major paradigms in contemporary sociology and is also implemented in other social and formal sciences.

1.2 Networks with Complex Structural Properties

A network is simply a collection of connected objects. The structure of a network is usually described by a given set of nodes and edges. In mathematics, networks are often referred to as graphs and in the scientific literature, the terms network and graph are frequently used interchangeably. Suppose a graph G is a network having N nodes and L edges (or links), we can label all the nodes and edges in the network to be $\{n\}_{n=1}^{N}$ and $\{l\}_{l=1}^{L}$. The links of a network can be directed or undirected. For directed (undirected) networks a link corresponds to an ordered (unordered) pair of nodes. For directed and undirected networks of N nodes without multiple connections, the network structure can be represented by an $N \times N$ adjacency matrix $\mathbf{A}$ of ones and zeros, where a one indicates the presence of a connection and each entry A_{mn} is nonzero if and only if a link exists from node m to node n. In a weighted network, the entries of A_{mn} can be non-unitary.

Network models serve as a foundation to understanding interactions within empirical complex networks. The following are some types of networks that have been well studied: regular, lattices in low dimensional spaces, random graphs such as Erdős-Rényi model [39], Watts-Strogatz small world model [154], and Barabási-Albert preferential attachment model [10] and so on. Various random network formation models produce structures that may be compared to real-world complex networks.

Here we introduce some basic network concepts and properties that are fundamental in social

network analysis.

- **Degree, average degree and degree distribution** - Degree (or connectivity in graph theory) is the number of edges that connect a node. We denote with k_n the degree of the n^{th} node in the network. In an undirected network the total number of links, L, can be expressed as the sum of the node degrees:

$$L = \frac{1}{2}\sum_{n=1}^{N} k_n.$$

There is a $1/2$ in front of the sum because every edge is counted twice. Average degree is an important quantity of a network, and in an undirected network it is defined as:

$$\langle k \rangle = \frac{1}{N}\sum_{n=1}^{N} k_n = \frac{2L}{N}.$$

The degree distribution p_k of a network is defined to be the fraction of nodes in the network with degree k. This p_k is a probability, hence,

$$\sum_{k=0}^{\infty} p_k = 1.$$

Note that one also has

$$\langle k \rangle = \sum_{k=0}^{\infty} k p_k.$$

- **Node centrality** - Network centrality is the answer to the question "What characterizes an important vertex?" The word "importance" has a wide number of meanings, leading to many different definitions of centrality [23]. Centrality concepts first originated in social network analysis, and many of the terms used to measure centrality reflect their sociological origin. The following are some types of network centralities: degree centrality, closeness centrality, betweenness centrality, eigenvector centrality, Katz centrality. In social networks, nodes with high centrality may play important roles in the overall composition of a network.

- **Clustering coefficient** - A clustering coefficient is a measure of the degree to which nodes in a graph tend to cluster together. Evidence suggests that in most real-world networks, and in particular social networks, nodes tend to create tightly knit groups characterized by a relatively

high density of ties, or put it another way, friends of friends are often one's friends. The following are the two common definitions of clustering coefficient.

The global clustering coefficient [151] is based on triplets of nodes. A triplet consists of three connected nodes. A triangle therefore includes three closed triplets, one centered on each of the nodes. The global clustering coefficient is defined as:

$$C = \frac{3 \times \text{number of triangles}}{\text{number of connected triplets of nodes}} = \frac{\text{number of closed triplets}}{\text{number of connected triplets of nodes}}.$$

The local clustering coefficient [154] captures the degree to which the neighbors of a given node link to each other, that is, it quantifies how close its neighbors are to being a clique (complete graph). For a node n with degree k_n the local clustering coefficient is defined as

$$C_n = \frac{2L_n}{k_n(k_n - 1)}$$

where L_n denotes the number of edges between the k_n neighbors of node n. Furthermore, the degree of clustering of a whole network is represented by the average clustering coefficient $\langle C \rangle$, and it is defined as

$$\langle C \rangle = \frac{1}{N} \sum_{n=1}^{N} C_n.$$

Note that all the global, local and average clustering coefficients are between 0 and 1. The clustering coefficient is also known in social network analysis as transitivity. In this thesis, we consider the global clustering coefficient in Chapter 2 and the local clustering coefficient in Chapter 3, and for simplicity, the clustering coefficient in this thesis means the different clustering coefficients accordingly.

- **Subgraph Motifs** - In social and real-world networks there are often some small structures that are more frequently shown than expectation. Network motifs are sub-graphs that repeat themselves in various networks [105]. Each of these sub-graphs, defined by a particular pattern of interactions between vertices, may reflect a framework in which specific functions are achieved efficiently. Motifs are of notable importance primarily because they may reveal functional properties. They have recently gathered much attention as a useful concept to

uncover topological design principles of complex networks.

- **Community Structure** - A network is said to have community structure if the nodes of the network can be easily grouped into sets of nodes such that each set of nodes is densely connected internally, or, subsets of nodes within which node and node connections are denser, but between which connections are less dense. In the study of social networks, it is common to see people have the same traits or experience such as race, ethnicity, location, income, hobby, or ideology would form groups or communities. This homophily effect makes individuals have a stronger bond with similar others, and this effect is also widely studied in social networks. In network science, detecting community structures in different levels is also a very significant topic of research [50, 113].

1.3 Network Dynamics and Coevolving Networks

When studying a dynamical process, one is concerned with its behavior as a function of time, space, and its parameters. Real networks are not simply lists of nodes where some pairs are linked, and others aren't. Nodes may have locations, opinions, affiliations, and demographic characteristics that change over time; links between them have timing, durations, capacities, and so on. Hence, nodes may come and go and edges may crash and recover. Substantial progress has been made both in the classification of real and synthetic networks and in the study of dynamical models of networks.

The phrase "network dynamics" can be interpreted as the study of dynamical systems on or of networks [111, 125]. The notion of dynamical networks has so far referred to either one of two distinct concepts. "Dynamics on networks" refers to the different classes of processes taking place on networks, e.g. biological contagion [16], social contagion [75], coupled oscillators [143], diffusion [91], percolation [22], etc. The effectiveness of such processes is deeply influenced by the topology of the network. On the other hand, "dynamics of networks" mainly refers to various phenomena that happen to the network structure to bring about certain changes over time in the topology of the network. The Barabási-Albert preferential attachment model, interpreted such that the addition of each new node is a time step, is an example of this kind of dynamics. New nodes could join the network and edges could be formed or deleted.

Therefore, it has become clear that properties in dynamical systems such as stability, bifurcation,

robustness, periodicity, phase transition, etc. could be discussed on and of the network dynamics. And the study of dynamical processes on and of networks are among some of the hottest theoretical challenges for complex network research.

Static networks are networks with fixed topology that do not change with time. The static network has been studied widely, and many phenomena are also explored. However, on networks with static topology, the coupling of topology and information flow is only a one-way road. The states of nodes do not affect the structure of such static networks.

Coevolving or adaptive networks are obtained by combining the dynamics on and of networks [59, 60, 74]. A coevolving network is a network whose network topology and states of nodes coevolve, that is, its links change according to its states, and vice versa, resulting in a dynamic interplay between the state and the structure of the network. Most networks in real life are coevolving networks to some extent. Hence, lots of examples in coevolving networks models could be applied to different fields of science. The study of coevolving networks is a fast growing topic in epidemiology, social and economic networks, and biological networks. Perhaps the most typical example is in epidemiology, with an infectious disease spreading on a network. To control the epidemic, an infected individual might be quarantined, hence, the local topology of the node is changed by losing its susceptible neighbors [101]. In the study of terrorist networks [40], not only are the networks temporal, the number of links one node has is strongly dependent on its activeness at a specific time.

In this thesis, we will study three different models of coevolving networks and explore the interaction between states of nodes and structure of networks.

1.4 Analytical Methods

Dynamics in real life are extremely complicated, and it is almost impossible to analyze or predict the outcome without simplification. The framework and analytical methods offered by statistical physics could allow us to explore the dynamics of various systems using simplified yet, insightful models. To capture the dynamics in mathematical models, and more specifically, networks, we need to reply on some level of approximation. Various degrees of simplification have different analytical or computational cost, and yield different accuracy. Because of such simplifications, mathematical and statistical inference and informative discoveries can and have been made. In the study of this thesis,

we focus on the study of binary-state dynamics on networks, that is, a node (or, as we will encounter in Chapter 6, a link) could only take one of two possible states, e.g. susceptible-infected-susceptible (SIS) dynamics on networks. Here we introduce the analytical methods we use in this thesis to study the dynamics of our models.

In statistical physics, mean field (MF) theory studies the behavior of large and complex stochastic models by investigating a simpler model of average interactions [11, 15, 18, 115]. Such models simply assume the environment of the system is well-mixed, and the effect of all the other individuals on any given individual is approximated by a single averaged effect, thus reducing a many-body problem to a one-body problem. In binary-state dynamics, the MF method only uses one differential equation to describe the dynamics, since the other one is redundant (by conservation of the total number of nodes, the fraction in one state minus the fraction in the other). Mean field theory simplifies the system dynamics hugely by only focusing on the change of quantities of different classes, whereas this method ignores the network topology and may not be accurate when systems have more complicated structures. Usually, this method works well when the network is sparse and locally tree-like, which is often interpreted to require that there are fewer cliques inside the network. However, there are some studies that show mean field theory can yield a good approximation of the network dynamics (see, e.g., [99] for an investigation of the accuracy of heterogeneous mean field theory, wherein the variables describing the system capture the fractions of nodes in each state for each distinct degree).

Pair approximation (PA) is an improvement for the mean field method [35, 88, 142, 146]. This method keeps track of the quantities of pairs or the frequencies of neighbor-site pairs of each possible type in the systems. For example, in the SIS dynamics in a system, one could follow the quantities of S nodes, SS, and SI edges (other information is redundant) to study the dynamics. Hence, in binary-state dynamics, the PA method uses three differential equations to describe the dynamics. Pair approximation has often provided accurate qualitative information about spatial stochastic models for epidemic, population, and evolutionary dynamics especially when the network topology is not complicated. Generally speaking, a large network essentially has an infinite hierarchical system, and the information of one level of approximation depends on its next level. Mean Field theory makes a closure approximation for the numbers of edges (that is, pairs) in terms of the number of nodes. Similarly, the differential equations of pairs depend on the densities of triplets, so Pair Approximation assumes a closure for the number of connected triples in terms of the numbers of

pairs, closing the system so that the densities of triplets are not explicitly tracked.

Master equations are used to portray the dynamics of a system that can be modeled as being in exactly one of the states at any given time, and where switching between states is treated probabilistically. The equations are usually a set of differential equations for the variation over time of the probabilities that the system occupies each of the different states. The approximate master equations (AME) framework [52, 53, 90, 97] on networks considers both the state and degree of nodes and the states of their immediate neighbors, generating a system of differential equations to model the co-evolution of the dynamics of states and network structure. For example, in the SIS dynamics, one can write down the differential equations of $S_{k,m}$, that is, the change of an S node that has degree k and m infected neighbors. Similarly, one can also write down the $I_{k,m}$ compartment. In binary-state dynamics, the AME method generates $O(k_{\max}^2)$ number of differential equations, where $k_{\max}$ denotes the maximum degree cutoff of a system. The AME method usually provides a very accurate approximation of the evolution of networks, including near the critical point of the dynamics. Moreover, the AME method performs well in both static and coevolving networks, since more equations are being used to gain this accuracy.

The differential equations of these systems keep track of the quantities of different classes of nodes, and in PA and AME, also their neighbors' states. The MF, PA, and AME above are categorized as node classification methods. Beyond the method of AME, [159] provides a link-based formalism method that includes the information not only of nodes but every set of links. Again in the SIS dynamics, for an SI edge, the classification is done by writing it as $S_{ij}I_{kl}$, that is, the S end has i neighbors, j of them are infected, and the I end has k neighbors, l of them are infected. The other systems could be formulated similarly. The link-based formalism method could provide slightly more accurate results compared with AME. However, this would also raise the computing costs to $O(k_{\max}^4)$ number of differential equations, where $k_{\max}$ denotes the maximum degree cutoff of a system. This method also provides subtly detailed information of degree correlation, and it could give a better approximation when the dynamics, say the spreading or rewiring process, is based on the degree of nodes. Since the method of AME has been slightly more widely used and its computational cost is more reasonable, here in the thesis we only use AME as our framework, though more extension could be explored in the future.

1.5 Overview of Thesis

- **Chapter 1** - In Ch. 1, we have provided an overlook and a broad introduction to network science. We defined the scope of our study – coevolving networks in the field of network dynamics. A survey of dynamics on and of networks was provided, and different level of analytical approximations have been briefly discussed. The importance and universality of coevolving networks makes such study an important topic of complex systems.

- **Chapter 2** - In Ch. 2, we provide a new transitivity reinforcement voter model. Rather than rewiring randomly, there is a certain probability that a node rewires to its distance two neighbors, close a triangle, and the clustering coefficient of the network increases. We study this new model on an initially Erdős-Rényi $G(N, l)$ random graph and also approximate the dynamics by using the method of approximate master equations. We investigate the parameter spaces, clustering coefficient, degree distribution in the stationary states, and the network evolution.

- **Chapter 3** - In Ch. 3, we provide a new clustering reinforcement model of the SIS dynamics. Rather than rewiring randomly, there is a certain probability that a node rewires to its distance two neighbors, and close a triangle. We study this new model on different structures of networks, and also approximate the dynamics by using the method of approximate master equations. We investigate the parameter spaces, the disease prevalence level, clustering coefficients, degree distribution in the stationary states, network evolution and finally, provide a bifurcation analysis.

- **Chapter 4** - In Ch. 4 we introduce a partner switching model in evolutionary games on networks. We explore the parameter space and study the dynamics thoroughly. By using the method of approximate master equations, we provide better estimation than existing methods. Furthermore, we use this semi-approximation technique to approximate the evolution of dynamics and degree distribution in stationary states. Lastly, we discuss the final cooperative level in this partner switching model.

- **Chapter 5** - Motivated by results in Ch. 4, we study another version of the partner switching model in Ch. 5, expanding the partner states that can be switched. We perform similar

investigations as in Ch. 4. The network evolution and the parameter spaces are explored. Also, the method of approximate master equations provides a good estimation of the network dynamics.

- **Chapter 6** - Motivated by results in Ch. 4 and Ch. 5, we study a theoretical extension of the partner switching model in Ch. 6. In the link-based network dynamics we study here, a node could play different strategies (or states) with its different neighbors. We provide simulations of the new model and discuss the possibilities of various levels of approximations.

- **Chapter 7** - We close this thesis with some concluding discussion and several directions of future work are indicated.

CHAPTER 2

Voter Model and Social Clustering on Complex Networks

2.1 Background Information

Almost all people have opinions about numerous topics, from weather, sports, environment, fashion, and the society to politics. These judgments can be either the result of sober reflection or, through the process of information spreading, formed through interactions with others that hold views on given issues. A large scale of media and social networking applications have made it possible for news, innovations, opinions and rumors to spread quickly, which affect and change our daily lifestyle significantly. People depend on others and the environment to shape their views of the world. To apprehend the process of opinion formation, it demands an exploration of the interaction between the structure of the social network and the dynamics that affects the system and human behavior.

Many researchers are dedicated to understanding the implication of different mechanisms and network structures and their interactions. Moreover, investigation of the opinion leaders, or zealots [98, 147], and external fields [79] has been implemented. Not only on synthetic networks, empirical [28, 153] and experimental [32, 109] studies have also contributed to the understanding of opinion dynamics. For example, social media such as Twitter, Facebook and Instagram have become important to lots of people's daily lives and are essential to the spread of opinions and information [5, 139]. Furthermore, television and internet ads also play crucial roles in elections and businesses [26, 153]. Hence, it is very natural to model, quantify and even give predictions to these social contagion dynamics in different settings, scopes, and mechanisms.

Various opinion dynamics models on complex networks have been brought up and investigated. In the setting of the threshold model [42, 55, 57, 152], a node turns active/infected if a sufficient number or ratio of its neighbors are already active/infected. The threshold model has been widely used in the study of fads, marketing, elections, disease propagation and contact process models.

Take the spreading of a fad, the size of the population getting it, its duration, the dynamics of spreading, and the interplay of network structure are usually the topics people study. The model is essentially asymmetric as when two nodes communicate only the inactive/susceptible node becomes active/infected thus resulting in a spread like dynamics.

The naming game is another model of opinion dynamics [13, 14, 95, 158]. It was first introduced in the context of linguistics and communications. This model describes how a global agreement or convention can automatically emerge in a population of artificial agents that interact locally with their peers, without any central control [85]. Hence, the formation of a language in a society could be studied. For example, in the context of a group of robots or sensor networks, the naming game model imitates the emergence of common communication schemes.

Models of continuous states of opinion dynamics have also been extensively investigated. In the bounded confidence model, opinions are not anymore binary or discrete, but it could be extended to a spectrum of values. First introduced by Krause and Hegselmann [67] and Deffuant et al. [30] independently, this is a probabilistic model for the evolution of continuous-valued opinions within a finite group of peers, and this could also be generalized to a network setting. The concept of bounded confidence is that artificial agents only interact if they share opinions close enough to each other. People study the emergence of the consensuses, the size of them, their duration, and distribution or the spatial properties of the various communities [92, 93].

A simpler model, the voter model is independently brought by Clifford and Sudbury [29], and by Holley and Liggett [70]. This is a mathematical model of opinion formation in which individuals, or voters, play as nodes in a complex network; each voter has an opinion at each time, and a randomly chosen voter accepts the opinion of one of its neighbors. It is also a stochastic process that is a peculiar type of interacting particle system. The voter model is a sequential dynamical system, and it is also similar to disease propagation and contact process. At random times, a random node or link is selected, and the voter's opinion is changed in agreement with some probabilistic rule. To be more specific, pick one node and choose a neighbor of this node, the neighbor's opinion could transfer to the chosen node following some stochastic rule. Or the chosen voter could see his or her neighbors' majority or minority opinion and act accordingly. Therefore, network topologies also plays an important role in the dynamics. Theoretical efforts have been devoted to fathom and quantify features in the dynamics of spread of opinions or contagions considering various local and

global structural attributes of the underlying complex systems [133, 138].

The voter model has been studied on many network topologies, and the underlaying networks could be static or adaptive. Investigations have been performed in networks with homogeneous and heterogeneous degree distributions [137], scale-free networks [24], small world networks [25], and multilayer networks [31]. In coevolving networks, networks structures could change depending on the states of nodes, usually by the mechanism of rewiring [19, 34, 71, 116, 135]. Individuals could have their preference to stay with others sharing the same opinions with them and break their links with people with discordant opinions. Although mainly people study only binary-state dynamics, lots of phenomenon such as graph fission and community structure could be explored.

In the study of opinion formation on complex networks, one of the critical components has been missing: the influence of clustering in coevolving networks on the resulting dynamics and network structure. Clustering is one of the central properties of social networks, arising from the ubiquitous tendency among individuals to connect to friends of a friend, and can significantly impact a coevolving network system. The role of clustering and environment could play a vital role in the network dynamics [96]. Random graph models and random rewiring processes usually lead to networks with zero clustering coefficients, which is a result not very realistic in social networks. Hence, in our study, we want to find a simple model that could lead to nontrivial local clustering of networks and investigate how this mechanism could lead to different network dynamics.

The outline of the Chapter is as follows. In Section 2, we define our model and in Section 3, we derive our semi-analytical method. In Section 4, we compare the simulation results with the estimation we obtained. We investigate the rewiring parameter space, the final state of consensuses, the clustering coefficient, the degree distribution, and the comparison of simulation and semi-analytical results. Finally, in Section 5, we give our conclusions and some further remarks.

2.2 Model Description

In this Chapter, we introduce and study a new model of opinion formation with clustering reinforcement. Our goal is to try to build a mechanism that fits one of the most fundamental observation of social network: friends of friends' friend are often ones' friends. We incorporate the clustering effect into the evolution of network, that is, we want to construct a mechanism such that

the clustering coefficient of network increases as the opinions are formed. Therefore, we introduce a simple preferential attachment to an existing rewire-to-random opinion formation model. Under our new model, there is a certain probability that if a rewiring happens, a node rewires to its neighbors' neighbor, a triangle is closed, and the local clustering extent is thus increased.

To begin with, consider a network $G(N, l)$, that is, a network with N nodes and l edges. Each node in the network has an opinion, or state, attached to it: 0 or 1. We want to investigate how these two opinions change with the evolution of networks. At each time step, we pick a discordant edge, or an edge with different states at its two ends. With probability $1 - \alpha$, a node at the end of the discordant edge would change its state to imitate the state on the other end. We call this process voting. With probability α, a node at the end of the discordant edge dismisses its neighbor and rewires to some node in the network. We call this process rewiring. When the rewiring process happens, there is also a probability γ that the node rewires to its neighbors' neighbor, or the distance two neighbor, otherwise, the node would rewire to a random node in the network. Hence, in our new model, when we update a discordant edge, the voting process happens with probability $1 - \alpha$, one node rewires to its distance two neighbor with probability $\alpha\gamma$, and one node rewires to a random node in the network with probability $\alpha(1 - \gamma)$. Hence, whenever a rewiring to neighbor's neighbor happens (with probability $\alpha\gamma$), a triangle is closed, and the clustering coefficient of the network increases. We illustrate this process in Figure 2.1.

We simulate networks with total number of nodes $N = 100,000$, total number of edges $l = 800,000$, and hence the mean degree of the network is fixed to be $\langle k \rangle = 4$. Initially, we start the networks to be an Erdős-Rényi $G(N, l)$ random graph model, that is, a network is chosen uniformly at random from the collection of all graphs which have N nodes and l edges. Hence with N large enough, we could approximate the initial degree distribution of the networks by a Poisson distribution,

$$p_k = \frac{\langle k \rangle^k e^{-\langle k \rangle}}{k!}.$$

Also, initially, we let 50% of nodes have opinion 0 and 50% of nodes have opinion 1. Then we start the opinion formation with clustering reinforcement process. At each time step, a discordant edge is picked and updated. The whole dynamic stops if there are no discordant edges in the network, and we say the network reaches its consensus state or final state. Hence, the network structure and

the state of nodes coevolve during the evolution of the network and the network stops changing until there are no discordant edges. Note that during the evolution of the network, both the total number of nodes N and the total number of edges l are fixed to be constants.

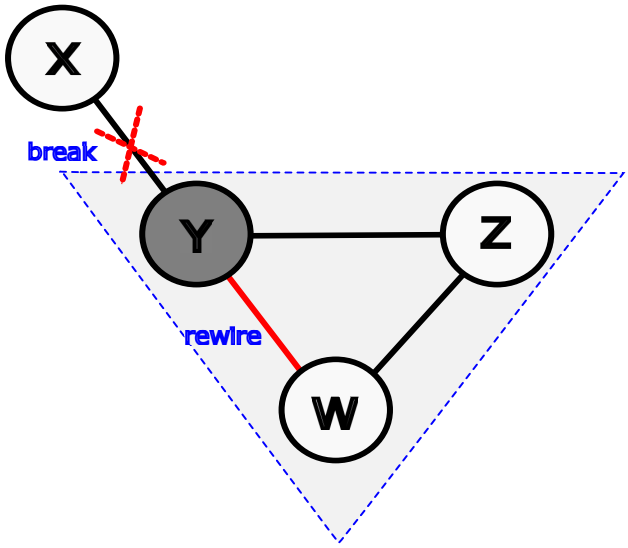

Figure 2.1: Illustration of the clustering reinforcement mechanism. At each time step, a discordant edge is picked. There is probability $\alpha\gamma$ for one node rewires to its neighbor's neighbor and closes a triangle. In this figure, white nodes are with opinion 0 and gray nodes are with opinion 1. A discordant edge XY is picked and node Y dismisses X and it rewires to its distance two neighbor W.

2.3 Semi-analytical Methods

In the voter model, consider the effect of the γ term, the probability of a node rewiring to its neighbor's neighbor. Now a node has probability $\alpha\gamma$ rewiring to its neighbors' neighbor. Let N_0 be the number of vertices with opinion 0, and N_1 be the number of vertices with opinion 1. N_{ij} is the number of oriented i-j links, and N_{ijk} is the number of oriented triples x-y-z having states i, j and k. Note that in this notation, $N_{01} = N_{10}$ and N_{00} counts every unoriented 0-0 link twice. Let $S_{k,m}(t)$ and $I_{k,m}(t)$ be the fraction of nodes with opinion 0 and 1, respectively, of degree k which have m neighbors of opinion 1.

We follow [53] to develop differential equations describing the evolution of the objects $S_{k,m}(t)$ and $I_{k,m}(t)$. First we note that $S_{k,m}(t)$ and $I_{k,m}(t)$ obey a few conservation laws: conservation of

nodes leads to

$$\sum_{k,m} S_{k,m}(t) + \sum_{k,m} I_{k,m}(t) = 1,$$

and conservation of edges leads to

$$\left(\sum_{k,m} S_{k,m}(t)\right)^2 + \left(\sum_{k,m} I_{k,m}(t)\right)^2 + 2\sum_{k,m} S_{k,m}(t) \sum_{k,m} I_{k,m}(t) = \langle k \rangle.$$

If an ϵ amount of nodes are made to hold opinion 1 at random at $t = 0$ then the initial conditions for $S_{k,m}$ and $I_{k,m}$ are given by

$$S_{k,m}(0) = (1-\epsilon)p_k(0)\binom{k}{m}\epsilon^m(1-\epsilon)^{k-m},$$

and

$$I_{k,m}(0) = \epsilon p_k(0)\binom{k}{m}\epsilon^m(1-\epsilon)^{k-m}.$$

Where $p_k(0)$ is the initial degree distribution, we assume it to be a Poisson distribution as our starting topology is a random network, and we have set $\epsilon = 0.5$, i.e., half of the nodes hold opinion 0 and the other half holds opinion 1.

To write a differential equation governing the evolution of $S_{k,m}$ we will require to know the probability of center S having a neighbor's neighbor (distance 2 neighbor) with opinion 0. We represent this probability by $P(nn0 \mid S_{k,m})$ and estimate it as:

$$P(nn0 \mid S_{k,m}) = \frac{m-1}{k-1} \cdot \frac{l_{10}}{\frac{1}{2}l_{11} + l_{10}} + \frac{k-m}{k-1} \cdot \frac{\frac{1}{2}l_{00}}{\frac{1}{2}l_{00} + l_{01}}.$$

Similarly we can obtain this probability for $P(nn0 \mid S_{k,m+1})$

$$P(nn0 \mid S_{k,m+1}) = \frac{m}{k-1} \cdot \frac{l_{10}}{\frac{1}{2}l_{11} + l_{10}} + \frac{k-m-1}{k-1} \cdot \frac{\frac{1}{2}l_{00}}{\frac{1}{2}l_{00} + l_{01}}.$$

We have the following ODE governing the time evolution of the $S_{k,m}$ compartment:

$$
\begin{aligned}
\frac{d}{dt}S_{k,m} &= \alpha\gamma\big\{ -\big[1+P(nn0 \mid S_{k,m})\big]mS_{k,m} + P(nn0 \mid S_{k,m+1})(m+1)S_{k,m+1} + (m+1)S_{k+1,m+1}\big\} \\
&+ \alpha(1-\gamma)\big\{ -(2-u)mS_{k,m} + (1-u)(m+1)S_{k,m+1} + (m+1)S_{k+1,m+1}\big\} \\
&+ \alpha\gamma\Big\{ -\big[\big(\frac{m}{k}\cdot\frac{l_{10}}{\frac{1}{2}11+l_{10}}\big)\cdot\frac{l_{01}}{N_0} + \big(\frac{k-m}{k}\cdot\frac{\frac{1}{2}l_{00}}{\frac{1}{2}l_{00}+l_{01}}\big)\cdot\frac{l_{01}}{N_0}\big]\cdot S_{k,m} \\
&- \big[\big(\frac{m}{k}\cdot\frac{\frac{1}{2}11}{\frac{1}{2}11+l_{10}}\big)\cdot\frac{l_{10}}{N_1} + \big(\frac{k-m}{k}\cdot\frac{l_{01}}{\frac{1}{2}l_{00}+l_{01}}\big)\cdot\frac{l_{10}}{N_1}\big]\cdot S_{k,m} \\
&+ \big[\big(\frac{m-1}{k-1}\cdot\frac{\frac{1}{2}11}{\frac{1}{2}11+l_{10}}\big)\cdot\frac{l_{10}}{N_1} + \big(\frac{k-m}{k-1}\cdot\frac{l_{01}}{\frac{1}{2}l_{00}+l_{01}}\big)\cdot\frac{l_{10}}{N_1}\big]\cdot S_{k-1,m-1} \\
&+ \big[\big(\frac{m}{k-1}\cdot\frac{l_{10}}{\frac{1}{2}11+l_{10}}\big)\cdot\frac{l_{01}}{N_0} + \big(\frac{k-m-1}{k-1}\cdot\frac{\frac{1}{2}l_{00}}{\frac{1}{2}l_{00}+l_{01}}\big)\cdot\frac{l_{01}}{N_0}\big]\cdot S_{k-1,m}\Big\} \\
&+ \alpha(1-\gamma)\frac{l_{01}}{N}\big\{ -2S_{k,m} + S_{k-1,m-1} + S_{k-1,m}\big\} \\
&+ (1-\alpha)\big\{ -mS_{k,m} + (k-m)I_{k,m}\big\} \\
&+ (1-\alpha)\big\{ -\beta^s(k-m)S_{k,m} + \beta^s(k-m+1)S_{k,m-1} - \gamma^s mS_{k,m} + \gamma^s(m+1)S_{k,m+1}\big\}
\end{aligned}
\tag{2.1}
$$

where

$$
\begin{aligned}
\beta^s &= \frac{\sum_{k,m} mS_{k,m}}{\sum_{k,m} S_{k,m}} = \frac{\tau_{001}}{l_{00}} \\
\gamma^s &= \frac{\sum_{k,m}(k-m)^2 I_{k,m}}{\sum_{k,m}(k-m)I_{k,m}} = \frac{\tau_{010}}{l_{01}} + 1,
\end{aligned}
$$

i.e., β^s is the number of 1 neighbors of a 0-0 edge and γ^s gives the number of 0 neighbors of the 1 at the end of a 0-1 edge and the $+1$ counts the 0 on the conditioning edge.

In a $S_{k,m}$ class, the probability that the center has a neighbor's neighbor (the distance two neighbor) with opinion 0 is estimated by $P(nn0 \mid S_{k,m})$. Similarly, in a $S_{k,m+1}$ class, the probability that the center has a neighbor's neighbor with opinion 0 is estimated by $P(nn0 \mid S_{k,m+1})$. Here β^s is the estimated number of 1 neighbors of a 0-0 edge. Moreover, γ^s gives the estimated number of 0 neighbors of the 1 at the end of a 0-1 edge and the $+1$ counts the 0 on the conditioning edge.

Following the same procedure as stated above for $S_{k,m}$, we obtain the following differential equation governing the evolution of the $I_{k,m}$:

$$
\begin{aligned}
\frac{d}{dt}I_{k,m} = {} & \alpha\gamma\{-[1+P(nn1|I_{k,m})](k-m)I_{k,m} + P(nn1|I_{k,m-1})(k-m+1)I_{k,m-1} + (k-m+1)I_{k+1,m}\} \\
& + \alpha(1-\gamma)\big\{-(1+u)(k-m)I_{k,m} + u(k-m+1)I_{k,m-1} + (k-m+1)I_{k+1,m}\big\} \\
& + \alpha\gamma\Big\{-\big[\big(\frac{m}{k}\cdot\frac{l_{10}}{\frac{1}{2}11+l_{10}}\big)\cdot\frac{l_{01}}{N_0} + \big(\frac{k-m}{k}\cdot\frac{\frac{1}{2}l_{00}}{\frac{1}{2}l_{00}+l_{01}}\big)\cdot\frac{l_{01}}{N_0}\big]\cdot I_{k,m} \\
& - \big[\big(\frac{m}{k}\cdot\frac{\frac{1}{2}11}{\frac{1}{2}11+l_{10}}\big)\cdot\frac{l_{10}}{N_1} + \big(\frac{k-m}{k}\cdot\frac{l_{01}}{\frac{1}{2}l_{00}+l_{01}}\big)\cdot\frac{l_{10}}{N_1}\big]\cdot I_{k,m} \\
& + \big[\big(\frac{m-1}{k-1}\cdot\frac{\frac{1}{2}11}{\frac{1}{2}11+l_{10}}\big)\cdot\frac{l_{10}}{N_1} + \big(\frac{k-m}{k-1}\cdot\frac{l_{01}}{\frac{1}{2}l_{00}+l_{01}}\big)\cdot\frac{l_{10}}{N_1}\big]\cdot I_{k-1,m-1} \\
& + \big[\big(\frac{m}{k-1}\cdot\frac{l_{10}}{\frac{1}{2}11+l_{10}}\big)\cdot\frac{l_{01}}{N_0} + \big(\frac{k-m-1}{k-1}\cdot\frac{\frac{1}{2}l_{00}}{\frac{1}{2}l_{00}+l_{01}}\big)\cdot\frac{l_{01}}{N_0}\big]\cdot I_{k-1,m}\Big\} \\
& + \alpha(1-\gamma)\frac{l_{01}}{N}\big\{-2I_{k,m} + I_{k-1,m-1} + I_{k-1,m}\big\} \\
& + (1-\alpha)\{-(k-m)I_{k,m} + mS_{k,m}\} \\
& + (1-\alpha)\{-\beta^i(k-m)I_{k,m} + \beta^i(k-m+1)I_{k,m-1} - \gamma^i mI_{k,m} + \gamma^i(m+1)I_{k,m+1}\} \qquad (2.2)
\end{aligned}
$$

where

$$
\begin{aligned}
P(nn1 \mid I_{k,m}) &= \frac{m}{k-1}\cdot\frac{\frac{1}{2}11}{\frac{1}{2}11+l_{10}} + \frac{k-m-1}{k-1}\cdot\frac{l_{01}}{\frac{1}{2}l_{00}+l_{01}} \\
P(nn1 \mid I_{k,m-1}) &= \frac{m-1}{k-1}\cdot\frac{\frac{1}{2}11}{\frac{1}{2}11+l_{10}} + \frac{k-m}{k-1}\cdot\frac{l_{01}}{\frac{1}{2}l_{00}+l_{01}}.
\end{aligned}
$$

To understand the differential equations, take an $S_{k,m}$ class of Equation (2.1). The first line of the right-hand side represents the center actively rewiring to a distance two neighbor, the second line means the center actively rewires to any node in the network, the third to sixth lines are the case the center is passively rewired by its distance two neighbors, the seventh line means the center is passively rewired by any node in the network. Finally, the last two lines are the case no rewiring happens and the nodes just simply update their opinions.

There are $2(k_{\max}+1)^2$ equations of the $S_{k,m}(t)$ and $I_{k,m}(t)$ governing ODEs, where $k_{\max}$ is the maximum degree a node could have in the system. MATLAB's ode45 solver was used starting with a Poisson degree distribution with averaged degree $\lambda = 4$. We set $k_{\max} = 20$ and we observe that the results are not appreciably affected by increasing $k_{\max}$. The illustration of some rewiring processes

is shown in Figure 2.2.

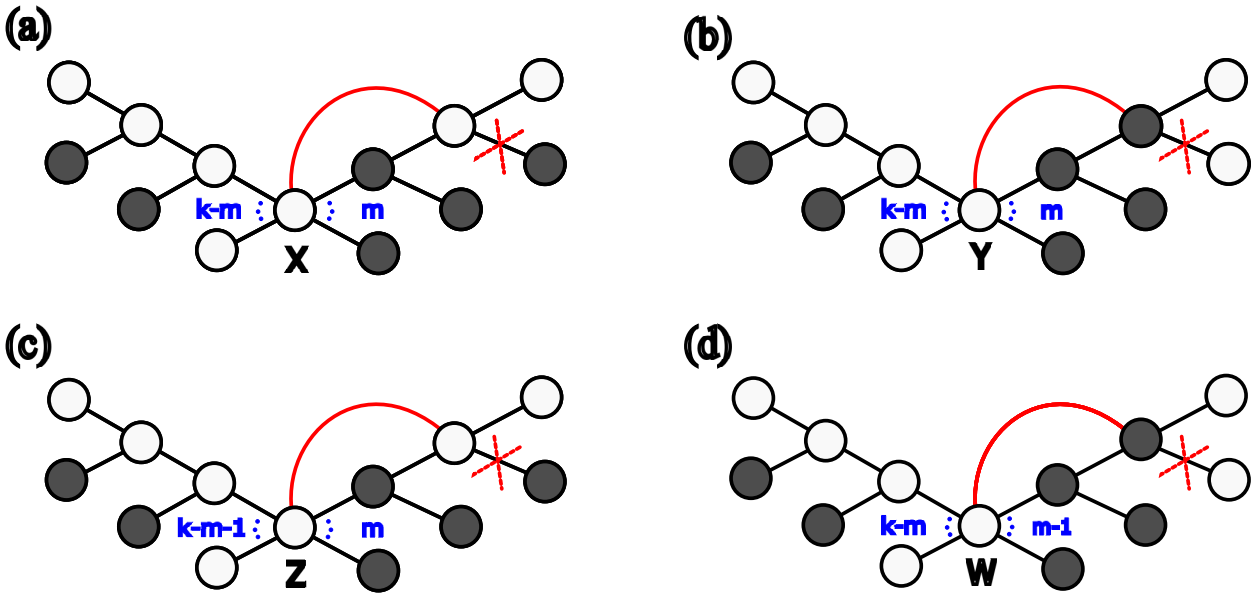

Figure 2.2: Suppose the center is a node with opinion 0. The following are illustrations of the center passively rewired by different distance two neighbors: (a) 0 rewires to node X, a class of $S_{k,m}$, (b) 1 rewires to node Y, a class of $S_{k,m}$, (c) 0 rewires to node Z, a class of $S_{k-1,m}$ and (d) 1 rewires to node W, a class of $S_{k-1,m-1}$. The case of the center with opinion 1 is similar.

2.4 Numerical Experimentation and Discussion

2.4.1 Consensus States of the Networks

Results in this subsection were led and provided by my collaborators Nishant Malik and Feng Shi.

In our opinion formation with clustering reinforcement model, both network topology and state of nodes change during the evolution of networks. The dynamic stops when there are no discordant edges, and networks become static. We denote the stopping time of the dynamics to be t_f, which means the network reaches its final state. We also call the final state of the network a consensus state, since there would be no discordant edge in this state. Note that $l(t_f) = l_{00}(t_f) + l_{11}(t_f)$.

The consensus state of the network could be characterized by two different consensuses: hegemonic consensus and segregated consensus. To see these outcomes, we define a variable ρ to be the fraction of nodes holding minority opinions in the consensus states; and also we define a variable s_1 to be the size of the largest connected component in the consensus state. In the hegemonic consensus state,

there exists a dominant opinion in the network, ρ is close to 0, and s_1 is close to 1. In this scenario, a giant component with a size close to the whole network has nodes with the same opinion. On the other hand, in the segregated consensus state, there is no dominant opinion in the network, ρ is close to 0.5, and s_1 is close to 0.5. In this scenario, a graph fission happens such that the final network comprises two nearly equal-sized components, each having nodes with a single opinion. In Figure 2.3, we plot ρ and s_1 with different combinations of α and γ.

Furthermore, in Figure 2.3, we observe that there exists a sharp transition of α for networks to have a graph fission. Fixing the level of γ, there is a critical value of α, or $\alpha_c(\gamma)$, which separates the hegemonic and segregated consensus states. This critical value $\alpha_c(\gamma)$ suggests the importance of γ in this dynamic. When α is large enough ($\alpha \geqslant 0.7$), regardless of different values of γ, there is a graph fission of the network. However, when α is not large enough, as γ increases, the critical value of $\alpha_c(\gamma)$ decreases. This shows us the significance of the parameter γ we introduce to the network dynamic. To see a graph fission, the rewiring probability does not need to be large if there is a strong tendency for an individual to rewire to his or her neighbors' neighbor. Or put it another way, if individuals have a high preference to cut the links of discordant neighbors and resort to a closer neighbor to form small groups, then it will be hard for the network to have a dominant consensus and a giant component in its final state.

2.4.2 Clustering Coefficients

Results in this subsection were led and provided by my collaborators Nishant Malik and Feng Shi.

To show that this opinion formation with clustering reinforcement model could indeed increase the clustering coefficient in the networks, in Figure 2.4, we provide the evolution of the clustering coefficients with different values of γ with $\alpha = 1$. In this figure, circles are the highlight of the clustering coefficient in the consensus states. As we can see, if $\gamma = 0$, the clustering coefficient stays at 0 as the network evolves. On the other hand, for a nonzero γ, the clustering coefficient grows approximately linearly until the networks stop evolving. In Figure 2.4 (b), we plot the clustering coefficients of networks in their final consensus states at time t_f with circles and provide an estimation of the clustering coefficients with the gray straight line. The higher the γ is, the higher the final clustering coefficients would be. Using mean-field arguments we could acquire the final clustering

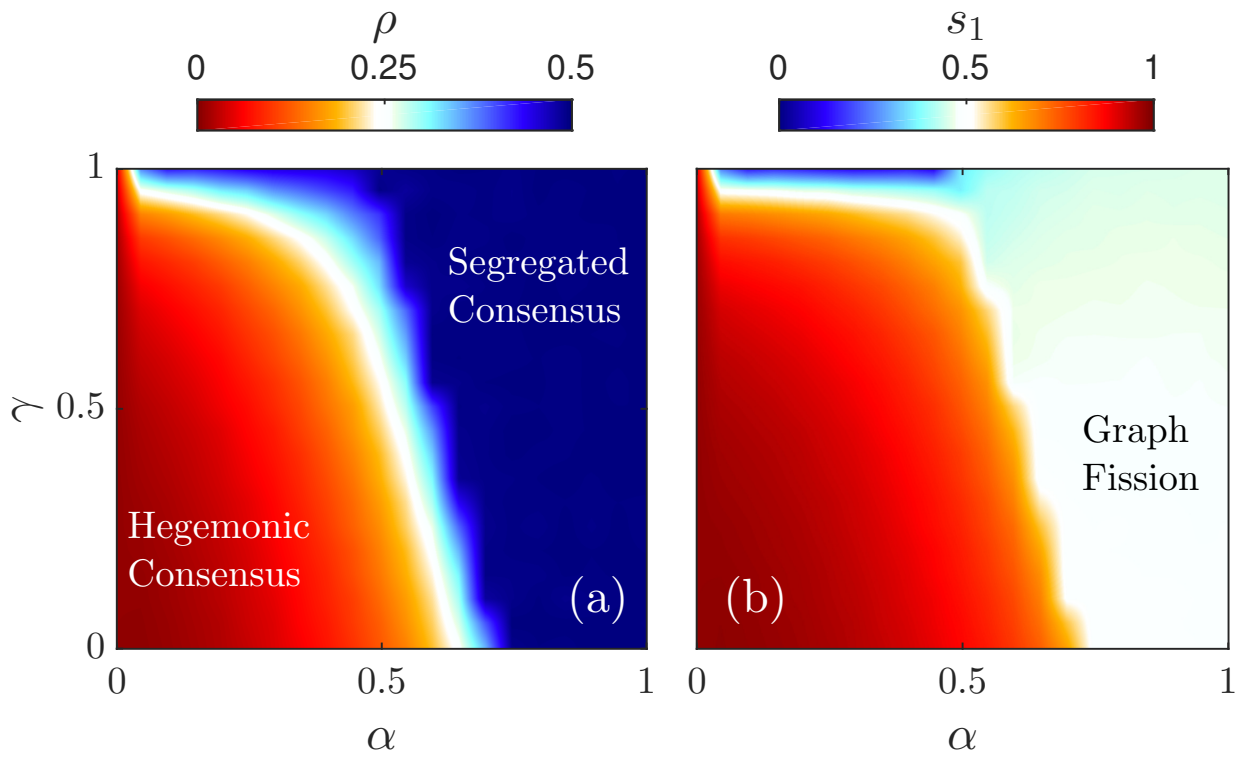

Figure 2.3: (a) Levels of ρ, the fraction of nodes holding minority opinions in the consensus states with different combinations of α and γ. In the hegemonic consensus state region, the minority opinion fraction is close to 0. However, in the segregated consensus state region, the minority opinion fraction is close to 0.5. Note that when γ increases, the region of the hegemonic consensus shrinks. (b) Levels of s_1, the size of the largest connected component in the consensus state with different combinations of α and γ. In the hegemonic consensus state region, the largest connected component in the consensus state is close to 1, the original size of the network. On the other hand, in the segregated consensus state region, the largest connected component in the consensus state is close to 0.5, half of the original size of the network.

coefficients in their consensus states, and we found that

$$C(t_f) = \frac{3\gamma}{3\langle k \rangle - 2}.$$

These two results match very well, and we can also see how γ plays a role with the final clustering coefficient. We include the derivation of this estimated final clustering coefficient in Appendix A.1.

2.4.3 Degree Distribution

Results in this subsection were led and provided by my collaborators Nishant Malik and Feng Shi.

We now want to study another fundamental measurement of complex networks: degree distribu-

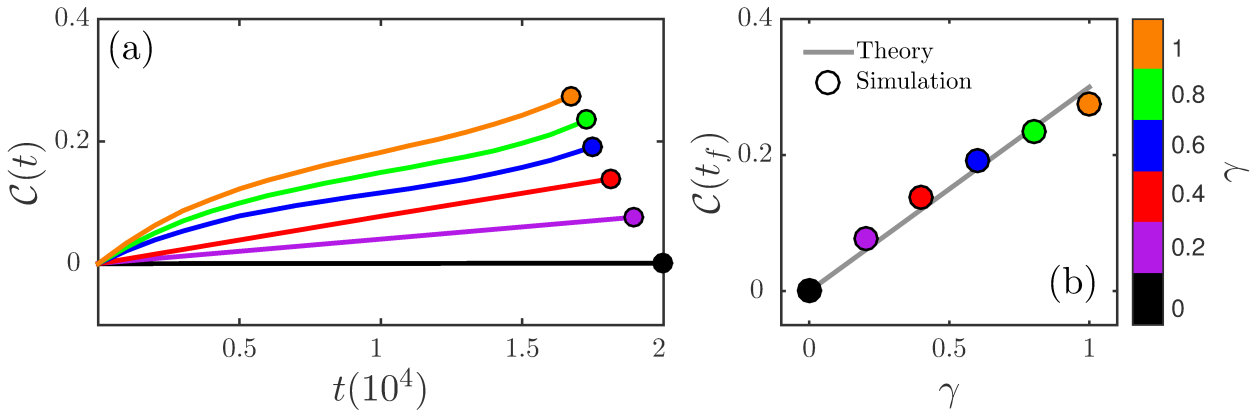

Figure 2.4: (a) Evolution of clustering coefficients with different values of γ with $\alpha = 1$. Circles are the clustering coefficients in the consensus states. (b) The clustering coefficients with different values of γ with $\alpha = 1$ in the consensus states at time t_f. Circles denote the simulation results, and the line denotes the theoretical estimation.

tion. Degree distribution usually tells how connected a network is. In the opinion formation with clustering reinforcement model, the interaction of the two mechanisms: voting and rewiring, would together generate nontrivial outcomes of the final degree distribution in the consensus states.

In Figure 2.5, we plot the initial and final degree distributions in the consensus states with different values of α and γ. Note that as we mentioned before, we start the networks as an Erdős-Rényi $G(N, l)$ random graph model. Hence, with N large enough, we could approximate the initial degree distribution of the networks by a Poisson distribution,

$$p_k = \frac{\langle k \rangle^k e^{-\langle k \rangle}}{k!}.$$

Here we have the initial degree distribution highlighted by thick gray bands in each subfigure. When $\alpha = 0$, there is no rewiring happening in the dynamics. Nodes only change their opinions back and forth, but the network structure does not change. Therefore, regardless of γ, the degree distribution remains the same.

The most interesting scenario must be the cases when α is small ($\alpha = 0.2$ and $\alpha = 0.4$). In these two cases, the effects of voting and rewiring are of the same magnitude. The voting mechanism makes nodes nearby competing for their opinions with each other. On the other hand, the rewiring mechanism makes nodes escaping from nodes with different opinions. To put it another way, the voting process promotes convergence to consensus states, but the rewiring process slows this down by

encouraging graph fission. Since these two mechanisms have the same magnitude, it takes networks longer time to reach their final consensus states. The network structures are shuffled so much for a long time that the final degree distributions have more deviation from the initial ones. We can also see the greater the γ is, the larger the deviation is.

When α gets greater, the rewiring mechanism starts dominating the network evolution. Nodes in the networks quickly find the components they belong to or the components of nodes with the same opinion by rewiring. This takes shorter time of networks to reach their consensus states. Although α is greater, the actual rewiring event is not more than the previous case when α is small. Hence, the deviation of the degree distribution is also small in this case.

To study the impact of γ on the final degree distributions, we perform a numerical analysis of data in Figure 2.5 and obtain the following best fit of the distribution:

$$p(k) = \begin{cases} \frac{\langle k \rangle^k}{k!} e^{-\langle k \rangle}, & \text{if } \alpha = 0 \\ \frac{b_1}{1.25\langle k \rangle} (\frac{k}{1.25\langle k \rangle})^{b_1} e^{-(\frac{k}{1.25\langle k \rangle})^{b_1}}, & \text{if } \alpha \neq 0 \end{cases}$$

Where the $\alpha \neq 0$ case is captured by Weibull distribution with b_1 as the shape parameter and scale parameter fixed constant equal to $1.25\langle k \rangle$, and b_1 is also a parameter depends on α and γ. This parameter b_1 encapsulates the variance in the degree distribution introduced by the interplay of the voting mechanism and the preferential rewiring towards closing the triangles, that is, it contains the information of both α and γ. The values of the parameter b_1 are provided in Appendix A.2.

2.4.4 Qualitative Exploration

Results in this subsection were led and provided by my collaborators Nishant Malik and Feng Shi.

In Section 2.4.1, we discuss the sharp transition of α for networks to have a graph fission without appreciable change in the populations of voters. This critical value of α depends on γ. Moreover, we have observed in Figure 2.3 that for $\alpha > \alpha_c(\gamma)$, the minority opinion fraction ρ is close to 0.5. On the other hand, for $\alpha < \alpha_c(\gamma)$, the minority opinion fraction ρ trends to 0 with decreasing α. To have a better understanding of the model, here we provide a holistic picture in Figure 2.6 and take a closer look at the dynamics.

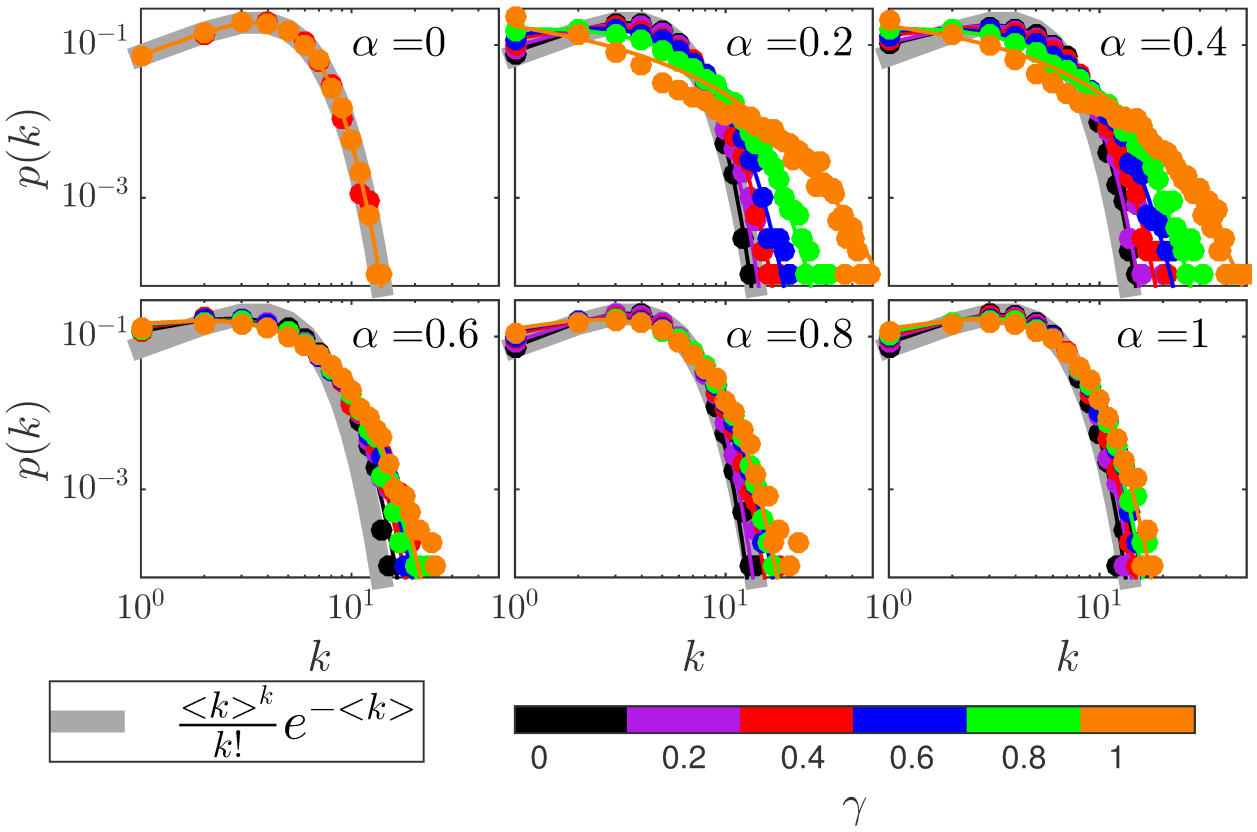

Figure 2.5: Initial and final degree distributions in the consensus state with different values of α and γ. We start with Erdős-Rényi networks with mean degree $\langle k\rangle = 4$, which has a Poisson distribution, highlighted by thick gray bands in each subfigure. We see a various level of deviation from the initial degree distribution as α and γ change.

In Figure 2.6 (a), we plot the dynamics of the opinion formation with clustering reinforcement model in the phase space of variables l_{01} and n_1. Fixing the value of α, different values of γ are labeled with different colors in the figure. We start with half of the population with opinion 0 and half of the population with opinion 1. At each time step, we pick a discordant edge l_{01} and update it. We see in the cases when α is large ($\alpha = 0.8$ and $\alpha = 1$), l_{01} drops to 0 relatively quickly, the final n_1 is around 0.5, and the dynamics stop. When α is smaller, different arches appear, the dynamics spend lots of time doing random walk on the arches, gradually reaches the $l_{01} = 0$ level, and the dynamics stop. The smaller the α is, the wider the arch span, as explored in detail (but restricted to our $\gamma = 0$ case) in [34]. We also see that in Figure 2.6 (b), fixing $\alpha = 0.4$, the greater the γ is, the narrower the arch. When $\gamma = 1$, the arch breaks and this makes the minority opinion fraction ρ closed to 0.5, and it is consistent with our previous $\alpha_c(\gamma)$ argument.

For $\alpha < \alpha_c(\gamma)$, the density of discordant edges at time t, or $l_{01}(t)$, can be approximated by

$$l_{01}(t) = c_1(1 - n_1(t))n_1(t) + c_2,$$

where $n_1(t)$ is the density of number of nodes having the opinion 1 and c_1 and c_2 are constants. We drop the argument t for the sake of simplicity later. Solving the quadratic equation for l_{01}, we get $n_{1_\pm} = 1/2 \pm 1/2\sqrt{1 + 4c_2/c_1}$. We denote n_{1_+} to be the state when n_1 is the majority opinion and n_{1_-} to be the state when n_1 is the minority opinion. The minority opinion fraction ρ here is the smaller solution of these two, which is $\rho = 1/2 - 1/2\sqrt{1 + 4c_2/c_1}$. In Figure 2.6 (a-b) we show the arches described by the quadratic equations above, as α and γ increase, these arches disappear for $\alpha > \alpha_c(\gamma)$. As we mentioned before, these arches behave like attracting manifolds for the dynamics, in Figure 2.6 (b), we observe that as γ increases, the arches are squeezed, i.e., the area enclosed within the arches contracts.

We estimate c_1 and c_2 using the data generated from simulations (see Appendix A.3). For $\alpha \neq 0$ we found that $\alpha_c(\gamma)$ could be found by solving the equation

$$\alpha^{2.1\exp(-0.75\gamma)} = 0.5.$$

To demonstrate the existence of this transition point in Figure 2.6 (c) we plot ρ for different α and γ vs. $\alpha^{2.1\exp(-0.75\gamma)}$, we observe that for $\alpha^{2.1\exp(-0.75\gamma)} > 0.5$, $\rho \simeq 0.5$ (segregated consensus). For $\gamma < 0.8$ we observe that all the data for ρ fall onto the same universal curve.

2.4.5 Semi-analytical Approximation

Lastly, we compare the numerical simulation results with the semi-analytical approximation we have. In Figure 2.7, fixing $\alpha = 0.4$, with different values of γ, the approximate master equation (AME) estimation also gives us different levels of arches as the simulation results suggest. We set different values of the stopping time $t = 500, 1000$, and 2000, and we see that the AME results stay on the arches for a long time. In the opinion formation with clustering reinforcement model we provide, eventually, the discordant edges l_{01} disappear. But it takes a long time for the simulation results to reach this state. The simulations would do random walks on the arches, gradually go to

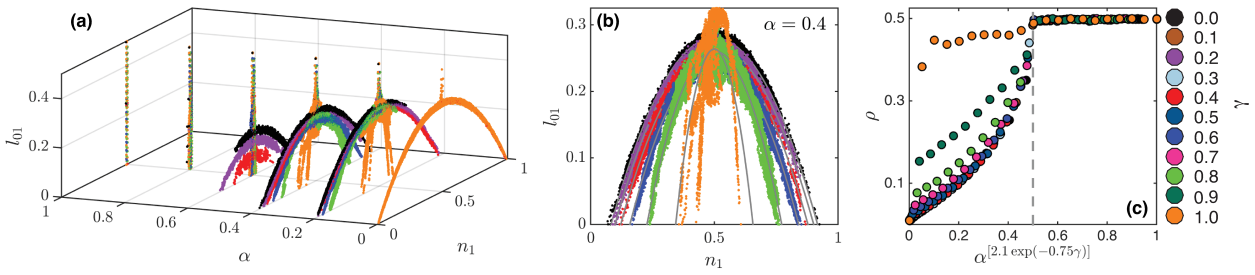

Figure 2.6: (a) The dynamics of the clustering reinforcement model in the phase space of l_{01} and n_1 with different values of α and γ. Note that the dynamics forms arches when α is small, and as α increases, the size of the arch shrinks. When $\alpha = 0.8$ and $\alpha = 1$, there are no such arches formed. Fix $\alpha = 0.4$, the dynamics of the model plotted as l_{01} versus n_1. The width of the arches is squeezed as we increase γ, and when $\gamma = 1$, the arch is destroyed. (c) Levels of ρ, the fraction of nodes holing minority opinions in the consensus states versus α. Here we transformed α into $\alpha^{2.1\exp(-0.75\gamma)}$. Note that this transformation forces all the data for $\gamma < 0.8$ collapses onto one universal line. Moreover, there is a clear transition in when $\alpha^{2.1\exp(-0.75\gamma)} = 0.5$.

$l_{01} = 0$ and stop evolving. The arches are just temporary states of the network dynamic. Hence, the difference of the AME and simulation results on the n_1 axis, i.e., $l_{01} = 0$ level, would be the error of our semi-analytical approximation. Note that the smaller the γ is, the better the estimations one can get from the AME method. This is because the AME method and, in particular, the model terms in our equations for rates of rewiring to second nearest neighbors, assumes a network to be locally tree-like, and when γ is greater, the greater this assumption is violated. Therefore, AME could give us a good qualitative estimation of the simulation results, and also good predictions of the final fraction of opinions when γ is not large.

In Figure 2.8, we compare the numerical simulations and the semi-analytical solution by Approximate Master Equation (AME) at $\alpha = 0.4$ with different levels of γ on a $n_1 - l_{01}$ coordinate system. The AME approximation gives us a good estimation of the qualitative behavior of the simulations. As we discussed previously, the smaller the γ is, more accurate result the AME method could provide.

2.5 Conclusion

All social networks in the real world have one thing in common: high local clustering. This is a nontrivial trait of social networks that few coevolving or adaptive network dynamics models deal with directly. Its influence on a variety of contagion dynamics occurring on social or real-world networks

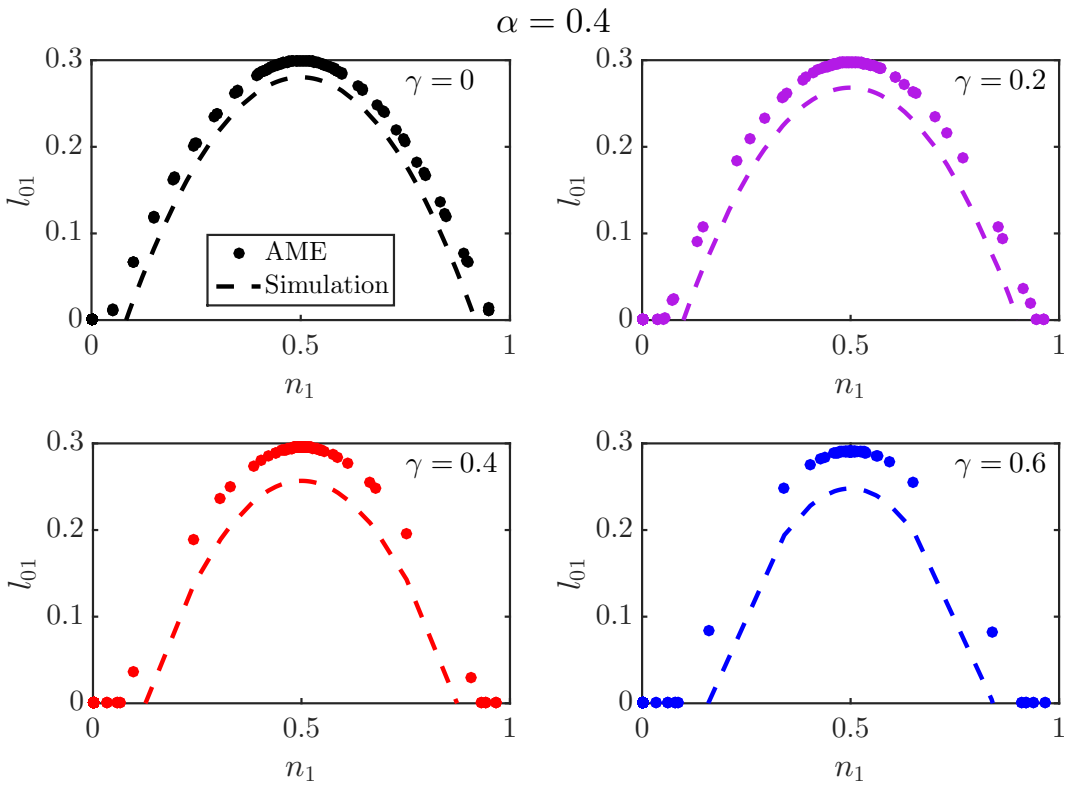

Figure 2.7: Comparison between Approximate Master Equation (AME) and simulations for $\alpha = 0.4$. Solutions for AME were sampled at $t = 500, 1000, 2000$.

has been studied in some detail, but systematic studies investigating its role in more realistic models such as the ones with coevolving network component are still lacking.

Here, we provide an opinion formation model with simple clustering reinforcement. We introduce a preferential attachment to an existing rewire-to-random opinion formation model. Under our new model, there is a certain probability that if a rewiring happens, a node rewires to its neighbors' neighbor, a triangle is closed, and the local clustering extent increases. We show that this new mechanism we establish indeed fundamentally affects the network dynamics, and leads to different qualitative and quantitative results.

We explore the parameter spaces and find out that there are mainly two types of consensus could be reached in our model, namely the hegemony consensus and the segregated consensus. The clustering coefficient of networks indeed increases in our clustering reinforcement dynamics. By using some mean field arguments, we give an estimation of the final clustering coefficient of the networks. We also investigate the final degree distribution and discuss how the parameters we introduce would

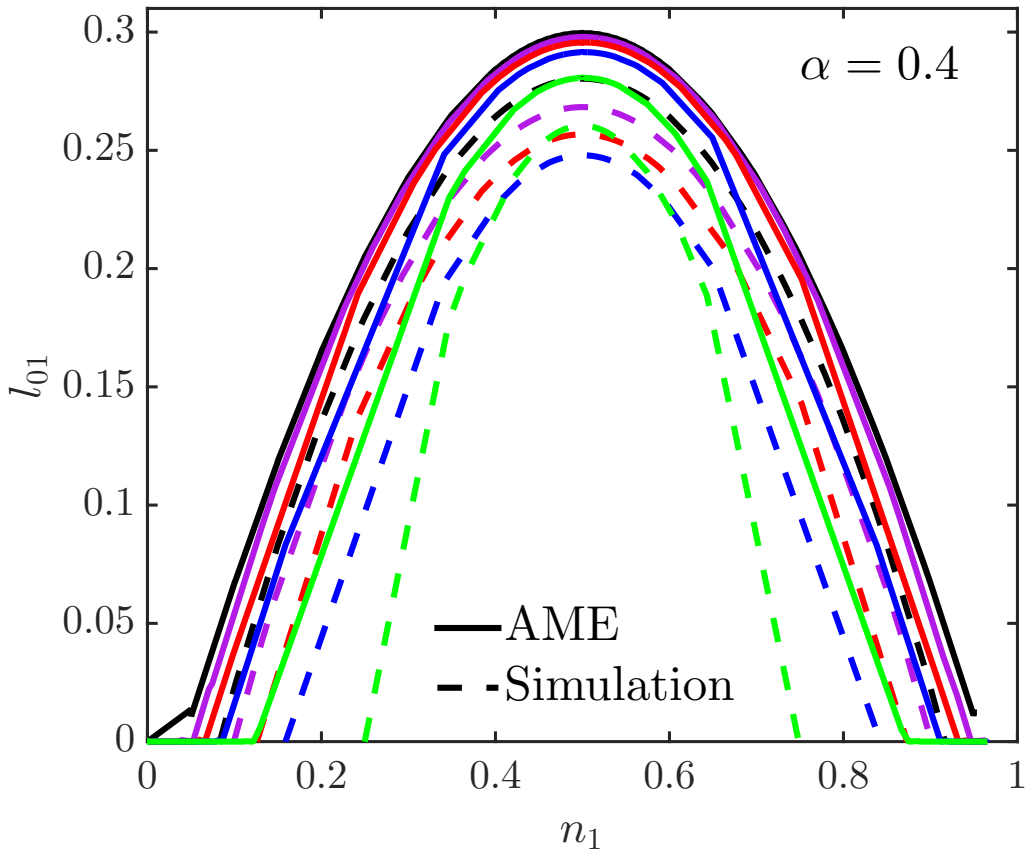

Figure 2.8: Comparison between numerical simulations and the semi-analytical solution by Approximate Master Equation (AME) at $\alpha = 0.4$. Different colors represents different values of γ, the color scheme used here is the same as in Figure 2.4 and Figure 2.5 above.

impact it. Moreover, we provide a full investigation of the qualitative behavior of the network dynamics; we see in some cases arches are formed, and how these related to the final fraction of minority opinions. Furthermore, we also provide a semi-analytical framework based on approximate master equation (AME) to study models with reinforcement of clustering. Using this estimation, we could accurately predict the dynamical behaviors of the model for a variety of parameter settings.

CHAPTER 3

SIS Model and Social Clustering on Complex Networks

3.1 Background Information

Mathematical modeling has provided significant insights into the processes involved in the spread of epidemics [4, 81]. In recent years, the study of dynamical processes on complex networks has caught much attention in this field [80, 112]. Loosely speaking, there are two types of dynamics that are studied in the context of modeling epidemic spread on networks: in the first type, each node is allowed to change its state with no evolution of the underlying network structure through time, while in the second the temporal evolution of the network structure co-evolves or is adaptive with the states of the nodes [58, 132]. Dynamics on coevolving networks may be more appropriate for modeling epidemic spread, as people might avoid contact with individuals infected by a infectious disease while readily building connections to healthy individuals. Such a preference in attachment between individuals will not only lead to change in the social network but thus also influences the spread of disease. Therefore, studying the interplay between dynamics and the adaptive coevolving structure of networks has a potential to provide several critical insights into the processes involved in the spread of epidemics.

Many real world networks are coevolving to some extent, and there are numerous studies on coevolutionary networks in epidemic models, with several important analytical and computational results [38, 58, 71, 132]. People studied fluctuations and the spread of disease as an SIS or SIR model on large static or coevolving networks [48, 134, 157]. Many studies also focus on preventing infectious diseases [21, 86, 150]. Moreover, network topology has a great impact on propagation dynamics [73, 87, 107]. Recently, percolation or epidemic processes on networks with clustering have also been studied broadly [51, 114]. More specifically, [103] shows that the clustering of networks could raise the epidemic threshold and reduce the epidemic size from networks comparing to networks with the same degree correlations but without clustering.

One of the critical components that has been missing in these studies is the influence of clustering in coevolving networks on the resulting dynamics and network structure. Clustering is one of the central properties of social networks, arising due to the ubiquitous tendency among individuals to connect to friends of a friend, and can greatly impact a coevolving network system [96]. In this paper, we generalize a model for coevolution of disease spreading on an adaptive network, in order to investigate the role of local clustering. We also explore the additional complexity induced by reinforcement of clustering with a new parameter which has preferential rewiring to close triangles.

The outline of the Chapter is as follows. In Section 2, we define our model and in Section 3, we derive our semi-analytical method. In Section 4, we compare simulation results with the estimation we obtained. We investigate the rewiring parameter space, study the change of degree distribution and the evolution of clustering coefficients. We also carry out a numerical bifurcation analysis. Finally, in Section 5, we give our conclusions and some further remarks.

3.2 Model Description

Social networks are observed to have high clustering, because of the natural tendencies in social ties for friends of friends being friends themselves. Therefore it is unrealistic to study dynamics on social networks without taking clustering coefficient into account. We also know that in real world networks, especially in networks in epidemiology, network topologies are often coevolving with the dynamics on them. The change of network topologies could be modeled through the process of rewiring. If individuals catch an infectious disease, the infected ones may be quarantined or avoided by healthy individuals, resulting in losses of their social ties. We here introduce an additional component in this rewiring mechanism that reinforces the local clustering, i.e., a preference to rewire to friends of a friend.

We employ a susceptible-infected-susceptible (SIS) model on a coevolving network [20, 59]. We consider a network with constant numbers of nodes, N, and undirected links, $M = \langle k \rangle N/2$, where $\langle k \rangle$ is the average degree in the network. At a given time, each node is either in a susceptible (S) or infected (I) state. In every time step, infected individuals infect their susceptible neighbors with probability β, while recovering from the disease with probability α. Meanwhile, susceptible individuals break a link with an infected neighbor with probability γ and—generalizing previously

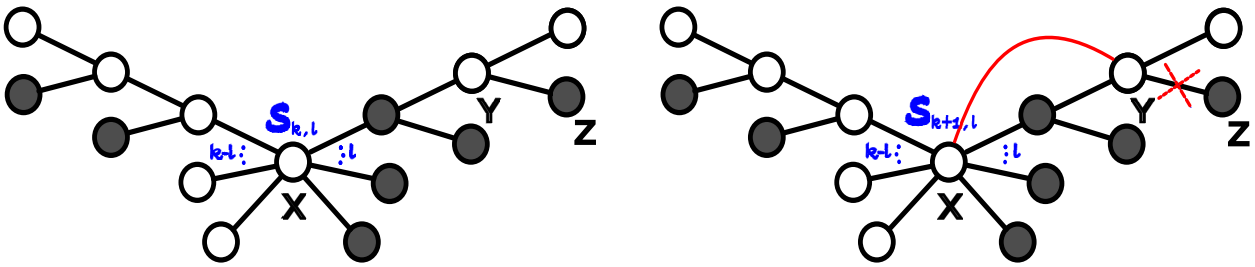

Figure 3.1: Illustration of rewiring to neighbors's neighbor. Before the rewiring, node X is of class $S_{k,l}$ (the left subfigure). Suppose a discordant edge YZ is picked, with probability η, Y would actively dismiss its infected neighbor and rewire to its neighbors's neighbor X. Then node X becomes of class $S_{k+1,l}$ (the right subfigure).

studied models—either rewire to a neighbors' neighbor with probability η, or rewire uniformly at random to another susceptible node in the network with probability $1-\eta$. Importantly, rewiring to a neighbors' neighbor closes a triangle between three nodes, directly reinforcing network transitivity, whereas rewiring uniformly at random can rapidly randomize any initial state of the network structure.

Here we illustrate the effect of rewiring to neighbor's neighbor, with probability η, in Figure 3.1.

3.3 Semi-analytical Methods

We study this generalized adaptive network model with a combination of simulations and approximate analytic models. The frameworks of Pair Approximation (PA) and Approximate Master Equations (AME) have both been used effectively as analytical tools in similar settings [34, 52, 80]. PA is a method for moment closure where the density of triplets is given by an approximate equation in terms of pairs, while AME can be used to achieve greater accuracy [52]. The AME framework considers both the infection state and degree of nodes and the states of their immediate neighbors, generating a system of differential equations to model the coevolution of the disease and network. The AME method generally provides accurate approximation of the evolution of networks, and it is still good around the critical point of the dynamics. Moreover, the AME method performs well in both static and coevolving networks.

Inspired by this improved compartmental formalism or master equation method, [159] used an approach (for studying adaptive SIS dynamics without any transitivity reinforcement) that treated

the links as the objects and classify them according to the disease states, the number of neighbors, and the number of infected neighbors of each node of its links. This link-based method could generally improve the accuracy compared to the AME method. However, it also enormously increases the computational cost from $O(k_{\max}^2)$ to $O(k_{\max}^4)$, where $k_{\max}$ is the maximum degree a node could have in the network.

We use an approach similar to the one used in [97] to combine AME with PA, extending the method to study the effect of reinforcement of clustering. Let $S_{kl}(t)$ and $I_{kl}(t)$ be the fraction of susceptible and infected sites of total degree k which have l infected neighbors at time t. Following the notation in [97], we also define the zeroth order moments of the $S_{kl}(t)$ and $I_{kl}(t)$ distribution by $S \equiv \sum_{kl} S_{kl}$ and $I \equiv \sum_{kl} I_{kl}$; the first order moments by $S_S \equiv \sum_{kl}(k-l)S_{kl}$, $S_I \equiv \sum_{kl} lS_{kl}$, $I_S \equiv \sum_{kl}(k-l)I_{kl}$ and $I_I \equiv \sum_{kl} lI_{kl}$; and the second order moments by $S_{SI} \equiv \sum_{kl}(k-l)lS_{kl}$, $S_{II} \equiv \sum_{kl} l(l-1)S_{kl}$, etc.

It is worth noting that while the network states and topologies coevolve, there are different conserved quantities the system should obey. For example, since the networks are not losing nodes, we always have $S + I = 1$, and this is the conservation of nodes. Similarly we always have $SS + SI + IS + II = \langle k \rangle$, and this is the conservation of edges. The system should conserve all its quantities at different orders of moments.

Again, let $S_{kl}(t)$ and $I_{kl}(t)$ be the fraction of susceptible and infected sites of total degree k which have l infected neighbors. We have the following ODE governing the time evolution of the S_{kl} compartment:

$$
\begin{aligned}
\frac{dS_{kl}}{dt} &= \alpha I_{kl} - \beta l S_{kl} + \alpha\big[(l+1)S_{k(l+1)} - lS_{kl}\big] \\
&\quad + \beta\frac{S_{SI}}{S_S}\big[(k-l+1)S_{k(l-1)} - (k-l)S_{kl}\big] \\
&\quad + \gamma\big[(l+1)S_{k(l+1)} - lS_{kl}\big] \\
&\quad + \gamma\eta\Big\{\Big[\frac{l}{k-1}\frac{I_S}{\frac{1}{2}I_I + I_S}\frac{S_I}{S} \\
&\qquad + \frac{k-l-1}{k-1}\frac{\frac{1}{2}S_S}{\frac{1}{2}S_S + S_I}\frac{S_I}{S}\Big]S_{(k-1)l} \\
&\quad - \Big[\frac{l}{k}\frac{I_S}{\frac{1}{2}I_I + I_S}\frac{S_I}{S} + \frac{k-l}{k}\frac{\frac{1}{2}S_S}{\frac{1}{2}S_S + S_I}\frac{S_I}{S}\Big]S_{kl}\Big\} \\
&\quad + \gamma(1-\eta)\frac{S_I}{S}\big[S_{(k-1)l} - S_{kl}\big].
\end{aligned}
$$

Similarly the ODE governing the time evolution of the I_{kl} compartment is:

$$\begin{aligned}\frac{dI_{kl}}{dt} &= -\alpha I_{kl} + \beta l S_{kl} + \alpha\big[(l+1)I_{k(l+1)} - lI_{kl}\big] \\ &+ \beta\big(1+\frac{S_{II}}{S_I}\big)\big[(k-l+1)I_{k(l-1)} - (k-l)I_{kl}\big] \\ &+ \gamma\big[(k-l+1)I_{(k+1)l} - (k-l)I_{kl}\big].\end{aligned}$$

To determine the initial condition, in each case, a fraction ϵ of nodes is initially infected at random. This gives us

$$S_{kl}(0) = (1-\epsilon)p_k(0)\binom{k}{l}\epsilon^l(1-\epsilon)^{k-l},$$

$$I_{kl}(0) = \epsilon p_k(0)\binom{k}{l}\epsilon^l(1-\epsilon)^{k-l},$$

and where $p_k(0)$ is the degree distribution at $t = 0$.

The differential equation system above contains $2(k_{\max}+1)^2$ differential equations. This level of complexity provides a reasonable accuracy we need for the new reinforcing clustering model and we do not need to deal with an $O(k_{\max}^4)$ system using the link-based formalism method. We use these differential equations to estimate the evolution of networks and solve their solutions numerically, arriving at a semi-analytical approximation of the network evolution.

3.4 Numerical Experimentation

We simulate networks with total number of nodes $N = 25,000$, and total number of edges $M = 25,000$, and hence our mean degree is fixed to be $\langle k\rangle = 2$. To implement the simulations, as in [97], we choose three different initial degree distributions of the networks. The first distribution is the Poisson distribution,

$$p_k^P = \frac{\langle k\rangle^k e^{-\langle k\rangle}}{k!},$$

and we could use this to approximate the degree distribution of an Erdős-Rényi model with large N. The second one is a truncated power law distribution,

$$p_k^{TPL} = \begin{cases} \frac{1}{C}k^{-\tau} & 0 < k \leqslant k_c \\ 0 & k > k_c, \end{cases}$$

where we choose $\tau = 2.161$ and $k_c = 20$ in order to make the mean degree $\langle k \rangle = 2$. The last one is a degree regular distribution:

$$p_k^{DR} = \delta_{k,k_0},$$

where δ is the Kronecker δ, hence every node would have the same degree k_0.

We perform Monte Carlo simulations of the disease propagation on a network. In each simulation, we use a Gillespie algorithm to accelerate the iteration process, and the step size here is a fixed number $1/M$. Self-loops and repeated links are not allowed in the simulation. Unless stated otherwise, we will do 1,000 simulations for each set of parameters.

3.4.1 Exploration of the Parameter Space

Since the effect of the parameter η depends on the rewiring parameter γ, the first thing we want to do is to explore the parameter space of γ and η. In order to compare with the original study in [97], we fix the infection rate $\beta = 0.04$ and the recovery rate $\alpha = 0.005$, and we want to see how γ and η would affect the disease prevalence I in the long run. The phase portrait of Figure 3.2 shows if γ is large, the susceptible nodes could easily get rid of the infected ones by breaking their links, and all networks become disease free. When $\gamma = 0$, there would be no rewiring process, network topology does not change, and η would have no effect on the network dynamics as well. More interesting behavior happens when γ is close but greater than zero, in this case η plays an important role for the disease prevalence I, and this is the case we are interested in. Hence in the rest of the experiments we will fix $\gamma = 0.04$ and change the value of η to see how it influences the network dynamics.

3.4.2 Network Dynamics and the Effect of η

We plot the disease prevalence I against time t with different η's in Figure 3.3. When $\eta = 0$ in Figure 3.3 (a), our model would go back to the previous case in [97]. We see networks with different initial topologies will lead to different results. In the Poisson and truncated power law cases, the disease prevalence I is always positive, and people call these networks to be endemic. However, in the degree regular case, the disease gradually disappears, and people call this situation disease free.

For an individual network, if the disease persists in it, the quantities of nodes being infected at each time would fluctuate. That is, the disease prevalence I will vary within a band when time

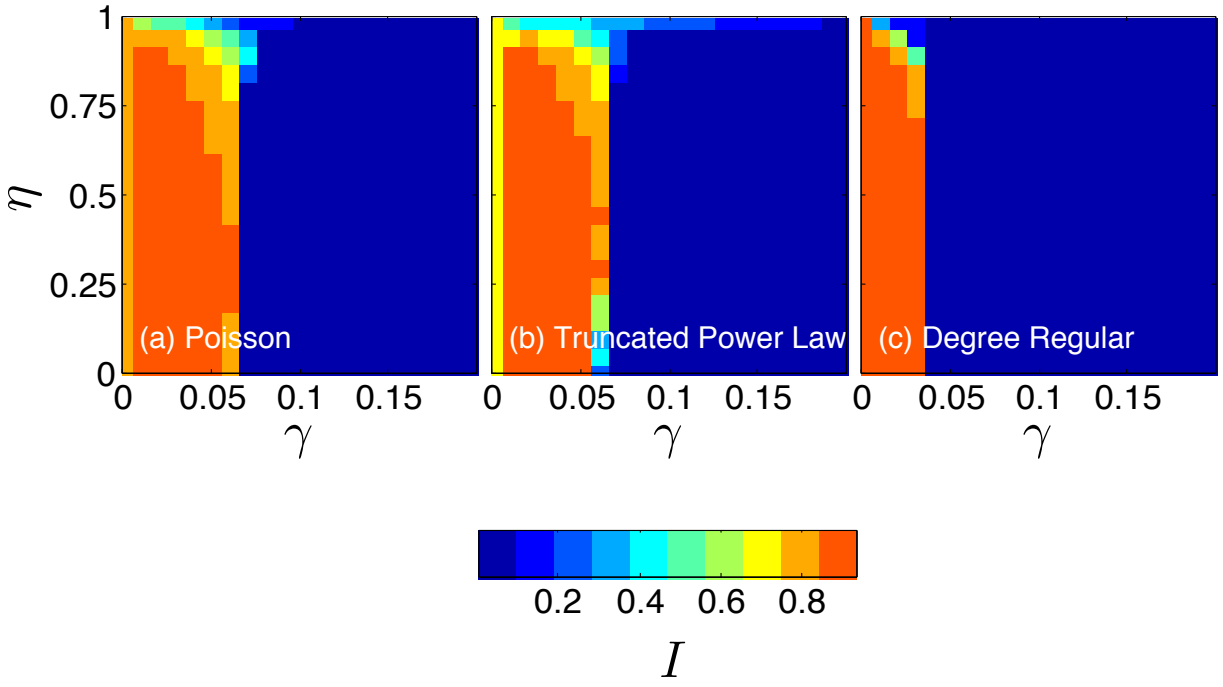

Figure 3.2: Phase plots in parameter space (γ, η) for the disease prevalence I on networks with an initial (a) Poisson, (b) truncated power law, and (c) degree regular degree distribution. Other parameters are $\beta = 0.04$, $\alpha = 0.005$ and $\epsilon = 0.1$. We choose $t = 10,000$, when most of the networks reach their stationary states. The disease prevalence I is averaged over 30 simulations in all cases.

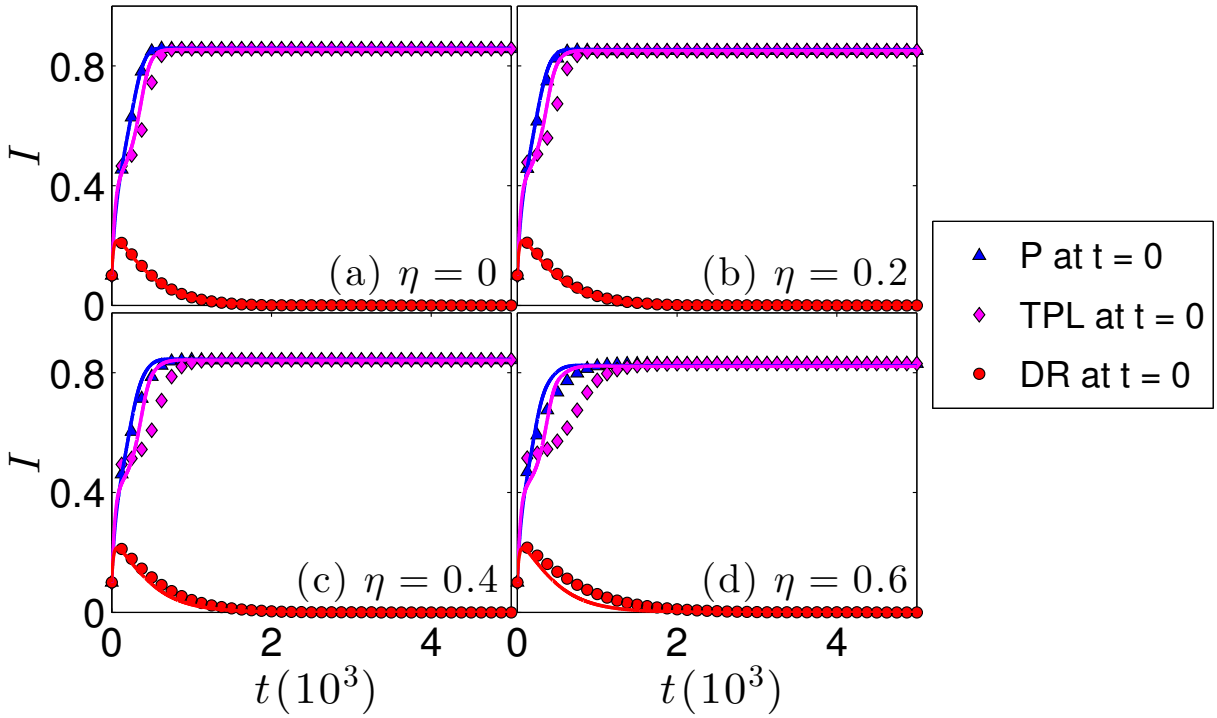

Figure 3.3: Disease prevalence I against time t on networks with mean degree $\langle k \rangle = 2$ but with different initial degree distributions (p_k^P (Poisson): blue, p_k^{TPL} (truncated power law): magenta, and p_k^{DR} (degree regular): red). Dots correspond to the mean computed over 1,000 simulations and lines are the semi-analytical approximations. Parameters are $\beta = 0.04, \gamma = 0.04$, $\alpha = 0.005$ and $\epsilon = 0.1$ in all cases. The η here are: (a) $\eta = 0$, (b) $\eta = 0.2$, (c) $\eta = 0.4$, (d) $\eta = 0.6$.

t is large enough. However, this stochastic variation would be averaged out if we perform more experiments and take the mean of their disease prevalence I. We declare a stationary state of the process when the average disease prevalences of the ensemble of networks between two consecutive steps differ by at most 10^{-5}, and we also define the stationary or final disease prevalence level to be I_∞. Under this definition, networks with all three different initial topologies reach their stationary states before $t = 5,000$ when η is not very large. Note that the disease prevalence I_∞ in stationary state decreases with η, indicating that η indeed affects the network dynamics. When the networks are still in their transient states, there are difference between simulations and our approximation, which might be accounted for if we use link-based formalism method used in [159]. But most importantly, our semi-analytical approximation captures the disease prevalence level of stationary states in all four cases $\eta = 0, 0.2, 0.4$, and 0.6.

3.4.3 Degree Distribution

One nice thing about our semi-analytical approximation is this gives us information of degree distribution of a network. AME uses (and keeps) degree information from nodes and their neighbors. In Figure 3.4, we choose different initial topologies with $\eta = 0.4$ and plot the degree distribution in their stationary states with a log-log scale. Our semi-analytical approximation provides a good estimation of the stationary degree distributions in each case. We then separate nodes into susceptible (S) and infected (I) classes and our method still captures their stationary degree distributions very well. Similarly, the Poisson and truncated power law cases show indistinguishable final degree distributions.

To see how η affects network degree distribution, we plot the initial and stationary degree distribution of networks with different η on a log-log scale in Figure 3.5. We separate the cases of networks with three different initial topologies, and plot their initial and stationary degree distributions. Our semi-analytical approximation also gives us good predictions up to $\eta = 0.8$. We see different η's do not make much difference of each stationary degree distribution. Again, the stationary degree distributions of Poisson and truncated power law cases become indistinguishable. Moreover, for the truncated power law case, the heavy tail property is gone after the rewiring processes that shuffle the network topologies.

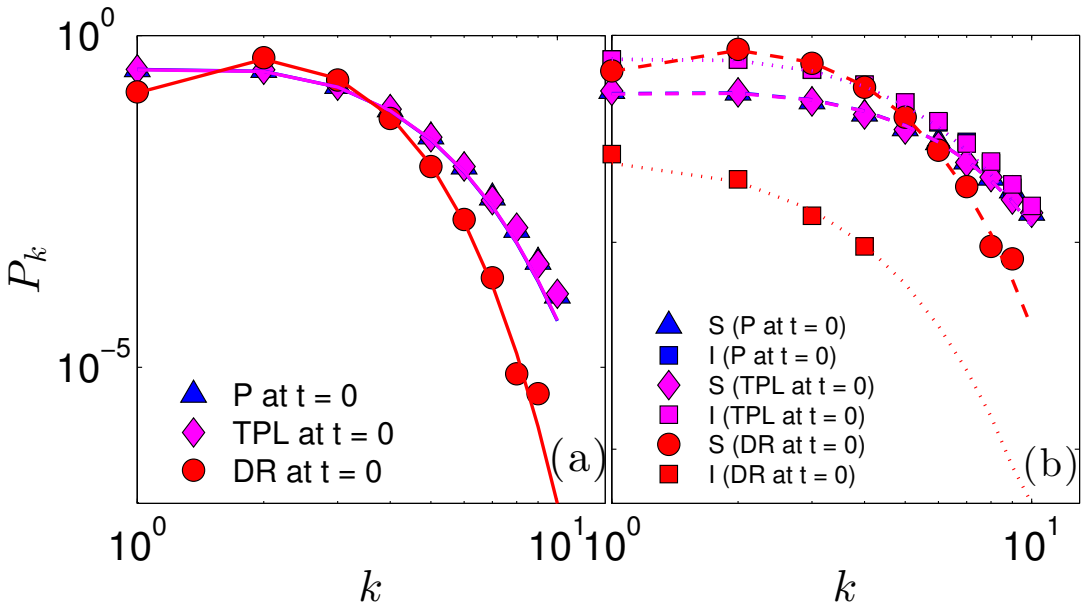

Figure 3.4: (a) Degree distribution and (b) degree distribution of S and I nodes on networks with mean degree $\langle k \rangle = 2$ on log-log scale but with different initial degree distributions (p_k^P (Poisson): blue, p_k^{TPL} (truncated power law): magenta, and p_k^{DR} (degree regular): red). Dots correspond to the mean computed over 200 simulations. Solid lines in (a) are the semi-analytical approximation of total degree, dashed lines and dotted lines in (b) are the semi-analytical approximation of degree distribution of S and I, respectively. Parameters are $\beta = 0.04, \gamma = 0.04, \alpha = 0.005, \epsilon = 0.1$ and $\eta = 0.4$.

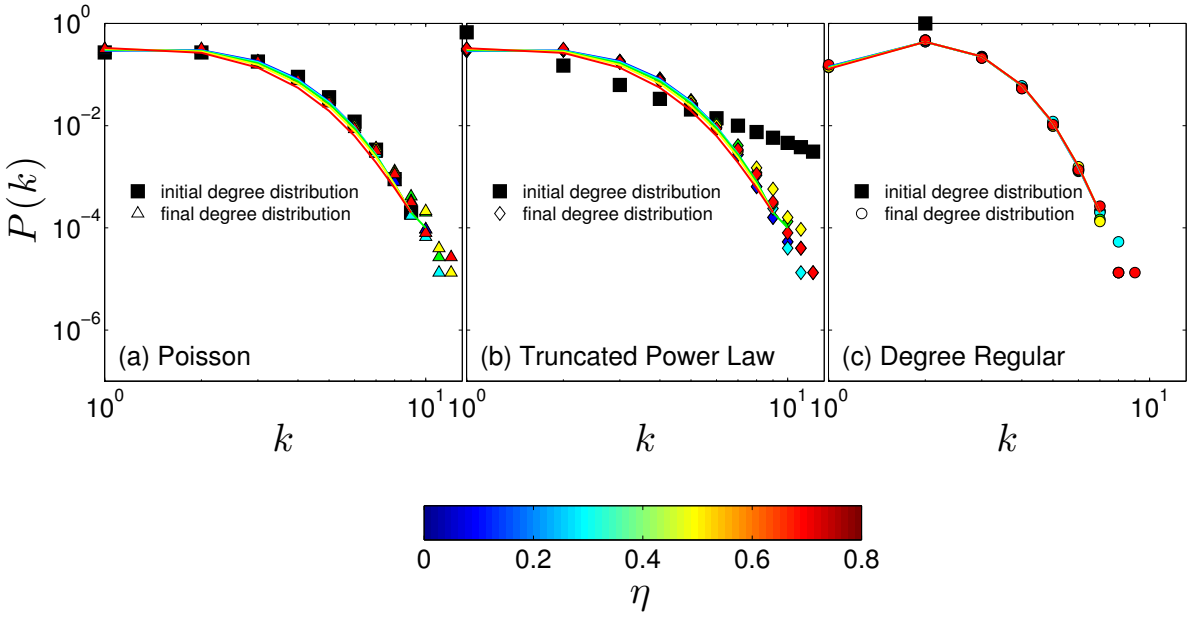

Figure 3.5: Degree distribution with mean degree $\langle k \rangle = 2$ on log-log scale on networks with an initial (a) Poisson, (b) truncated power law, and (c) degree regular degree distribution. We choose $\eta = 0, 0.2, 0.4, 0.6,$ and 0.8. Other parameters chosen are $\beta = 0.04$, $\gamma = 0.04$, $\alpha = 0.005$, and $\epsilon = 0.1$. We set $t = 5,000$, all networks reach their stationary states at this time. Squares in each subplot are the initial degree distributions. Dots correspond to the mean computed over 200 simulations. Lines are the semi-analytical approximation of the stationary state degree distributions.

3.4.4 Clustering Coefficient

In order to make sure that our model really provides us nonzero clustering coefficient and it reinforces the clustering while rewiring, we study the clustering coefficient against time. In Figure 3.6 (a), we explore η from 0 to 1, keep other parameters fixed and choose the initial degree distribution to be Poisson. Like before, the case of $\eta = 0$ would go back to the previous case in [97], and we can see the clustering coefficient stays at $C = 0$ all the time. As time evolves, for networks with nonzero η's, the clustering coefficients would rapidly increase and stop changing after these networks reach their stationary states. However, in the case $\eta = 1$, networks again do not reach their stationary states at time $t = 5,000$, but we could still see the increasing pattern of the clustering coefficient against time. We also study this on the other two initial topologies. In Figure 3.6 (b), we see the stationary clustering coefficients increase as we increase η. At time $t = 5,000$, except the case $\eta = 1$, all other networks reach their stationary states. As we showed before, networks with regular degree distributions initially at this time would be disease free and they have higher clustering coefficients comparing to the other two cases. Moreover, the initially Poisson and truncated power law degree distribution networks again show indistinguishable result of clustering coefficient when $\eta < 1$. We believe $\eta = 1$ is a special case in our model and we will study this case separately later.

3.4.5 Disease Prevalence

To study the whole picture of the parameter η, again, we explore η from 0 to 1, keep other parameters fixed and choose the initial degree distribution to be Poisson. We compare the simulation results and the semi-analytical approximation in Figure 3.7. As we increase η, the disease prevalence at the stationary state gets lower and the error between simulation and approximation gets larger. Although our approximation does not match the simulation result very well before they reach their stationary state, this approximation still captures the disease prevalence level I_∞ when η is not very large.

Unlike other cases are in their stationary states at the time $t = 5,000$, in the case $\eta = 1$, we see the disease prevalence I is still decaying gradually. Our semi-analytical approximation suggests that I_∞ would go to 0 when $\eta = 1$, but it's not clear what would be the disease prevalence level I_∞ of the simulation. So we increase time to $t = 10^7$ when $\eta = 1$ as shown in Figure 3.7. As we can see

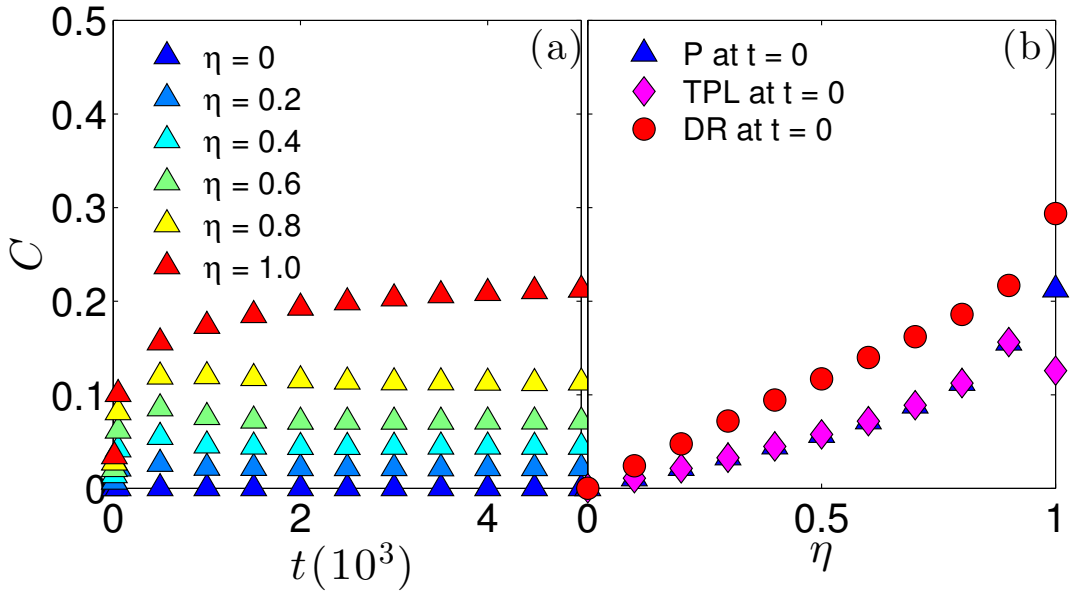

Figure 3.6: (a) Clustering coefficient C versus time t on networks with the same mean degree $\langle k \rangle = 2$ initial Poisson degree distributions. The parameters of the system are $\beta = 0.04, \gamma = 0.04, \alpha = 0.005$, and $\epsilon = 0.1$. Dots correspond to the mean computed over 30 simulations. Different chosen values of η are shown in the figure. (b) Clustering coefficient C at $t = 5,000$ versus η on networks with the same mean degree $\langle k \rangle = 2$ but different initial degree distributions (p_k^P (Poisson): blue, p_k^{TPL} (truncated power law): magenta, and p_k^{DR} (degree regular): red). At time $t = 5,000$, except the case $\eta = 1$, all other networks reach their stationary states.

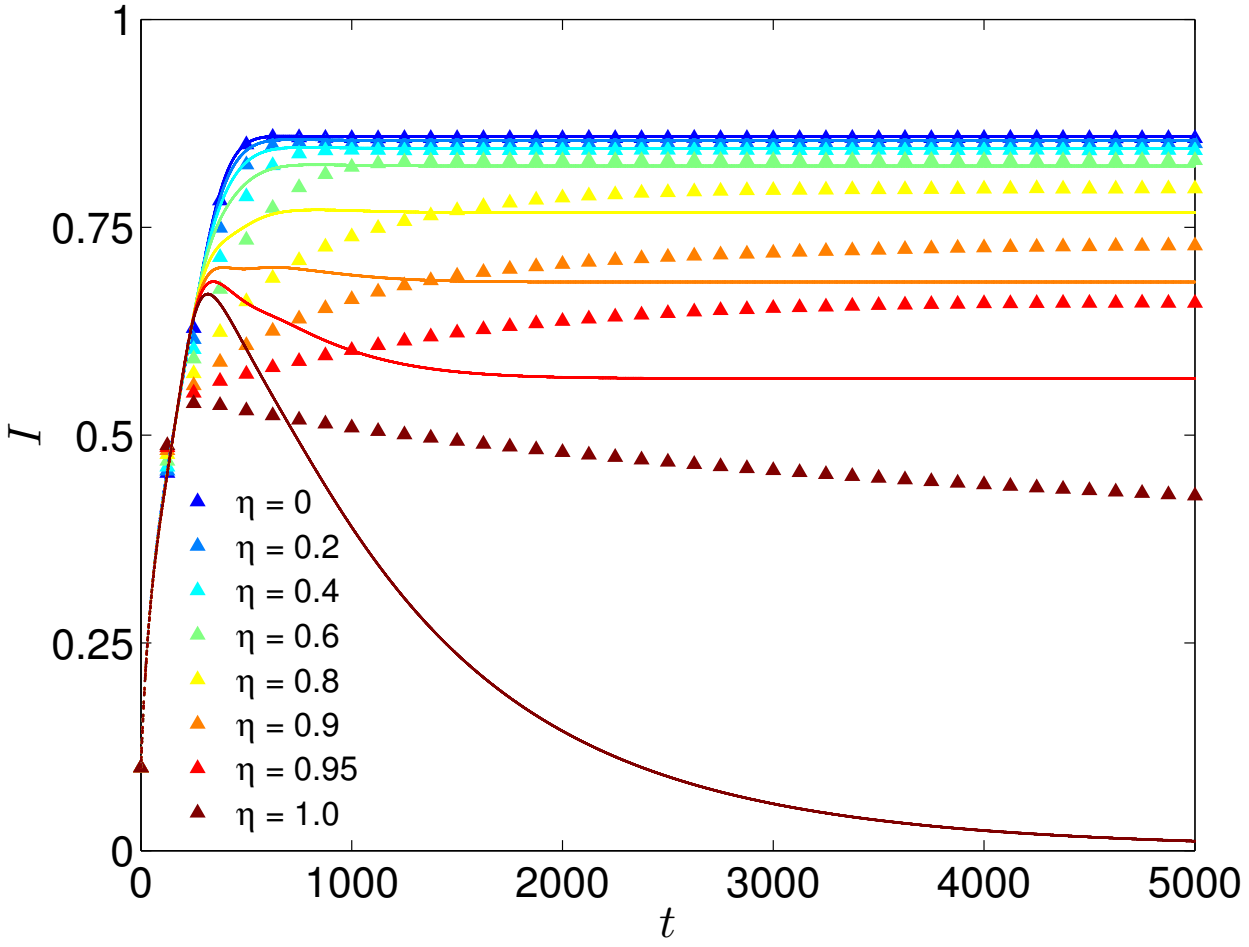

Figure 3.7: Disease prevalence I against time t on networks with the same mean degree $\langle k \rangle = 2$ initial Poisson degree distribution. The parameters of the system are $\beta = 0.04, \gamma = 0.04, \alpha = 0.005$, and $\epsilon = 0.1$. Dots correspond to the mean computed over 1,000 simulations and the lines are the semi-analytical approximation. Different chosen values of η are shown in the figure.

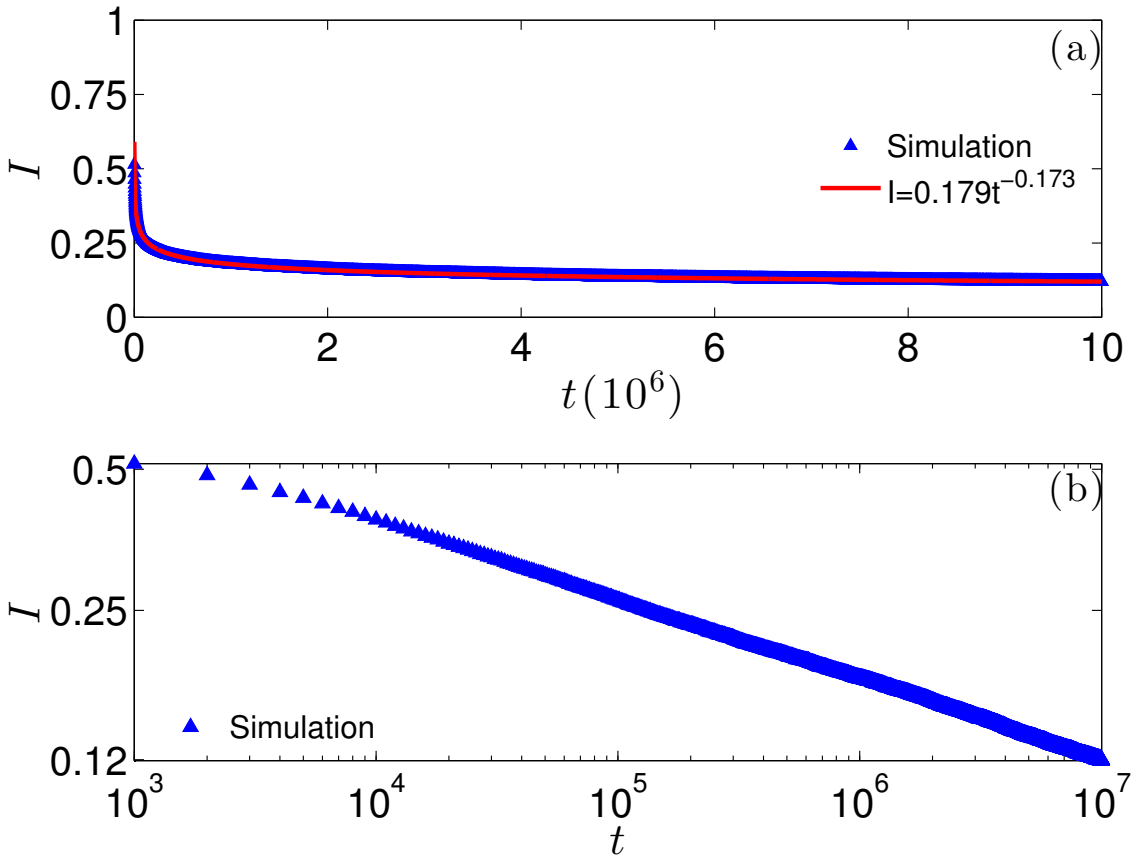

Figure 3.8: Disease prevalence I against time t until $t = 10^7$ in the case $\eta = 1$ on networks with mean degree $\langle k \rangle = 2$ initial Poisson degree distributions. (a) Dots are sampled every t = 1,000 correspond to the mean computed over 30 simulations. (b) The curve fitting on a $log - log$ plot of the data. We can see the data becomes a straight line and this suggests the data has a power law decay.

in Figure 3.8 (a), the disease prevalence I reaches 0.12 at $t = 10^7$ but we are not sure whether it will keep decreasing or not. If we plot I and t in the log-log scale, the simulation data becomes a straight line. This suggests that the disease prevalence I has a power law decay. Using the curve fitting software in MATLAB, the simulation result is well fitted by the curve $I = 0.179t^{-0.173}$. Hence although we do not know the disease prevalence level I_∞ when $\eta = 1$, we would say it is at most 0.12 and this will be our I_∞ we use later. Moreover, in our semi-analytical approximation, all the cases except $\eta = 1$ have positive disease prevalence levels I_∞. Combining this fact and the very different time scale, we surmise that there is a phase transition happening when $\eta = 1$, which deserves further investigation.

We have shown that networks with different initial topologies present different behaviors. Using the parameter set we chose before, networks starting with a degree regular degree distribution would become disease free. On the other hand, networks starting with Poisson or truncated power law degree distributions would be endemic. That is, in the degree regular case, networks have $I_\infty = 0$, and in the other two cases we see networks with different positive I_∞ depending on different η's. In Figure 3.9 (a), we plot the I_∞ against η in Poisson and truncated power law cases, and our semi-analytical approximation captures the I_∞ quite well when η is not close to 1. Moreover, networks with these two different initial topologies again show the indistinguishable I_∞ when $\eta < 1$ and $\eta = 1$ is a special case as in our previous discussion. In the degree regular case, since we know networks will be disease free, we plot the time networks reach their stationary states as in Figure 3.9 (b) and we call this time t_f. As η increases, t_f increases. Large η would also create higher clustering coefficient as we saw before and this makes the time for networks to become disease free longer. Although our semi-analytical approximation knows these network will become disease free, the t_f it predicts are not accurate. That means our approximation method is not very good when the networks are still in transient states, and again, this might be improved if people use link-based formalism method in the future.

3.4.6 Bifurcation Analysis

We plot two bifurcation diagrams of the systems in Figure 3.10 and Figure 3.11. in order to explore the properties of the systems at equilibrium. As we mentioned before, it takes longer time for the cases $\eta = 1$ to reach their stationary states so we plot these cases separately. In Figure 3.10, the first row is the case $\eta < 1$ and the second row is the case $\eta = 1$. When $\eta < 1$, in all three cases of initial topologies, there are small bistable regions around $\beta = 0.16$. The transition is discontinuous when $\eta = 0$ as we show in the insets in the plots, and the gap between the transition starts shrinking when we increase η. When $\eta = 0.8$, the transition becomes continuous and this means η could make a qualitative change of the dynamical system. In the case $\eta = 1$, the systems do not reach their stationary states in the given time $t = 10,000$ we set. However they still show continuous transitions, which are very different from the case $\eta = 0$. Last but not least, the critical value of β also decreases in the case $\eta = 1$.

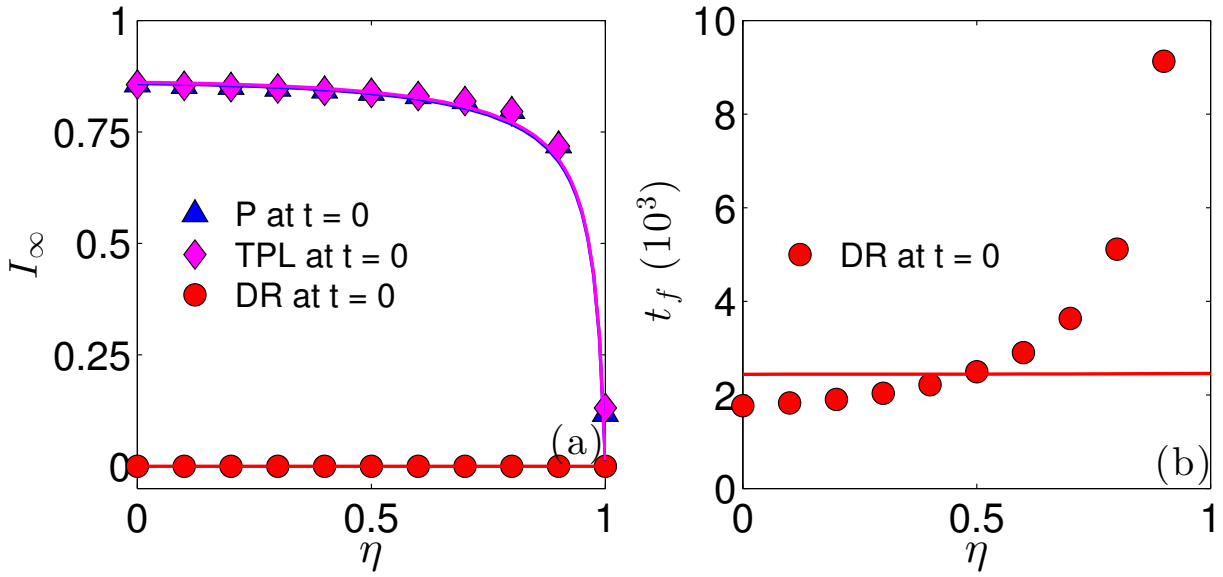

Figure 3.9: (a) Disease prevalence I versus η at time $t = 10,000$ on networks with the same mean degree $\langle k \rangle = 2$ but different initial degree distributions (p_k^P (Poisson): blue, p_k^{TPL} (truncated power law): magenta, and p_k^{DR} (degree regular): red). (b) t_f versus η on networks with the same mean degree $\langle k \rangle = 2$ initial degree regular degree distribution. Dots correspond to the mean computed over 30 simulations and the lines are the semi-analytical approximations.

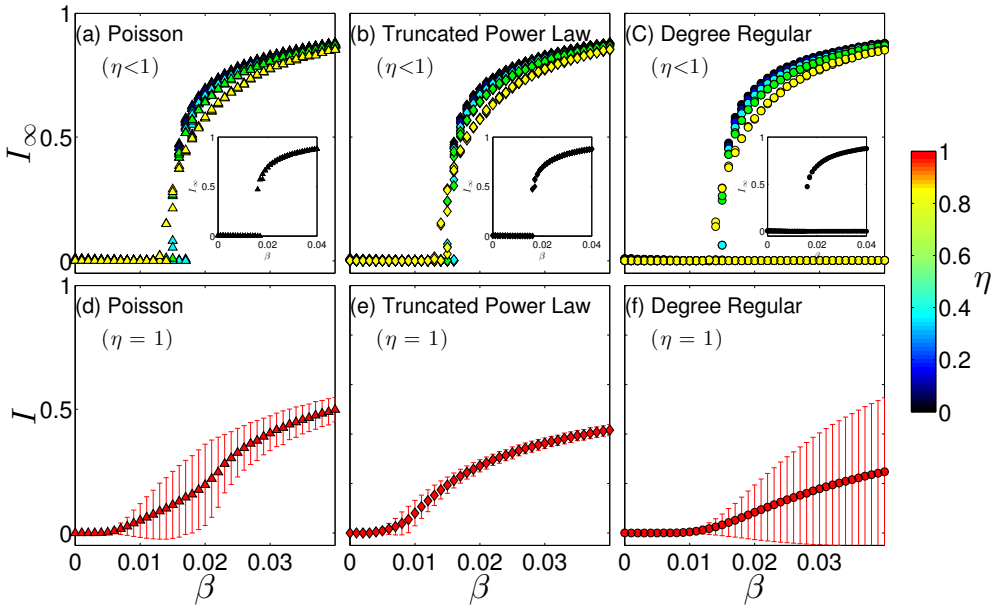

Figure 3.10: Bifurcation diagrams of the disease prevalence I versus η on networks with an initial (a) and (d): Poisson, (b) and (e): truncated power law, and (c) and (f): degree regular degree distribution. In (a), (b) and (c), we plot all the simulation results of 30 experiments. In (d), (e) and (f), dots and the error bar are the mean and standard deviation over 30 Monte Carlo simulations. The first row are the cases $\eta < 1$ and the second row are the cases $\eta = 1$. We vary the values of β and η. The other parameters of the system are $\gamma = 0.02$, and $\alpha = 0.005$. We run simulations for each value $\epsilon = 0.001, 0.01, 0.05, 0.99$, and, 0.999. We set $t = 10,000$, all networks with η not close to 1 reach their stationary states at this time.

Finally, using the same parameter set as before, we study the effect of η on bifurcation diagrams on the three initially different networks. Instead of fixing the initial infected fraction $\epsilon = 0.1$, we choose ϵ to be $0.001, 0.01, 0.2, 0.4, 0.6, 0.8, 0.99$, and, 0.999. We choose $t = 10,000$ and at this time, networks with η not close to 1 would reach their stationary states. In Figure 3.11, our semi-analytical approximation gives us the same disease prevalence curves in the three cases. But in the degree regular case, there is also a horizontal line $I = 0$ as in Figure 3.9 (a). In this case, if the initial infected fraction ϵ is not large enough, networks would stay disease free. And if ϵ is larger, networks would become endemic. On the other hand, in the truncated power law case, all networks with different ϵ would become endemic. The case in between is the Poisson case, when $\epsilon = 0.001$, about 5% of the networks would become disease free. The stochasticity of simulations plays a role here. In all networks with different initial topologies, when η is closed to 1, we could see the simulations spread more and this shows these networks are still in their transient states. If the networks are endemic in their stationary states, our approximation gives us a good prediction of the disease prevalence level I_∞. Moreover, in all these three cases, they share the same disease prevalence curve even though they have different stationary degree distributions as we showed in Figure 3.5. Our conjecture here is given a set of parameters, when the networks reach their stationary states, the disease prevalence level I_∞ would always fall on the same universal curve independent of the network topologies, and that is the endemic state of the network. On the contrary, networks could go to disease free if the initial infected fraction ϵ is not large enough. Like we showed in Figure 3.10, these are the two stable regions or fixed points of the dynamics.

3.5 Conclusion

In this chapter we have introduced a model that includes reinforcement of clustering during the rewiring process, hence providing a unique opportunity to study the role of clustering in altering the dynamics of epidemic spread. In this new model clustering is controlled by combination of rewiring parameter γ and parameter η. We also saw that the initial topologies of networks play important roles on network dynamics.

We explored the parameter space of the rewiring parameters γ and η, identified the regimes η affects network dynamics the most. By extending the AME method to its second and third layers

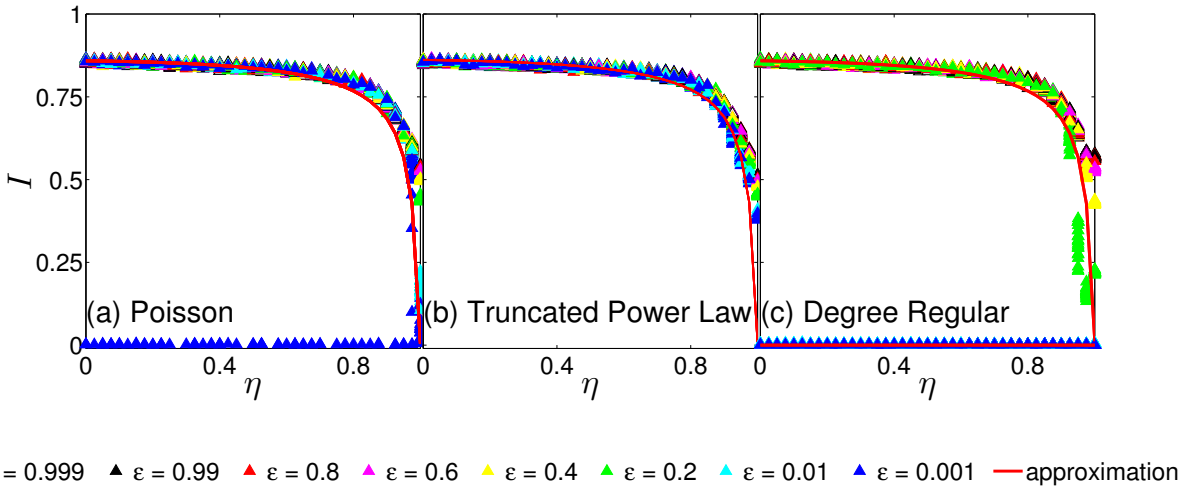

Figure 3.11: Bifurcation diagrams of the disease prevalence I versus η on networks with an initial (a) Poisson, (b) truncated power law, and (c) degree regular degree distribution. Lines are the predictions of our semi-analytical approach and dots are the outcome of 30 Monte Carlo simulations. We run simulations for each value $\epsilon = 0.001, 0.01, 0.2, 0.4, 0.6, 0.8, 0.99$, and, 0.999 and plot them with different colors. We set $t = 10,000$, all networks with η not close to 1 reach their stationary states at this time.

we were able to capture the dynamics on the networks when η is not very large. Our semi-analytical approximation gives a good prediction of the disease prevalence when networks reach their stationary states. In addition, this method also provides us a good estimation of network degree distribution as well.

We carried out a bifurcation analysis in order to understand the properties of the systems at equilibrium. We observed that introduction of the parameter η brought several quantitative changes to the dynamics. We found there are bistable regions correspond to endemic and disease free states of the systems. Moreover, there is a universal disease prevalence curve independent of network topologies and our semi-analytical approximation could capture the disease prevalence accurately when η is not close to 1.

A key assumption of our model is that the networks we investigate are locally tree-like. When η is large, this assumption will no longer be valid and our approximate master equation method was not able to provide a good estimation. We showed that there exists an apparent phase transition at $\eta = 1$. We also observed that for $\eta = 1$, the time evolution of the system is slower than compared to

any $\eta < 1$ case.

We provided a simple scheme that reinforces the clustering effect on coevolving networks. Our semi-analytical method takes the information of the status and degree of nodes, their neighbor nodes, and their distance 2 or 3 neighbors. Using similar semi-analytical method, people could study more complicated rewiring methods based on the degree of a node or arbitrary distance from a node.

CHAPTER 4

Evolutionary Games on Complex Networks

4.1 Background Information

Game theory is the study of strategic decision making and the analysis of mathematical models of conflict and cooperation between intelligent rational participants [49, 62, 108]. Game theory is mainly used in biology, economics, political science, computer science, psychology, and even military research. Classical game theory requires that all of the rational actors make their choices to optimize their individual payoffs, that is, they make their strategic choices on a wholly rationally determined evaluation of probable outcomes, or utility. Therefore, it is essential that in game theory each player must consider the strategic analysis that the players' opponents are making in determining their own strategic choice.

Evolutionary game theory [65, 69, 119, 136, 155] is the application of game theory to evolving populations of lifeforms in biology, and recently it has been expanded to various areas in social science. Evolutionary game theory is useful in this context by defining a framework of contests, strategies, behaviors, and analytics into which competition can be modeled. The key point in the evolutionary game theory model is that the success of a strategy is not just determined by how good the strategy is in itself, it is a question of how good the strategy is in the presence of other alternative strategies, and of the frequency that other strategies are employed within a population. How good the strategy is of course matters because in the biological world a successful strategy will eventually dominate a population and competing individuals in it end up facing identical strategies to their own.

One of the great difficulties of Darwinian theory, and one recognized by Darwin himself was the problem of altruism [106]. The exploited cooperators are worse off than defectors. Hence according to the basic principles of Darwinian selection, it would seem that the extinction of cooperation is almost certain to happen. If the basis for selection is at the individual level, altruism is a hard to

interpret phenomenon. But universal selection at the group level, or, for the "greater good", fails to pass the test of the assumption of individuals maximizing their own utility of game theory and is certainly not found to be the general case in nature. In many social animals altruistic behaviors can be found, and often altruism could be fundamental for species to survive [41].

The solution to this paradox can be demonstrated in the application of evolutionary game theory to the prisoner's dilemma game [7, 104], a game which tests the outcomes of cooperating or in defecting from cooperation. Cooperation is usually analyzed in game theory by means of a non-zero-sum game. The prisoner's dilemma game is a standard example of a game analyzed in game theory that shows why two completely rational individuals may not cooperate, even if it appears that it is in their best interests to do so. It is certainly the most studied game in all of game theory.

As with all games in evolutionary game theory the analysis of prisoner's dilemma is as an iterative game [100]. This repetitive nature affords competitors the possibility of retaliating or defecting based on the results of previous rounds of the game. There is a multitude of strategies which have been tested by the mathematics of evolutionary game theory and in computer simulations of contests [43] and the conclusion is that the best competitive strategies are general cooperation with a reserved retaliatory response if necessary. The most famous and perhaps one of the most successful of these strategies is Tit for Tat which carries out this approach by executing a simple algorithm [7, 117].

In recent years, investigations have taken place on different games played on random graphs and social networks [1, 37, 45, 46, 64, 68, 77, 83, 89, 118, 124, 129]. For example, individuals could play a prisoner's dilemma game on a graph with various strategies and the option to switch partners, hence, this game could be put into a framework of coevolving networks. On a coevolving or adaptive network with a game, the vertices represent players and the edges denote the pairwise partnership, or game interaction, between individuals.

The studies devoted to evolutionary games on complex networks are extensive. We can broadly say that one of the most important goals of such studies is to find what kind of mechanism of dynamics, different game rules, or various network topologies can provide cooperation among selfish and unrelated individuals.

The settings of spatial structure could enable cooperators to form small groups or clusters to protect themselves against exploitation by defectors [118]. Studies have shown that the spatial structure can promote cooperation [82], but there is also evidence that suggests the spatial structure

may not necessarily favor cooperation [64]. Many studies have elaborated on different aspects of cooperation on scale-free [54, 126], square lattice [123, 128], small world [84, 130, 141], social and real-world networks [44, 72, 94], and multilayer networks [149].

In addition to network reciprocity inherent to games on complex networks, other notable rules encouraging cooperative behavior are kin selection [61], group selection [33, 145], direct reciprocity [122], indirect reciprocity [120, 121], social diversity [131, 156], voluntary participation [27, 63, 66], and reputation [45]. All of these have been studied as interesting mechanisms that may promote cooperation in evolutionary games.

In this Chapter, we focus our study on how players play a prisoner's dilemma game with the ability to change their strategies and switch partners if they are exploited by their neighbors. We are interested in exploring the cooperative level among the individuals. By using the technique of approximate master equations, we will provide a better approximation of the evolution of the network structure and the individual status. We will compare the existing analytical methods and the new approximation we developed, and provide qualitative and quantitative estimations of various network properties. In Section 2, we introduce the model we investigate. We then describe the improved approximation method in Section 3. In Section 4 we provide the numerical results and comparison of the approximation methods. Lastly, in Section 5 and Section 6, we make concluding remarks.

4.2 Model Description

We study the partner switching model in [46], on a coevolving network with a game, the vertices represent players and the edges denote the pairwise partnership between individuals. We want to study how players play a prisoner's dilemma (PD) game with the ability to change strategies based on the links they have and switch partners. We start with an Erdős-Rényi network with N nodes and M edges. Each node has an equal probability to be a cooperator (C, denoted by two-dimensional unit vector $s = [1, 0]^T$) or defector (D, $s = [0, 1]^T$) on one end of each link and engages in pairwise interactions with his immediate neighbors defined by the partner network. That is, individual i

plays a PD game with all his social partners and obtains an income as

$$P_i = \sum_{j \in \mathcal{N}_i} s_i^T P s_j,$$

where $\mathcal{N}_i$ represents the neighborhood set of i and the 2-by-2 payoff matrix P is

$$\begin{array}{c} \\ C \\ D \end{array} \begin{array}{c} \begin{array}{cc} C & D \end{array} \\ \begin{pmatrix} 1 & 0 \\ 1+u & u \end{pmatrix} \end{array}$$

where a single-parameter cost-to-benefit ratio $u \in (0, 1)$ is used to rescale the relative benefits of outcomes in the payoff matrix. That is, if the player i plays C and the player j plays C, then both of them get the payoff of 1; if the player i plays C and the player j plays D, then the player i gets the payoff of 0 and the player j gets the payoff of $1 + u$, and so on.

In each time step, we first randomly pick an edge that connects a pair of players with different strategies, i.e., a CD link denoted by E_{ij} to update. Later on, we will extend the model to allow all individuals to switch their defective partners, that is, both CC and DD links can be rewired. With a given probability w, node i and node j connected by the edge E_{ij} update their strategies; otherwise, E_{ij} is rewired (with probability $1 - w$). When one node updates its strategy, the node has a probability ϕ given by the Fermi function to change its state, as first proposed by [140], and specified in detail below. When link E_{ij} is rewired, the player with end state C unilaterally gets rid of the partnership with its neighbor with end state D on the edge E_{ij}. Suppose node i has the end with state C, then it will randomly pick a player k from the remaining population as its new partner. Figure 4.1 shows an illustration of the rewiring process.

When a strategy updating event occurs, node i and j consider play in the PD game with all of their neighbors respectively, envisioning a total payoff P_i and P_j as calculated above. Then the strategy j replaces that of i on the edge E_{ij} with likelihood given by the Fermi function

$$\phi(s_i \leftarrow s_j) = \frac{1}{1 + \exp[\alpha(P_i - P_j)]},$$

where α represents the intensity of the selection [47, 144], or equivalently, its inverse $1/\alpha$ could also

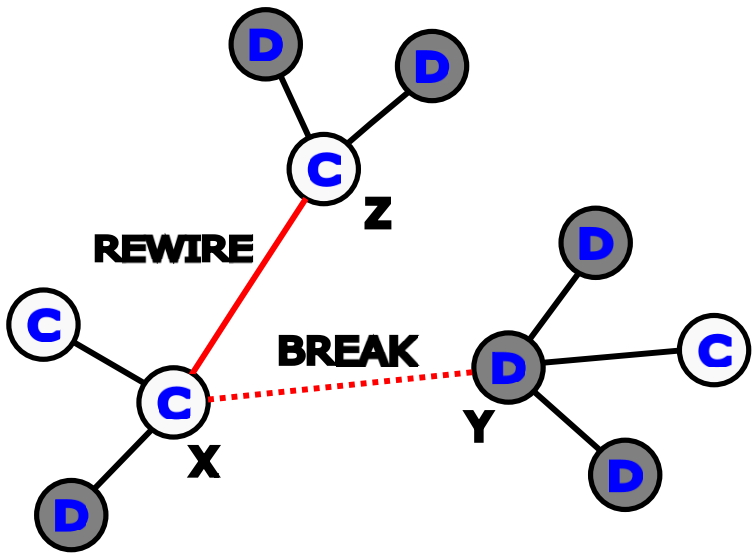

Figure 4.1: Illustration of the rewiring process. Pick a discordant edge XY. Suppose node X is of state C and node Y is of state D. Then with probability $1 - w$, the rewiring process happens. Node X would dismiss its defective neighbor Y and rewire to a random node Z in the network, regardless of the state of node Z.

represent the amplitude of noise [127, 148]. To be more specific, $\alpha \to 0$ leads to random drift while $\alpha \to \infty$ leads to deterministic imitation dynamics. Otherwise, the strategy of i replaces the strategy of j on the edge E_{ij} with likelihood $\phi(s_j \leftarrow s_i) = 1 - \phi(s_j \leftarrow s_i)$. Figure 4.2 shows an illustration of the rewiring process.

This partner switching evolution game model stops evolving when there are no discordant edges remaining in the network. In the stationary state of the system, there are no CD edges, only CC and DD edges exist. Hence, the final state creates a fission of these two (cooperative and defective) groups of individuals. In Figure 4.3, we provide a visualization of the model shortly before fission occurs.

4.3 Semi-analytical Methods

We study this generalized coevolving network model with a combination of simulations and approximate analytic models. The frameworks of Mean Field theory (MF), Pair Approximation (PA) and Approximate Master Equations (AME) have all been used effectively as analytical tools in similar settings. Among these approximations, AME can be used to achieve greater accuracy [53].

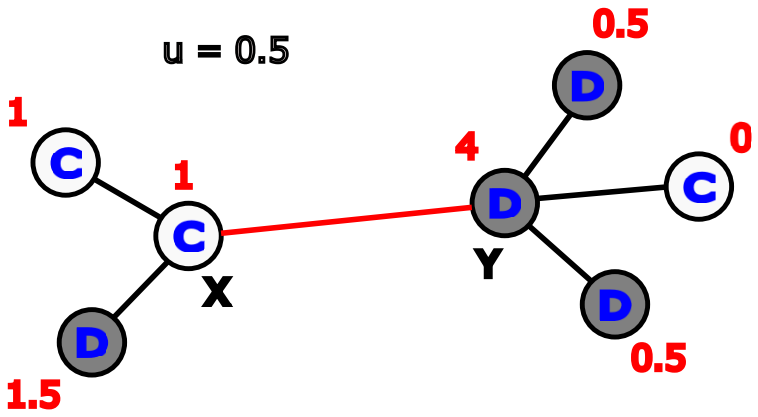

Figure 4.2: Illustration of the strategy updating process. Pick a discordant edge XY. Suppose node X is of state C and node Y is of state D. Then with probability w, the strategy updating process happens. Node X and Y would compare their utility and the node with lower utility would change its strategy with probability according to the Fermi functions. Suppose $u = 0.5$, then node X has 1 unit of utility and node Y has 4 units of utility. By the Fermi function, $\phi(s_X \leftarrow s_Y) = \frac{1}{1+\exp[\alpha(P_X - P_Y)]} = \frac{1}{1+\exp[30(1-4)]} \approx 1$, that is node X has a probability close to 1 to imitate node Y's state.

The PA estimation was obtained by [46], and here we provide the AME approximation.

The AME method is widely used in both static and coevolving networks. The difficulty of the derivation of AME in this model is that usually the transition probabilities of states are constant or depending on their neighbors' states. For example, in the SIS model, the recovery rate is often a constant μ while in the voter model, the probability for a node to change its state could rely on its neighbors' majority opinion. In the partner switching evolutionary game model, for a node to change its state, at each time we need to compute its utility and compare with its neighbors' utility, plug it in the Fermi function, and obtain the transition probability. AME only contains the information of the state of nodes, their degree and the state of their neighbors. Hence, we need some clever way to estimate the utility of every node in the network and be able to compare them. We will explain how we approximate these equations after we introduce the equations.

Let $C_{kl}(t)$ and $D_{kl}(t)$ be the fraction of cooperative and defective nodes of total degree k which have l defecting neighbors at time t. We also define the zeroth order moments of the $C_{kl}(t)$ and $D_{kl}(t)$ distribution by $N_C \equiv \sum_{kl} C_{kl}$ and $N_D \equiv \sum_{kl} D_{kl}$; the first order moments by $N_{CC} \equiv \sum_{kl}(k-l)C_{kl}$, $N_{CD} \equiv \sum_{kl} lC_{kl} + (k-l)D_{kl}$ and $N_{DD} \equiv \sum_{kl} lD_{kl}$; and the second order moments by $N_{CCD} \equiv \sum_{kl}(k-l)lC_{kl}$, $N_{CDD} \equiv \sum_{kl} l(l-1)D_{kl}$, etc.

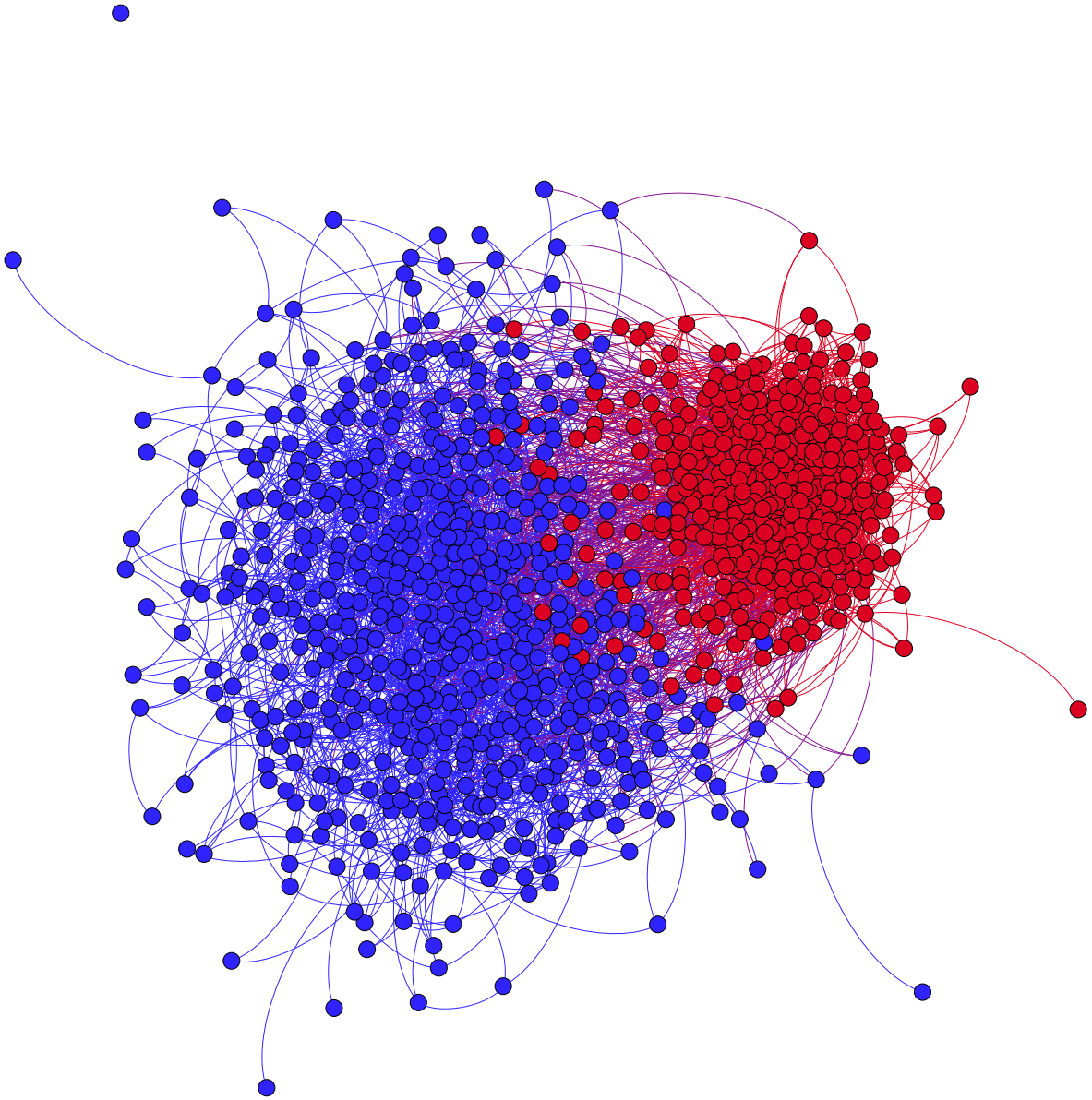

Figure 4.3: Visualization of the partner switching model soon before fission occurs, for $N = 1,000$ nodes, $M = 5,000$ edges, cost-to-benefit ratio $u = 0.5$, strategy updating probability $w = 0.1$, and initial fraction of defectors $\rho = 0.5$. Colors correspond to the two states of node; blue: cooperative and red: defective.

It is worth noting that while the network states and topologies coevolve, there are different quantities that must remain conserved by the system. For example, since the networks are not gaining or losing nodes, we have conservation of nodes $N_C + N_D = 1$. Similarly we always have conservation of edges $N_{CC} + N_{CD} + N_{DD} = \langle k \rangle$.

The following pair approximation method was derived by Fu *et al.* [46],

$$\begin{aligned}
\frac{dN_C}{dt} &= w \cdot N_{CD} \cdot \tanh\left[\frac{\beta}{2}(\overline{\pi}_C - \overline{\pi}_D)\right] \\
\frac{dN_{CC}}{dt} &= w \cdot \left(N_{CD}\phi_{C\to D} - 2N_{CD}\frac{N_{CC}}{N_C}\phi_{D\to C} + N_{CD}\frac{N_{CD}}{N_D}\phi_{C\to D}\right) \\
&\quad + (1-w)\cdot\frac{N_C}{N}N_{CD} \\
\frac{dN_{DD}}{dt} &= w \cdot \left(N_{CD}\phi_{D\to C} - 2N_{CD}\frac{N_{DD}}{N_D}\phi_{C\to D} + N_{CD}\frac{N_{CD}}{N_C}\phi_{D\to C}\right)
\end{aligned} \tag{4.1}$$

Again, let $C_{k,l}(t)$ and $D_{k,l}(t)$ be the fraction of cooperative and defective sites of total degree k which have l defective neighbors. We have the following ODE governing the time evolution of the $C_{k,l}$ compartment:

$$\begin{aligned}
\frac{dC_{k,l}}{dt} &= w\Big\{\phi^D_{k,l}(k-l)D_{k,l} - \phi^C_{k,l}lC_{k,l} \\
&\quad + \phi^C_{k,l+1}\gamma^C(l+1)C_{k,l+1} - \phi^C_{k,l}\gamma^C lC_{k,l} \\
&\quad + \phi^C_{k,l-1}\beta^C(k-l+1)C_{k,l-1} - \phi^C_{k,l}\beta^C(k-l)C_{k,l}\Big\} \\
&\quad + (1-w)\Big\{\frac{N_C}{N}\big[(l+1)C_{k,l+1} - lC_{k,l}\big] \\
&\quad + \frac{N_{CD}}{N}\big[C_{k-1,l} - C_{k,l}\big]\Big\}
\end{aligned} \tag{4.2}$$

Similarly the ODE governing the time evolution of the $D_{k,l}$ compartment is:

$$\begin{aligned}\frac{dD_{k,l}}{dt} = w\Big\{ & -\phi^D_{k,l}(k-l)D_{k,l} + \phi^C_{k,l} l C_{k,l} \\ & + \phi^D_{k,l+1}\gamma^D(l+1)D_{k,l+1} - \phi^D_{k,l}\gamma^D l D_{k,l} \\ & + \phi^D_{k,l-1}\gamma^D(k-l+1)D_{k,l-1} - \phi^D_{k,l}\gamma^D(k-l)D_{k,l}\Big\} \\ & + (1-w)\Big\{\big[(k-l+1)D_{k+1,l} - (k-l)D_{k,l}\big] \\ & + \frac{N_{CD}}{N}\big[D_{k-1,l} - D_{k,l}\big]\Big\}\end{aligned} \tag{4.3}$$

To see how the AMEs are derived, we will focus on explaining the $C_{k,l}$ compartment, as the derivation of the $D_{k,l}$ compartment is similar. The first three lines of equation (4.2) with w are the effect of strategy updating and the last two lines with $1-w$ are the effect of rewiring. To write the AMEs, we need to keep track of all the quantities flowing in and out each time to our center class, $C_{k,l}$. Refering to Figure 4.4, there are six flows related to the $C_{k,l}$ compartment, and these are the first six terms in the $C_{k,l}$ equation. As we mentioned before, at each time step, one needs to know the utility of the center and compare it with their neighbors' utility. The first term is for a $D_{k,l}$ class, the center node with state D compares its utility with one of its C neighbors, changes its states to C, and thus $D_{k,l}$ becomes $C_{k,l}$, which is a positive change for the class $C_{k,l}$. And the second term is for a $C_{k,l}$ class, where the center node with state C compare its utility with one of its D neighbors, changes its states to D, and thus $C_{k,l}$ becomes $D_{k,l}$, which is a negative change for the class $C_{k,l}$.

Here we need to use the Fermi function ϕ to find all the transition probabilities. Recall that the payoff matrix of a game is

$$\begin{array}{c} \\ C \\ D \end{array} \begin{array}{c} \begin{array}{cc} C & D \end{array} \\ \begin{pmatrix} 1 & 0 \\ 1+u & u \end{pmatrix} \end{array}$$

where $u \in (0,1)$. For a $D_{k,l}$ class, the center node is of state D, it has k neighbors and l of them are of state D. Hence we can compute the center's utility as

$$P_D = l \cdot u + (k-l) \cdot (1+u).$$

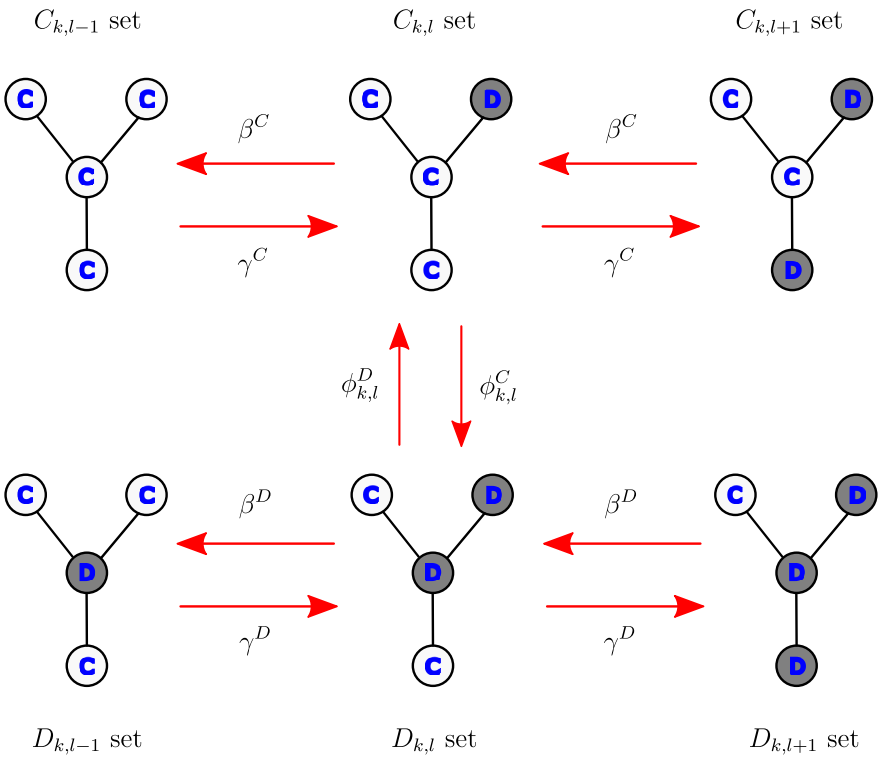

Figure 4.4: Illustration of transitions to/from the $C_{k,l}$ and $D_{k,l}$ sets in the AME. For each set, only parts of its neighbors are shown here, and the classes of sets are shown next to the corresponding compartments.

But, we do not have information about the neighbors of the center node's C neighbors. We can only approximate their utility by averaging the total payoff across all C nodes. Therefore here we have

$$P_C = 1 \cdot \frac{2N_{CC}}{N_C} + 0 \cdot \frac{N_{CD}}{N_C}.$$

Then we compare the center node D's utility with one of its C neighbor's utility by using the Fermi function, and we denote this as:

$$\phi^D_{k,l}(D \leftarrow C) = \frac{1}{1 + \exp[\alpha(P_D - P_C)]}.$$

Likewise, for a $C_{k,l}$ class, the center node is of state C, it has k neighbors and l of them are of state D. We can compute the center's utility as

$$P_C = l \cdot 0 + (k - l) \cdot 1.$$

Then we estimate their D neighbors' utility by

$$P_D = (1 + u) \cdot \frac{N_{CD}}{N_D} + u \cdot \frac{2N_{DD}}{N_D}.$$

Lastly, we denote this transition probability as

$$\phi^C_{k,l}(C \leftarrow D) = \frac{1}{1 + \exp[\alpha(P_C - P_D)]}.$$

The third term to the sixth term in the $C_{k,l}$ equation are the effects of one of the neighbors changing its state and leading to a change of the total quantity of $C_{k,l}$. We use β to denote rates of C changing to D, γ for rates of D changing to C, and superscripts to represent the state of the center node. If the center is a C node and one of its neighbors changes its state from C to D, then we denote this probability by β^C. In similar fashion, if the center is a D node and one of its neighbors changes its state from D to C, then we denote this probability by γ^D. To compute β^C, we count the number of CC edges in the network at each time, and then compute the number of edges which switch from being CC to CD in the next time step. Here β^C provides the expected number of D

neighbors of a CC edge, that is, we define β^C as

$$\beta^C = \frac{\sum_{k,l}(k-l)lC_{k,l}}{\sum_{k,l}(k-l)C_{k,l}}.$$

Similarly we have

$$\beta^D = \frac{\sum_{k,l} l^2 C_{k,l}}{\sum_{k,l} lC_{k,l}},$$

$$\gamma^C = \frac{\sum_{k,l}(k-l)^2 D_{k,l}}{\sum_{k,l}(k-l)D_{k,l}},$$

and

$$\gamma^D = \frac{\sum_{k,l} l^2 D_{k,l}}{\sum_{k,l} lD_{k,l}}.$$

Following the six flows related to the $C_{k,l}$ compartment, we obtain the first three lines of equation (4.2), describing the strategy updating effect in the $C_{k,l}$ class.

The last two lines in the $C_{k,l}$ equations are the rewiring effect. The class $C_{k,l+1}$ would contribute to the $C_{k,l}$ if the center node C drops one of its defected neighbors and rewires randomly to a C in the network. Similarly, the class $C_{k,l}$ would decrease if for a $C_{k,l}$ node, the center node C drops one of its defected neighbors and rewires randomly to a C in the network. Lastly, a $C_{k-1,l}$ would contribute to $C_{k,l}$ if the center receives a C node during rewiring and the class $C_{k,l}$ would decrease if a $C_{k,l}$ center receives a C node during rewiring. The fourth line of equation (4.2) is an expression corresponding to the center node actively rewiring to some other node in the network while the fifth line describes the center node passively rewiring by the action of some other node in the network. Figure 4.5 and Figure 4.6 illustrate this active and passive rewiring.

By following a similar fashion, we can obtain the equation of the $D_{k,l}$ compartment as well.

The differential equation system above contains $2(k_{\max}+1)^2$ coupled differential equations, where $k_{\max}$ is the maximum degree a node can have in the network. Usually, $k_{\max}$ depends on network structure and the mean degree. Here we choose $k_{\max} = 50$. We use these differential equations to estimate the evolution of networks and solve their solutions numerically, arriving at a semi-analytical approximation of the network evolution. To solve these thousands of ODEs, we use the ode45 solver in MATLAB until the solutions converge to a steady state.

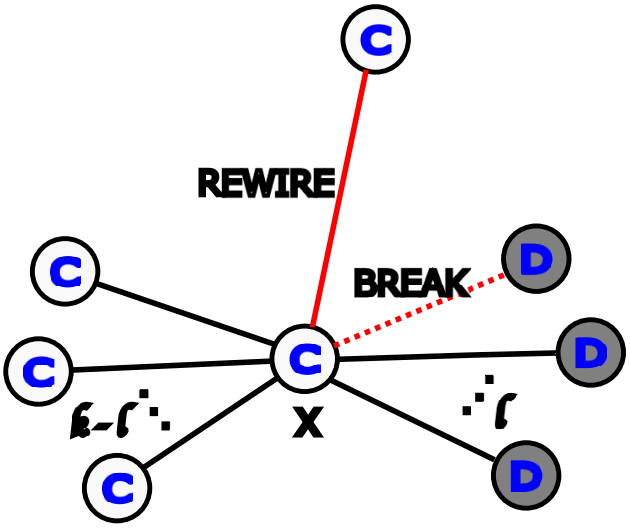

Figure 4.5: Illustration of active rewiring. Before the rewiring, node X is of class $C_{k,l}$. Suppose one of X's discordant edge is picked, and X actively dismisses its defective neighbor, rewiring to a random node in the network. If node X rewires to a node of state C, then node X becomes of class $C_{k+1,l}$. We recall that only C's actively rewire in the present model.

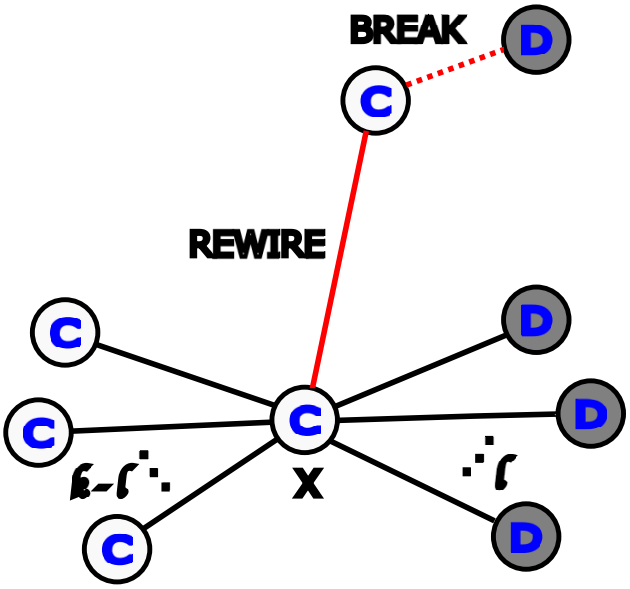

Figure 4.6: Illustration of passive rewiring. Before the rewiring, node X is of class $C_{k,l}$. Suppose in the rewiring process, node X is passively rewired by a random node in the network. Then node X becomes of class $C_{k+1,l}$. We recall that only C's actively rewire in the present model.

4.4 Numerical Experimentation

We simulate networks with $N = 1,000$ nodes and $M = 5,000$ edges, and hence the mean degree of the network is fixed to be $\langle k \rangle = 10$. We set the imitation parameter β in the Fermi function equal to 30. We also introduce a parameter ρ to denote the initial fraction of defectors. First, we set $\rho = 0.5$, and we will explore the effect of this parameter later. Initially, we start the networks to be an Erdős-Rényi $G(N, M)$ random graph model, that is, a network is chosen uniformly at random from the collection of all graphs which have N nodes and M edges. Hence with large N, we could approximate the initial degree distribution of the networks by a Poisson distribution,

$$p_k = \frac{\langle k \rangle^k e^{-\langle k \rangle}}{k!}.$$

We perform Monte Carlo simulations of the evolution of the networks. In each time step, we choose 100 edges and update them (as will be further explained below). In the case when only discordant edges (i.e., CD edges) are updated, the dynamics will stop when there are no discordant edges remaining or when the simulation reaches our selected stopping time $t = 1,000$. Unless stated otherwise, we do the Monte Carlo simulations 1,000 times for each experiment.

4.4.1 Exploration of the Parameter Space

In the stationary states of the network, either the dynamics would stop because of lacking discordant edges or the change of quantities in each state is balanced. In our setting of dynamics and parameter sets, every scenario we simulated reaches its stationary state before our stopping time $t = 1,000$. To see the effect of u and w, first, we investigate the final fraction of cooperators in the stationary states. For both u and w, we start from 0 and increase the step by 0.05 to 1, and we want to explore the cooperative levels in the stationary states. In Figure 4.7, we have the heat map of this result. When u is small, there is a high level of cooperators in the stationary states. And when w is close to 0, there is a medium level of cooperators in the stationary states. Other than small u or w, the networks would be full of defectors in the stationary states, which we will explore and explain this phenomenon with our semi-analytical approximation together in Figure 4.8 and Figure 4.9.

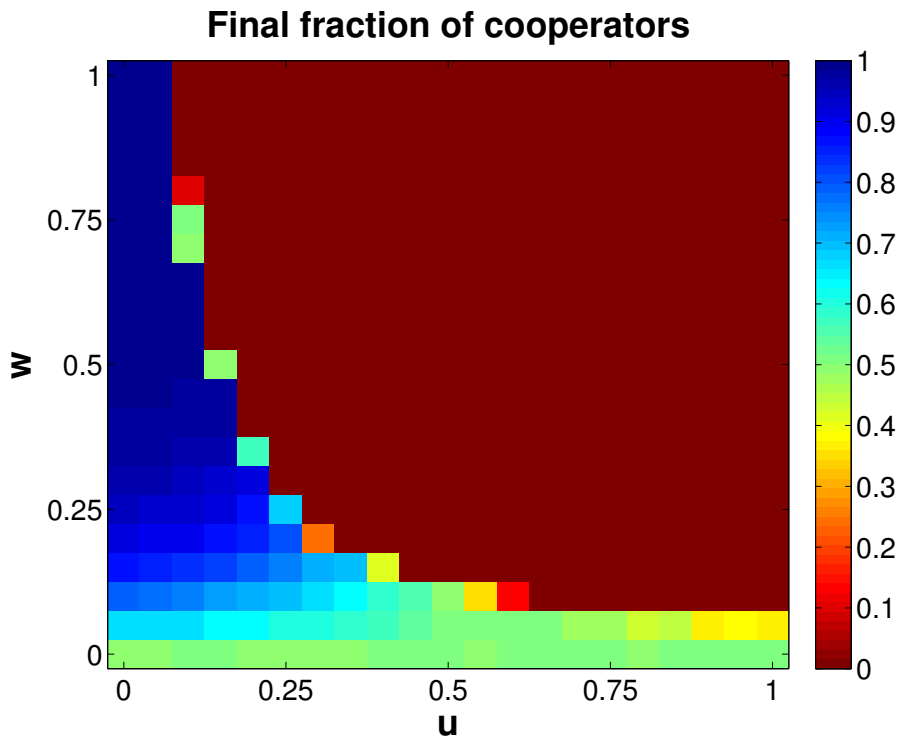

Figure 4.7: Simulation results of the final fraction of cooperators with different combinations of u and w. For both u and w axes, we pick the step to be 0.05 and plot the fraction of cooperators in the stationary states in simulations. We take the mean of 50 simulations of each parameter set here.

4.4.2 Final Level of Cooperation

Now we want to compare the simulation results and the two semi-analytical approximations. In Figure 4.8, we consider $w = 0$, $w = 0.05$, $w = 0.1$, and $w = 0.5$, plotting the fraction of nodes in state C in the stationary state of the networks against the cost-to-benefit ratio, u. There are three sets of outcomes here: markers are the simulation results, dotted lines are the PA approximation, and the dashed lines are the AME approximation. Although this figure only shows us the final fraction of C's, one also knows the final fraction of D's simply because the sum of C and D ratios should always be 1.

In the case $w = 0$, since there are no strategy updates happening in the networks, nodes couldn't change their states during the evolution. Hence, the final fraction of C and D will remain constant. Since first we set $\rho = 0.5$, regardless of u we should get 50% of C and 50% of D in the stationary states. In Figure 4.8, simulations, PA, and AME give us the same results, final ratio of C stays constant of 0.5 with regard to u. Therefore, both the PA and AME approximations are satisfying.

When $w > 0$, the strategy updating starts playing a role. The greater the cost-to-benefit u is, the stronger the incentive for nodes to defect. Hence, the final fraction of cooperators decreases as u increases. In the cases $w = 0.1$ and $w = 0.5$, simulation results decrease slowly at first and suddenly drop to zero around $u = 0.2$ and $u = 0.6$, respectively. This phenomenon is captured by AME approximation not only by the qualitative behavior but also the critical dropping value of u. On the other hand, although PA gives good qualitative estimation of the behavior, PA lines both drop earlier and fail to provide a good prediction of critical points. Hence, comparing to PA, AME offers better predictions of the simulation. Lastly, in the case $w = 0.05$, the simulation results gradually decrease when u increases. The gaps between simulation results and PA and AME gradually increase. The PA curve drops to zero around $u = 0.85$, however, the AME curve does not have this qualitative change. Therefore, throughout all the scenarios listed in this figure, AME always provides fitting qualitative approximations of the simulation results, and it gives accurate predictions at the critical points.

Similarly, we plot the final fraction in the stationary state of cooperators C versus w with different cost-to-benefit ratios, u in Figure 4.9. Here we consider four cases: $u = 0$, $u = 0.01$, $u = 0.2$, and $u = 0.8$. All of them start from $\rho = 0.5$ when $w = 0$, because when $w = 0$ there is no strategy

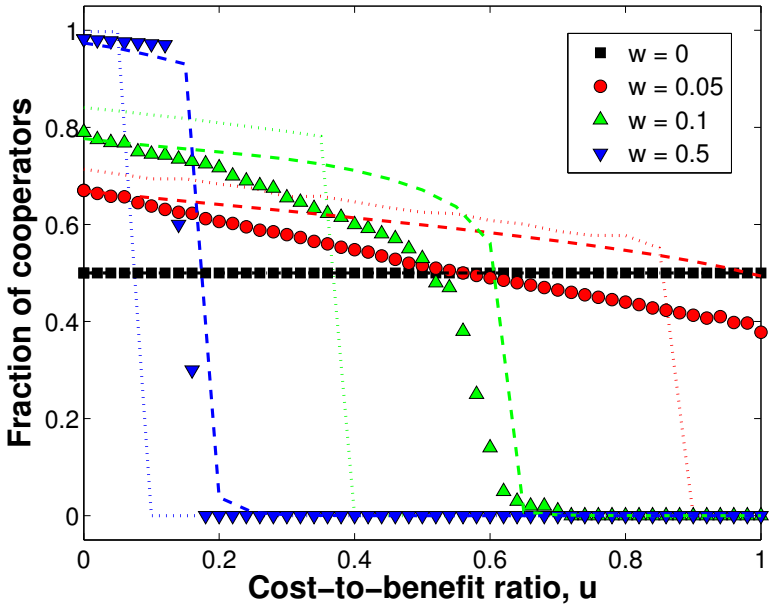

Figure 4.8: Fraction of cooperators versus cost-to-benefit ratio u with different strategy updating rates w in stationary states. Markers are the averages of 1,000 simulations results, dotted lines are the semi-analytical results of pair approximation (PA), and the dashed lines are the semi-analytical results of approximate master equations (AMEs). The PA results are different from the ones shown in [46], but we have confirmed the accuracy of our results in personal communication with the authors of that paper.

updating in the dynamics. Hence, all of the nodes only rewire but do not change their states. The final fraction of C's remains 50% in the networks. As w increases, the effect of strategy updating in the dynamics becomes stronger. In the cases $u = 0$ and $u = 0.01$, u is so small that there is almost no incentive to defect, so in the strategy updating process C's and D's are almost indistinguishable. However, because of the effect of rewiring, C would drop its defective neighbor D, reducing the number of partners for D. Comparing with C nodes, D nodes would not have as many neighbors and hence would have less payoff. This effect makes more D's change to C's and leads to the dominance of C's when u is small. In the cases $u = 0$ and $u = 0.01$, both PA and AME provide accurate results and behave well qualitatively.

When $u = 0.8$, as w increases, C nodes become more disadvantaged since the payoff of defecting is high. The final fraction of cooperators decreases to zero around $w = 0.1$, and both PA and AME capture this critical value of w well. Although both approximations have humps when w is small, they still give satisfying predictions and AME does not do worse than PA.

Finally, in the case $u = 0.2$, the incentive of defecting is not too large. The final fraction of cooperators would increase at first due to the rewiring effect, that is, C nodes gain more neighbors and have higher payoffs when comparing the payoffs with D nodes. But when w gets greater, the effect of rewiring diminishes, C nodes would not have more neighbors rewiring to them and start losing payoff to their D neighbors. This effect makes more C's become D's and the networks will be dominated by defectors. Both of the semi-analytical approaches capture this qualitative change of the dynamics. The fraction of final cooperators curve drop around $w = 0.35$, $w = 0.2$, and $w = 0.4$ for simulation, PA, and AME, respectively. Though not perfect, AME in this case still yields more accurate prediction than PA. Hence, generally speaking, we can see that AME improves the results PA could acquire in this figure.

4.4.3 Network Dynamics

Having explored the populations in the stationary states, now we explore how the networks evolve. We are aware that there are two things happening to the networks: the states of the nodes change and the structure of the networks also change. To see how the networks change with time, we investigate the evolution of five fundamental quantities of the networks: the fractions of nodes/edges

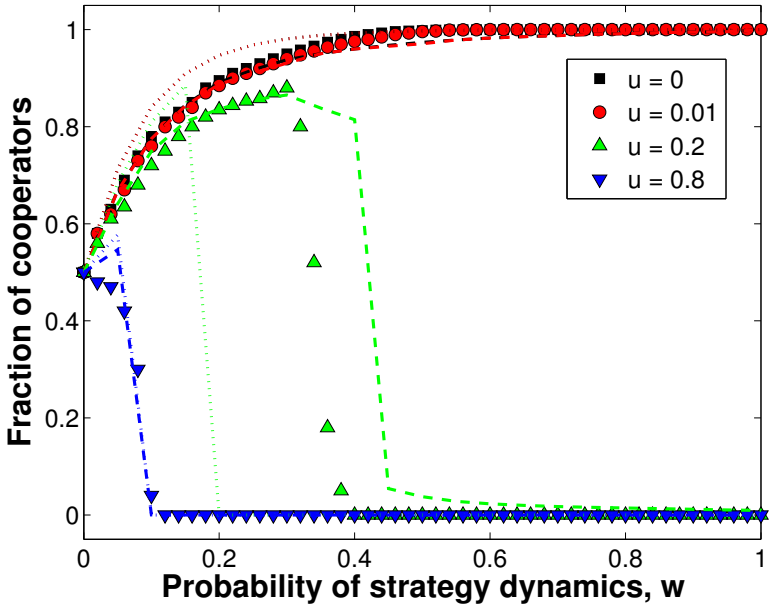

Figure 4.9: Fraction of cooperators versus w with different cost-to-benefit ratio u values in stationary states. Markers are the averages of 1,000 simulations results, dotted lines are the semi-analytical results of pair approximation (PA), and the dashed lines are the semi-analytical results of approximate master equations (AMEs).

in states C, D, CC, CD, and DD. We compare the simulation results with the two semi-analytical approximations we have. We choose a set of parameters $u = 0.5$ and $w = 0.1$, for which neither of the approaches perform very well here. Since the time scale of PA and AME are fixed to the equations, in order to keep our simulation results and semi-analytical results on the same time scale, we carry out 100 updates at each unit time in the simulations. In this fashion, the three results will enjoy the same time scale as we show in Figure 4.10. To perform the experiment, we do the 50 simulations and take the averages of them at each time step. In this figure, since the initial fraction of defectors ρ is set to be 0.5, and we follow the Erdős-Rényi $G(N, M)$ random graph model, both C and D are 0.5, CC and DD are 0.25, and CD is 0.5. These are also the initial conditions of PA and parts of the initial conditions of AME. One thing worth noting is that the total number of nodes and edges are constant during the evolution, requiring both $C + D$ and $CC + CD + DD$ to be equal to 1. The networks evolve with time until there are no discordant edges, i.e. when CD (the black markers) equals 0. At a time slightly before $t = 100$, the networks stop evolving and all five quantities keep constant after this stopping time. The PA method, in this case, stops evolving before $t = 10$, and it gives the prediction that the networks are occupied by defectors and their links, which is totally at odds with the simulations. On the other hand, the AME method stops evolving around $t = 160$, when the black line goes to zero and the other four lines stay constant. Although the final prediction of these five quantities is still off, the result is still better than PA. Not only does AME gives the correct order of these quantities, but during the evolution, AME provides qualitatively correct trajectories of how these quantities change with time. For example, the quantity of D first goes up and then goes down below the quantity of C. AME captures this phenomenon. There is a hump at the beginning of the red line and it goes down gradually below the blue line. The other AME curves have similar qualitatively correct trajectories. Hence compared to PA, even if AME does not give us an accurate prediction in this specific parameter set, this still works much better than PA.

In Figure 4.11, we compare the simulation results with AME approximation. Since we know AME does no worse than PA in all of our observed cases, we only compare AME and simulation results. We choose four different parameter sets here: $u = 0.2, w = 0.1$; $u = 0.2, w = 0.3$; $u = 0.5, w = 0.1$; and $u = 0.5, w = 0.3$. In each case, AME provides the correct order of C (blue), D (red), CC (green), CD (magenta), and DD (black) ratios in the stationary states. In cases like $u = 0.2, w = 0.1$;

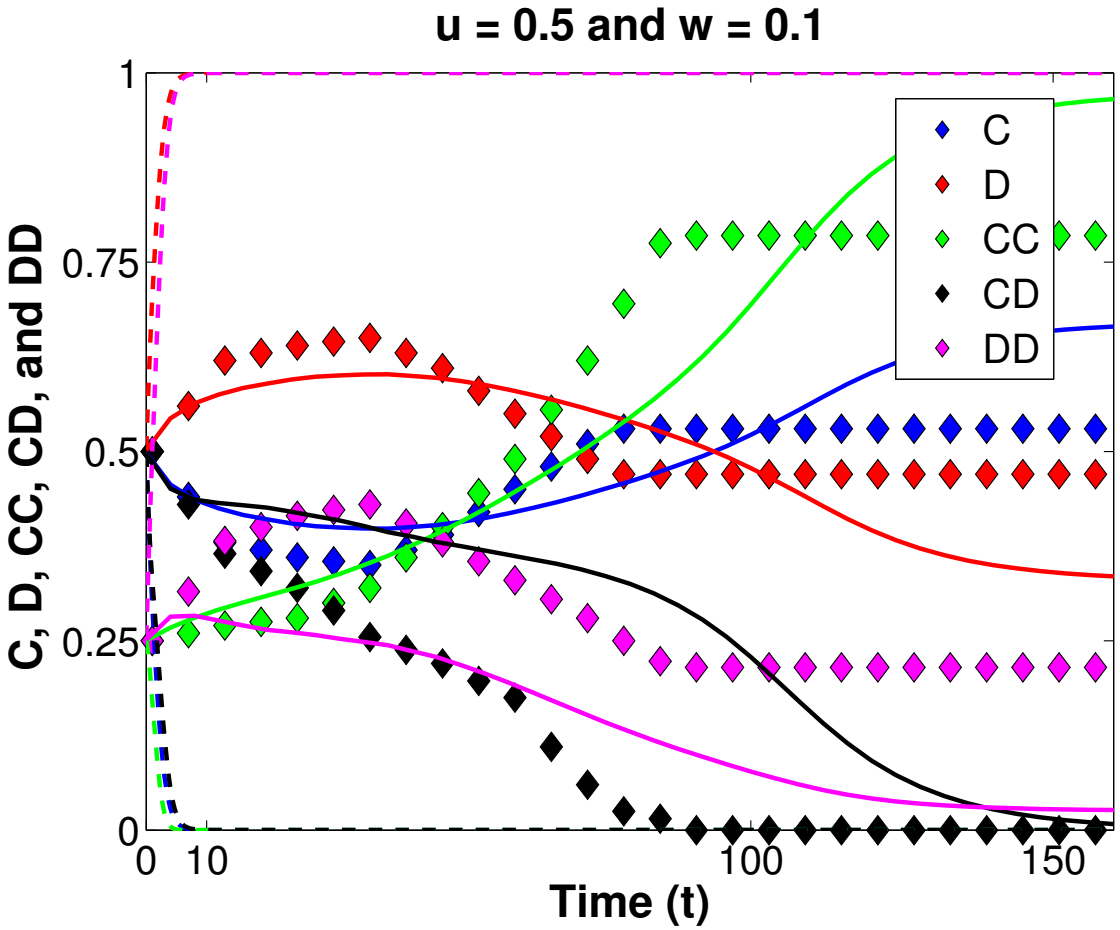

Figure 4.10: Evolution of five fundamental quantities versus time t when $u = 0.5$ and $w = 0.1$. We plot C (blue), D (red), CC (green), CD (magenta), and DD (black) ratios and compare these with two semi-analytical approximations. Markers are the averages of 50 simulations results, dotted lines are the semi-analytical results of pair approximation (PA), and the dashed lines are the semi-analytical results of approximate master equations (AMEs). PA dynamics stop around $t = 10$, and it gives bad estimations. On the other hand, AME provides better estimations of the simulation results.

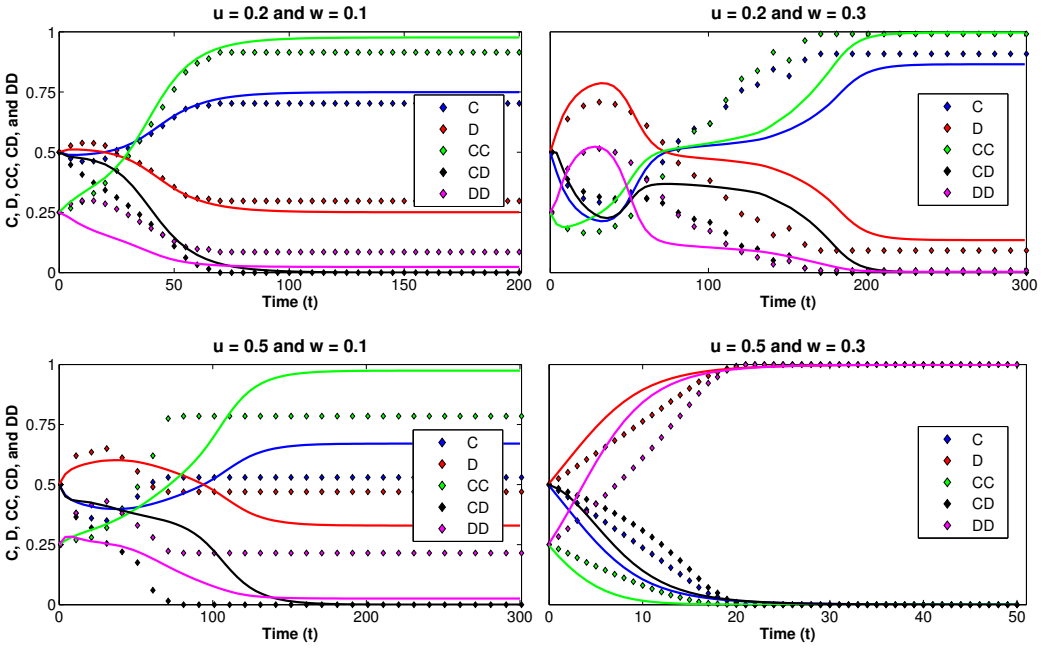

Figure 4.11: Evolution of five fundamental quantities versus time t in different parameter sets, upper left: $u = 0.2$, $w = 0.1$, upper right: $u = 0.2$, $w = 0.3$, lower left: $u = 0.5$, $w = 0.1$, and lower right: $u = 0.5$, $w = 0.3$. We plot C (blue), D (red), CC (green), CD (magenta), DD (black) ratios and compare these with our semi-analytical approximations. Markers are the averages of 50 simulations results and the lines are the semi-analytical results of approximate master equations (AMEs). AME provides qualitatively good estimations of the simulation results.

$u = 0.2, w = 0.3$; and $u = 0.5, w = 0.3$, AME method gives fairly accurate prediction of the final levels of these quantities. Moreover, throughout the evolution, AME generates similar qualitatively correct curves as the simulation results. Hence not only do we have a better idea of the final level of these important quantities, we can also get qualitatively good evolution trajectories by plotting the AME trajectories while solving these equations.

4.4.4 Degree Distribution

As we discussed before, the AME method takes in more information and has higher computational cost, but it can generally provide better approximation than PA. There are also things that AME could predict but PA could not, such as degree distributions. Since AME needs the information of the states of nodes, the states of nodes' neighbors, and the degree of nodes, this method can also give us this information during the network evolution. Therefore by examining the variables of in

the AME method, we can have knowledge of the degree distributions of the networks at any given time. We simply cannot get the same information from PA. Here in Figure 4.12, we plot the degree distribution of C and D nodes separately in the stationary states and compare the simulation results and AME approximation. In each case, since we initialize with random strategies on the Erdős-Rényi $G(N, M)$ random graph model, the initial degree distributions are approximately Poisson when the network size N is large enough. To see the degree distributions in the stationary states, we choose the same parameter sets as in the previous figure: $u = 0.2, w = 0.1$; $u = 0.2, w = 0.3$; $u = 0.5, w = 0.1$; and $u = 0.5, w = 0.3$. In the case $u = 0.5, w = 0.3$, the AME method yields very accurate prediction of C, D, CC, CD, and DD levels as we showed before. Not surprisingly, AME also gives us a superb prediction of the final degree distribution. In the stationary state of this case, D nodes dominate the whole network, and there is no C node left. The AME method successfully provides us the degree distribution of C and D nodes respectively. In the other three cases, although the AME predictions are not that accurate, we can still see it gives us a hint of how the degree distribution behaves. Hence, we know generally speaking, if the AME gives us good predictions of the dynamics, it will also give us a nice prediction of its degree distribution. And this is a result PA method can not provide.

4.4.5 Exploration of the Initial Fraction of Defectors, ρ

Finally, we explore the effect of the initial fraction of defectors parameter ρ in Figure 4.13 and Figure 4.14. In these two figures, we fix the parameter to be $w = 0.1$ in Figure 4.13 and $u = 0.2$ in Figure 4.14, and we change the other parameter u, and w, respectively, to see the final fraction of cooperators against ρ in stationary states. And we compare the simulation results (markers) with our AME approximation (lines). It is worth noting that in both figures, all the trajectories generated by simulation and approximation results would pass through the upper left and the lower right corners. This is because when $\rho = 0$, there are no D nodes in the networks, there is no discordant edge, and the networks would not evolve. The final fraction of cooperators remains 100%. The final fraction of cooperators is 0% for the similar reason in the case $\rho = 1$. In Figure 4.13, for all u curves, the final fraction of cooperators would first gradually decrease and drop to zero suddenly at different values of ρ, and AME method captures this qualitative behavior in different levels of u. Moreover,

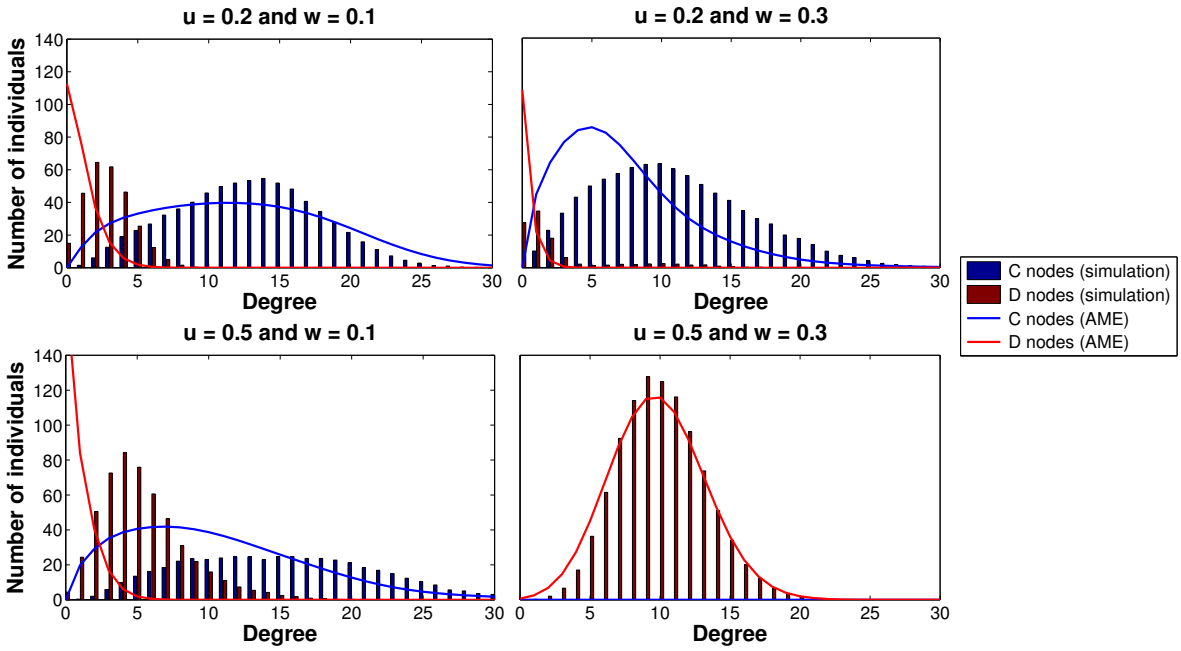

Figure 4.12: Degree distribution in the stationary states in different parameter sets, upper left: $u = 0.2$, $w = 0.1$, upper right: $u = 0.2$, $w = 0.3$, lower left: $u = 0.5$, $w = 0.1$, and lower right: $u = 0.5$, $w = 0.3$. Bars are the averages of 50 simulations results and the lines are the semi-analytical results of approximate master equations (AMEs). AME provides qualitatively good estimations of the simulation results. Blue bars and lines are degrees of cooperative nodes, and red bars and lines are degrees of defective nodes.

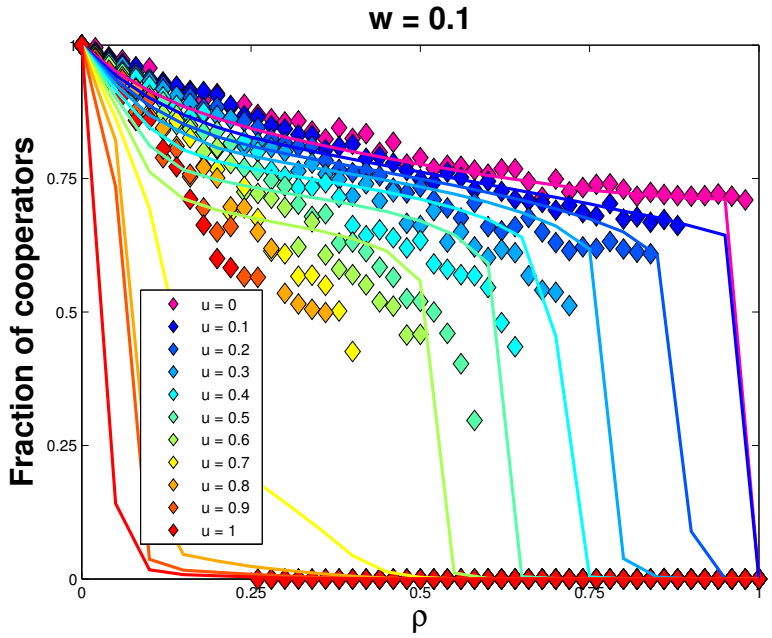

Figure 4.13: Fraction of cooperators versus ρ with $w = 0.1$ in stationary states. Different cost-to-benefit ratio u: 0, 0.1, ..., 1 are chosen. Markers are the averages of 50 simulations results and the dashed lines are the semi-analytical results of approximate master equations (AMEs).

fixing $w = 0.1$, smaller u would result in higher cooperative level, since the incentive of defecting is less when u is small. We also find out that AME is more accurate when u is small in this figure. In Figure 4.14, fixing $u = 0.2$, the diagonal line is the case $w = 0$, there are no strategy updates happening, hence the cooperative level remains the same during the evolution. The w curves drop to zero more quickly when ρ increases, that means the strategy updating effect is more sensitive to the initial fraction of defectors ρ. When w is large, the networks count more on the strategy updating dynamics, and the stationary cooperative level would drop to zero more quickly. As we show in this figure, the AME curves suddenly drop to zero when $w \geqslant 0.4$. Although not very accurate, AME method still gives us qualitatively correct predictions of these scenarios.

4.5 Discussion

We are interested in how to increase the final level of cooperation, that is, the final ratio of cooperators, and how to maximize the overall utility in the network. The first question could be answered by Figure 4.7, where we investigate the final fraction of cooperators with different

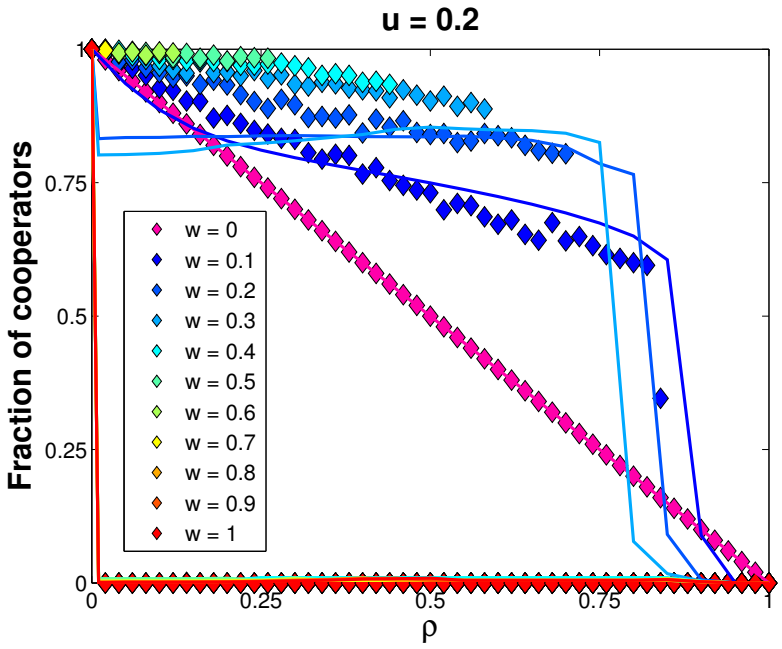

Figure 4.14: Simulation results of the final fraction of CC links with different combinations of u and w. For both u and w axes, we pick the step to be 0.05 and plot the fraction of cooperators in the stationary states in simulations. We take the mean of 50 simulations of each parameter set here.

combinations of u and w. To increase the final fraction of cooperators, the most effective way is to reduce the cost-to-benefit ratio, u in the model. Then nodes do not have much incentive to defect and this would increase the final cooperative level greatly, in many cases getting close to 1. Or one could also make the parameter w small. In this case, nodes do not have much chance to update their strategy; they do a lot of rewiring and the dynamics will stop when there are no discordant edges. However, this would only make the final cooperative level close to 0.5, the initial cooperative level. Furthermore, one can decrease the initial fraction of defectors parameter ρ. As we studied in Figure 4.13 and Figure 4.14, the smaller the ρ is, the greater of final cooperative level.

The second question, how to maximize the total utility or payoff is slightly different. In the partner switching evolutionary game model we study here, no matter how the structure of networks and the state of the nodes change, the total number of nodes and edges are fixed. Utility comes from every edge in the network. According to the model, the total utility of a CC edge is 2, the total utility of a CD edge is $1+u$, and the total utility of a DD edge is $2u$, where $u \in (0,1)$. Hence, the average utility of a CC edge is greater than CD and than DD. And this is a trait of a prisoner's

dilemma game. If we want to maximize the overall utility, we need to have more CC links. We not only wish to increase the fraction of C's, but we also need to make sure the links mostly belong to CC, not DD. As we will discuss next chapter, if we also let DD rewire, we can increase the overall utility even more.

We plot the final fraction of CC edges with different combinations of u and w in Figure 4.15. It generally shows the same pattern as in Figure 4.6, but when w is close to 0, the CC level increases to around 0.75. This is because when there is no strategy updating, nodes can not change their states, and the only thing for the nodes to do is to rewire until there is no discordant edge. If $w = 0$, then the network would stop evolving until all the C's in the CD edges dismiss their defective neighbors and rewire to the C nodes. Since no nodes could change their states, the final CC ratio would equal to 1 minus the initial DD ratio, that is 1 - 0.25 = 0.75.

We used PA and AME approaches to approximate the simulation results here. It is also worth noticing that [159] used an approach for studying adaptive SIS networks that treated the links as the objects and classifies them according to the disease states, the number of neighbors, and the number of infected neighbors of each node of its links. This link-based method could generally improve the accuracy compared to the AME method. However, it also enormously increases the computational cost from $O(k_{\max}^2)$ to $O(k_{\max}^4)$, where $k_{\max}$ is the maximum degree a node could have in the network.

4.6 Conclusion

Investigations have taken place on different evolutionary games played on random graphs and social networks. Individuals could play a prisoner's dilemma game on graphs with various strategies and the option to switch partners. Therefore, this game could be put into a framework of coevolving networks. We follow the node-based dynamics, which means each node can use only one strategy (cooperate or defect) towards all of his or her neighbors. We explore the overall parameter space and see the combination effect of the parameter related to partner switching and strategy updating. Also in our work, we improve the existing pair approximation (PA) by using approximate master equations (AMEs), and get more accurate approximations of the dynamics in the stationary states. We investigate the evolution of the dynamics and see how the AMEs could approximate this. We also use the AME method to estimate the degree distributions of different parameter sets in their

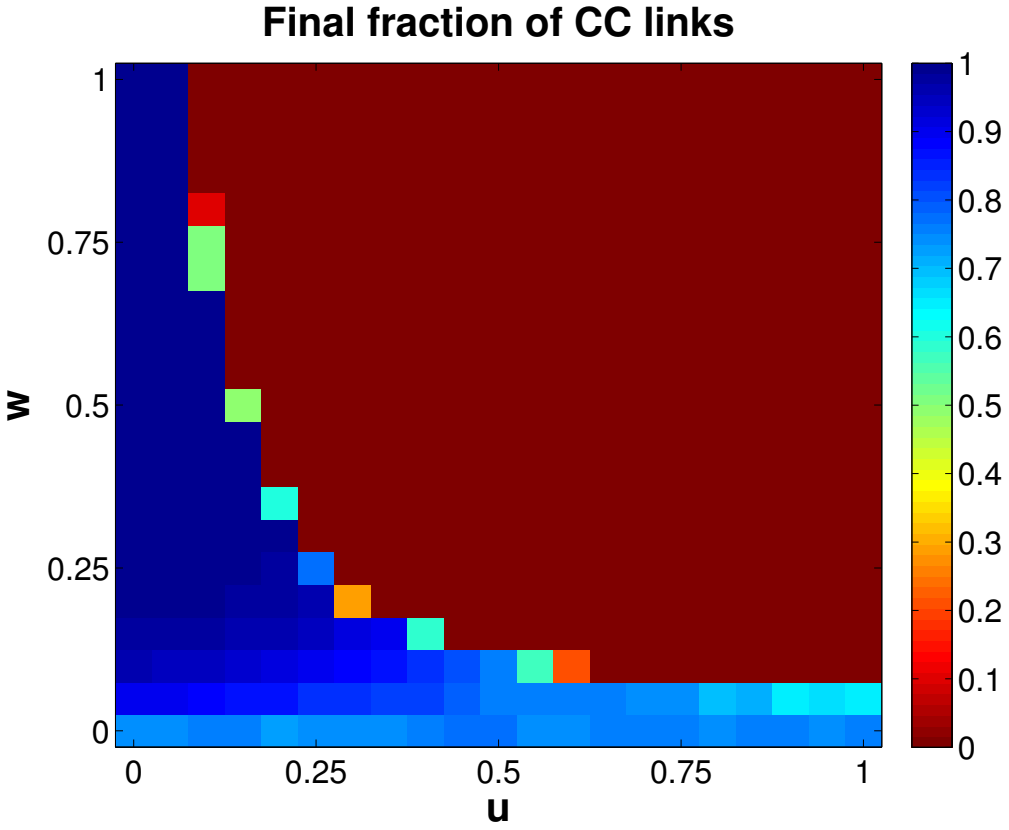

Figure 4.15: Simulation results of the final fraction of CC links with different combinations of u and w. For both u and w axes, we pick the step to be 0.05 and plot the fraction of cooperators in the stationary states in simulations. We take the mean of 50 simulations of each parameter set here.

stationary states, which PA is not able to predict. Furthermore, we explore the parameter ρ, the initial fraction of defectors, and see how it affects the final cooperative level.

Following the existing partner switching model, we holistically explore the effects of its parameters. We discuss how to increase the final cooperative level and improve the existing method to approximate the network dynamics. In the next chapter, we extend the current model and see how the networks behave if we change the network dynamics. We hope that our results provide insight into the understanding of the evolution of the games playing on coevolving networks.

CHAPTER 5

Evolutionary Games on Complex Networks – A Variation Model

5.1 Model Description

In this Chapter, we will study a slightly different dynamics of the partner switching evolution game model in the previous Chapter. We want to investigate the network evolution when we also let DD edges rewire, and we want to investigate how this dynamic affects the final cooperation level.

Following the previous Chapter, on a coevolving network with a game, the vertices represent players and the edges denote the pairwise partnership between individuals. We want to study how players play a prisoner's dilemma (PD) game with the ability to change strategies on each individual links they have and switch partners. We start with an Erdős-Rényi network with N nodes and M edges.

The strategy updating part is the same as in the previous Chapter. The only different thing is now we not only let CD edges but also DD edges to rewire. In each time step, we first randomly pick a CD or DD edge. If a CD edge is picked, then with probability w, the strategy updating process happens, and with probability $1 - w$, the player with state C unilaterally gets rid of the partnership with its neighbor with state D and rewires to an arbitrary node in the network. On the other hand, if a DD edge is picked, then with probability w nothing happens, and with probability $1 - w$ one end chosen randomly dismisses the other end and rewires to an arbitrary node in the network. Hence during the whole process, the total amount of nodes and edges remain constant.

This variation partner switching evolution game model stops evolving when there are no CD and DD edges in the system, or it also stops when there is only one state in the network. To put it another way, there would be two cases in the stationary state of the network. Case 1: C and D nodes coexist in the network, but there are no CD or DD edges. Case 2: There is only one state of nodes (either C or D) in the network. In both cases, there is no possibility for a node to change its state and hence, we stop the dynamics.

In Figure 5.1, we provide a visualization of the model in the stationary state (case 1). We choose cost-to-benefit ratio $u = 0.5$, strategy updating probability $w = 0.1$, and initial fraction of defectors $\rho = 0.5$. In this case, C and D coexist in the network, but there are no CD or DD edges. The C nodes own all the edges and they form a single component to defend the exploitation of D. Moreover, note that all the D nodes in this case are isolated nodes.

On the other hand, in Figure 5.2, we have another visualization of the model in the stationary state (case 2). We choose cost-to-benefit ratio $u = 1$, strategy updating probability $w = 0.5$, and initial fraction of defectors $\rho = 0.5$. In this case, only D nodes exist in the network, and all the edges are DD edge. The dynamics stops because of lacking of C nodes for D nodes to update their strategies. In contrast to many isolated nodes we see in the previous case, this final network forms a giant component instead.

5.2 Semi-analytical Methods

We study the second version of the partner switching models on coevolving networks with a combination of simulations and approximate analytic models. Likewise, we also compare the pair approximation (PA) and the approximate master equation (AME) approach with the simulation results.

Following the notation of the previous Chapter, here we derive the PA equations for this variation partner switching evolution game model.

$$\begin{aligned}
\frac{dN_C}{dt} =& w \cdot N_{CD} \cdot \tanh\left[\frac{\beta}{2}(\overline{\pi}_C - \overline{\pi}_D)\right] \\
\frac{dN_{CC}}{dt} =& w \cdot \left(N_{CD}\phi_{C\to D} - 2N_{CD}\frac{N_{CC}}{N_C}\phi_{D\to C} + N_{CD}\frac{N_{CD}}{N_D}\phi_{C\to D}\right) \\
&+ (1-w)\cdot\frac{N_C}{N}N_{CD} \\
\frac{dN_{DD}}{dt} =& w \cdot \left(N_{CD}\phi_{D\to C} - 2N_{CD}\frac{N_{DD}}{N_D}\phi_{C\to D} + N_{CD}\frac{N_{CD}}{N_C}\phi_{D\to C}\right) \\
&- (1-w)\cdot\frac{N_C}{N}N_{DD}
\end{aligned}$$

Suppose now both CD and DD could break their links. We also have the following ODE governing

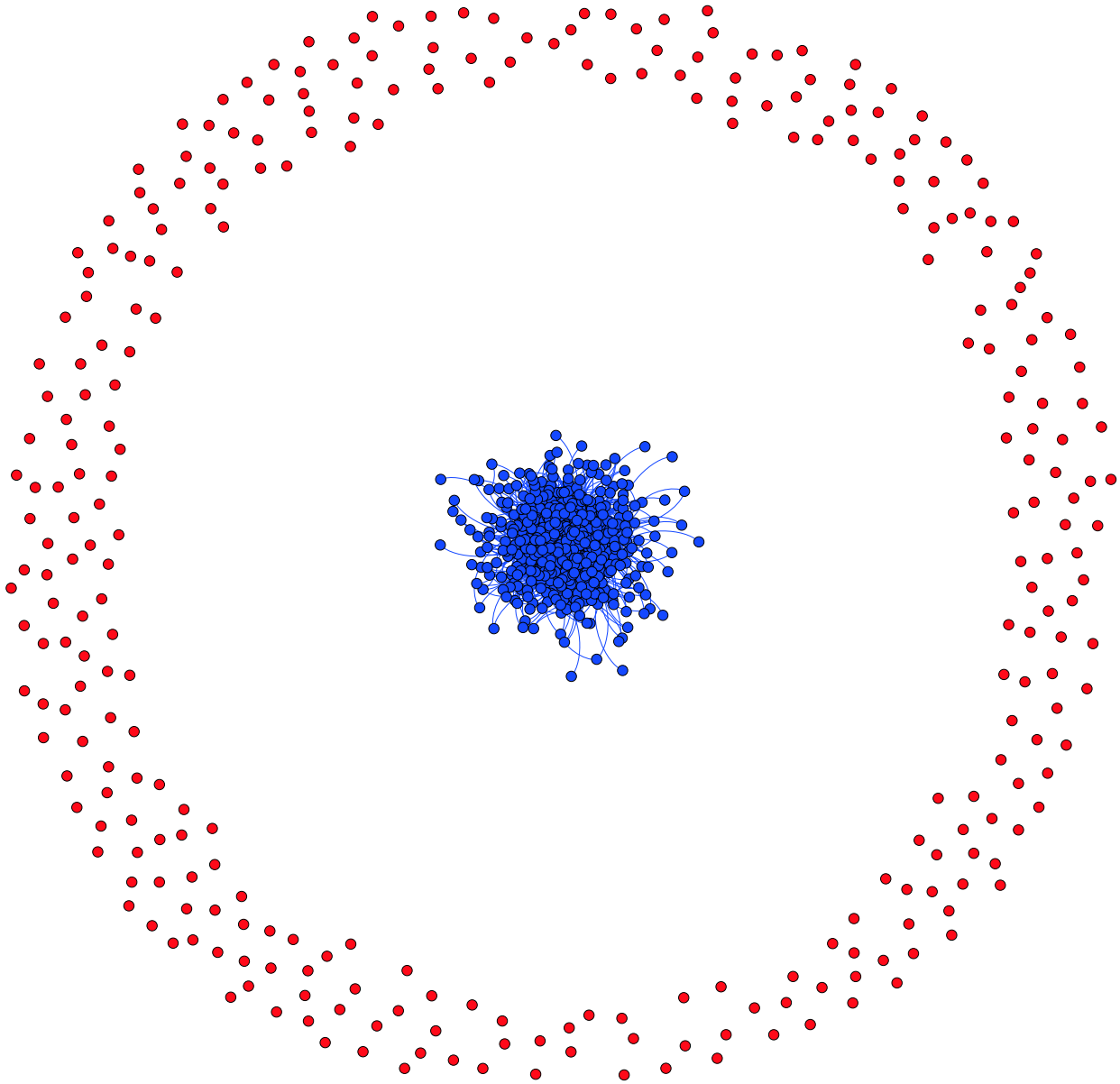

Figure 5.1: Visualization of the second partner switching model in the stationary state, for $N = 1,000$ nodes, $M = 5,000$ edges, cost-to-benefit ratio $u = 0.5$, strategy updating probability $w = 0.1$, and initial fraction of defectors $\rho = 0.5$. Colors correspond to the two states of node; blue: cooperative and red: defective. In this case, C nodes and D nodes coexist in the network, but there are no CD or DD edges.

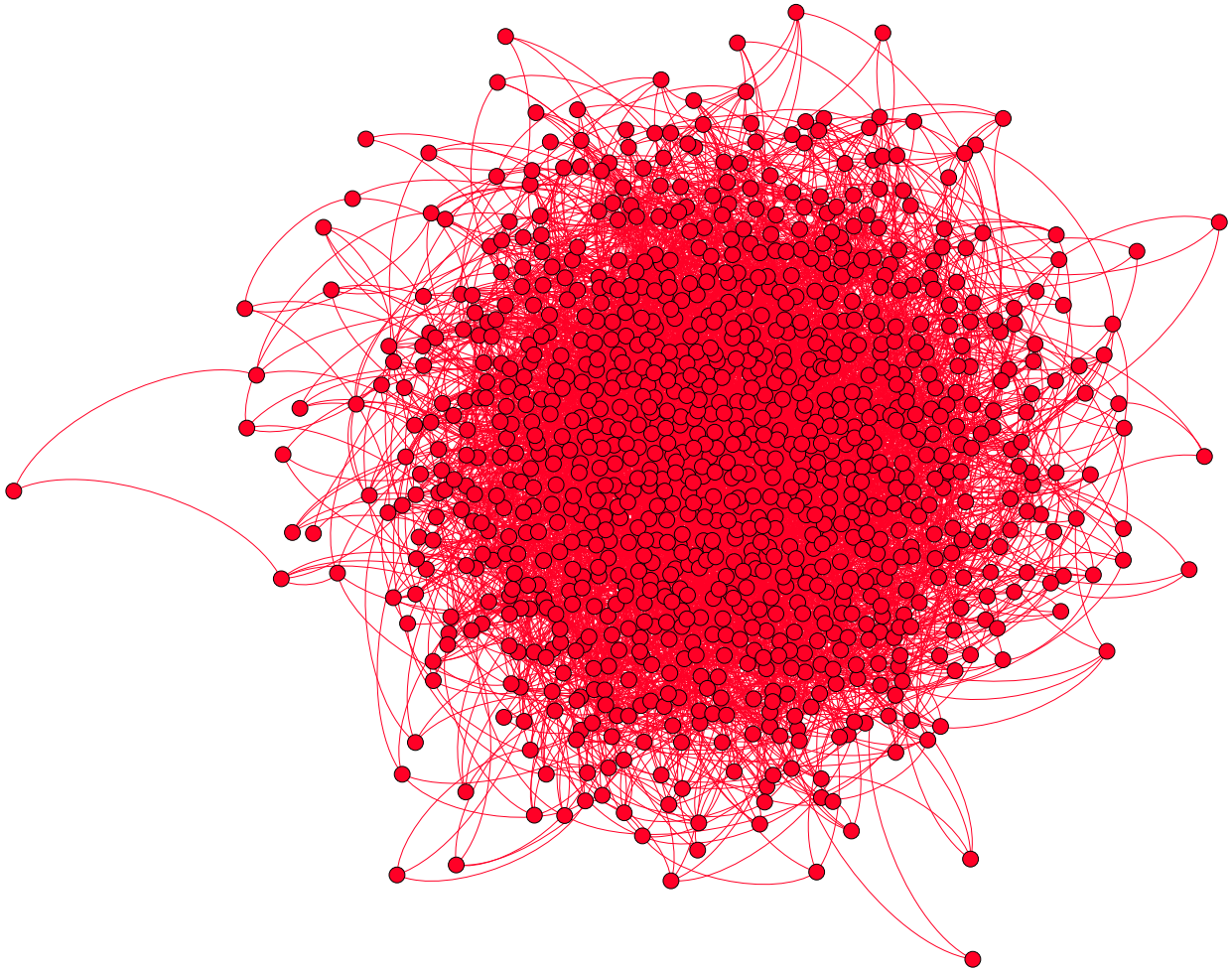

Figure 5.2: Visualization of the second partner switching model in the stationary state, for $N = 1,000$ nodes, $M = 5,000$ edges, cost-to-benefit ratio $u = 1$, strategy updating probability $w = 0.5$, and initial fraction of defectors $\rho = 0.5$. Colors correspond to the two states of node; blue: cooperative and red: defective. In this case, only D nodes exist in the network, and all the edges are DD edges.

the time evolution of the $C_{k,l}$ compartment:

$$\begin{aligned}\frac{dC_{k,l}}{dt} = w\Big\{ & \phi^D_{k,l}(k-l)D_{k,l} - \phi^C_{k,l} l C_{k,l} \\ & + \phi^C_{k,l+1}\gamma^S(l+1)C_{k,l+1} - \phi^C_{k,l}\gamma^S l C_{k,l} \\ & + \phi^C_{k,l-1}\beta^S(k-l+1)C_{k,l-1} - \phi^C_{k,l}\beta^S(k-l)C_{k,l}\Big\} \\ & + (1-w)\Big\{\frac{N_C}{N}\big[(l+1)C_{k,l+1} - lC_{k,l}\big] \\ & + \frac{N_{CD}}{N}\big[C_{k-1,l} - C_{k,l}\big] + \frac{N_{DD}}{N}\big[C_{k-1,l-1} - C_{k,l}\big]\Big\}\end{aligned}$$

Similarly the ODE governing the time evolution of the $D_{k,l}$ compartment is:

$$\begin{aligned}\frac{dD_{k,l}}{dt} = w\Big\{ & -\phi^D_{k,l}(k-l)D_{k,l} + \phi^C_{k,l} l C_{k,l} \\ & + \phi^D_{k,l+1}\gamma^I(l+1)D_{k,l+1} - \phi^D_{k,l}\gamma^I l D_{k,l} \\ & + \phi^D_{k,l-1}\gamma^I(k-l+1)D_{k,l-1} - \phi^D_{k,l}\gamma^I(k-l)D_{k,l}\Big\} \\ & + (1-w)\Big\{\big[(k-l+1)D_{k+1,l} - (k-l)D_{k,l}\big] \\ & + \frac{N_C}{N}\big[(l+1)D_{k,l+1} - lD_{k,l}\big] + \big[(l+1)D_{k+1,l+1} - lD_{k,l}\big] \\ & + \frac{N_{CD}}{N}\big[D_{k-1,l} - D_{k,l}\big] + \frac{N_{DD}}{N}\big[D_{k-1,l-1} - D_{k,l}\big]\Big\}\end{aligned}$$

The differential equation system above contains $2(k_{\max}+1)^2$ differential equations, where $k_{\max}$ is the maximum degree a node can have in the network. Usually, $k_{\max}$ depends on network structure and the mean degree. Here we choose $k_{\max} = 50$. We use these differential equations to estimate the evolution of networks and solve their solutions numerically, arriving at a semi-analytical approximation of the network evolution. To solve these thousands of ODEs, we use the ode45 solver in MATLAB when all the solutions converge.

5.3 Numerical Experimentation

As in the previous Chapter, we simulate networks with $N = 1,000$ nodes, $M = 5,000$ edges, and hence the mean degree of the network is fixed to be $\langle k \rangle = 10$. We set the imitation parameter α in

the Fermi function equal to 30. As before, we introduce a parameter ρ to denote the initial fraction of defectors. First, we set $\rho = 0.5$ and we will explore the effect of this parameter later. Initially, we start the networks to be an Erdős-Rényi $G(N, M)$ random graph model, that is, a network is chosen uniformly at random from the collection of all graphs which have N nodes and M edges. Hence with large N, we could approximate the initial degree distribution of the networks by the Poisson distribution,

$$p_k = \frac{z^k e^{-z}}{k!}.$$

We perform Monte Carlo simulations of the evolution of the networks. In each time step, we choose 100 edges and update them with the same reason provided in the previous Chapter, that is, to match the time scale of numerical simulations and the semi-analytical approximations. The dynamics will stop when there are no CD or DD edges, only one state of nodes in the network, or when it reaches our stopping time $t = 1,000$.

5.3.1 Exploration of the Parameter Space

To see the effect of cost-to-benefit ratio u and strategy updating probability w, first, we investigate the final fraction of cooperators and fraction of CC links in the stationary states. For both u and w, we start from 0 and increase the step by 0.05 to 1, and we want to explore the cooperative levels in the stationary states. In Figure 5.3 and Figure 5.4, we have the heat map of this result. There are not many differences with the heat map we got in the previous Chapter. When u is small, there is a high level of cooperators in the stationary states. And when w is close to 0, there is a medium level of cooperators in the final states. Most importantly, when w is small and u is large, the cooperative level is higher than the first model in Chapter 4. We see that letting DD to be able to rewire can increase the cooperation level when w is small. Other than small u or w, the networks are full of defectors in the stationary states, which we will explore and explain this phenomenon with our semi-analytical approximations together in Figure 5.5 and Figure 5.6.

Note that in the stationary state of this second model, there would only be CC links if C and D nodes coexist in the network; or in the other case, if there is no C node, only DD links would exist. There exist two clear regions in the parameter space where C or D nodes dominate, and on the boundary, that is the place where stochasticity of the dynamics happens. Sometimes C nodes

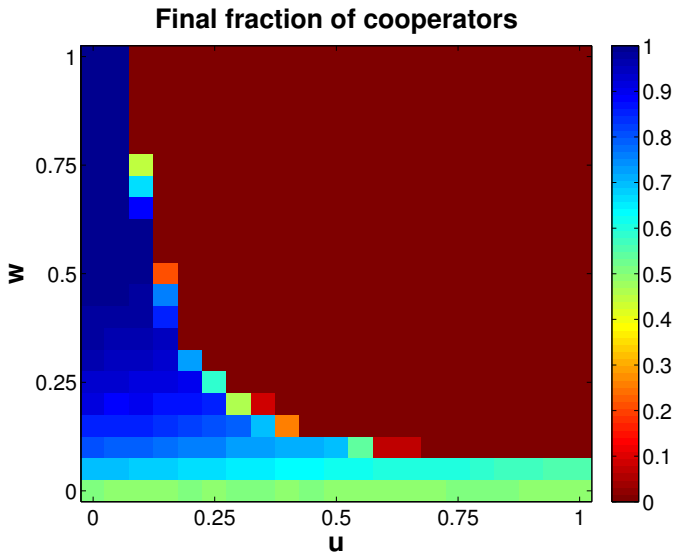

Figure 5.3: Simulation results of the final fraction of cooperators with different combinations of cost-to-benefit ratio u and strategy updating probability w. For both u and w axes, we pick the step to be 0.05 and plot the fraction of cooperators in the stationary states in simulations. We take the mean of 50 simulations of each parameter set here.

dominate and sometimes D nodes dominate so that we could see different colors on the boundaries of Figure 5.3 and Figure 5.4.

5.3.2 Final Level of Cooperation

Now we want to compare the simulation results and the two semi-analytical approximations. In Figure 5.5, fix $w = 0$, $w = 0.05$, $w = 0.1$, and $w = 0.5$, we plot the ratio of C's in the stationary state of the networks against the cost-of-benefit ratio, u. There are three sets of outcomes here: markers are the simulation results, dotted lines are the PA approximation, and the dash lines are the AME approximation. Although this figure only shows us the final fraction of C's, one could also know the final fraction of D's simply because the sum of C and D ratios should always be 1.

In the case $w = 0$, since there are no strategy updates happening in the networks, nodes couldn't change their states during the evolution. Hence, the final fraction of C and D will remain constant. Since first we set $\rho = 0.5$, regardless of u we should get 50% of C and 50% of D in the stationary states. In Figure 5.4, simulations, PA, and AME give us the same results, where the final ratio of C stays constant of 0.5 with regard to u. Therefore, both the PA and the AME approximations here are

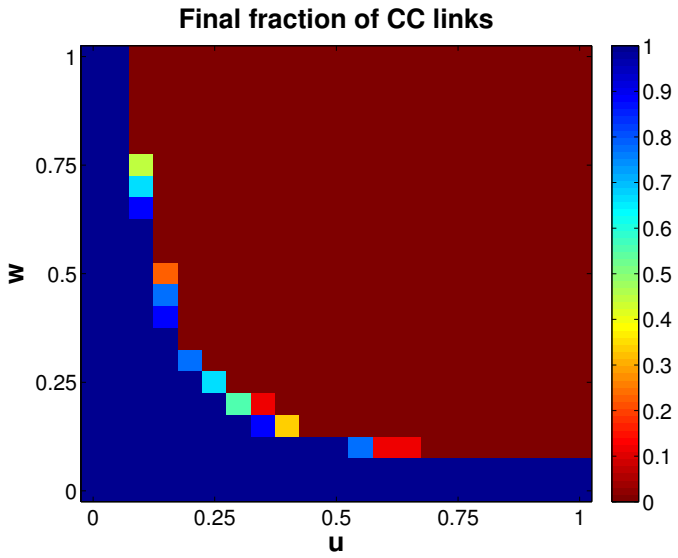

Figure 5.4: Simulation results of the final fraction of CC links with different combinations of cost-to-benefit ratio u and strategy updating probability w. For both u and w axes, we pick the step to be 0.05 and plot the fraction of cooperators in the stationary states in simulations. We take the mean of 50 simulations of each parameter set here.

accurate. When $w > 0$, the strategy updating starts playing a role. The greater the cost-of-benefit u is, the more incentive for nodes to defect. Hence, the final fraction of cooperators decreases as u increases.

In the cases $w = 0.1$ and $w = 0.5$, both simulation results decrease slowly at first and drop faster to zero around $u = 0.2$ and $u = 0.6$, respectively. This phenomenon is captured by the AME approximation not only by the qualitative behavior but also the critical dropping value of u. On the other hand, although PA could give us a good qualitative estimation of the behavior, PA lines both drop earlier and fail to provide a good prediction of critical points. Hence comparing to PA, the AME method offers better predictions of the simulation. Lastly, in the last case $w = 0.05$, the simulation results gradually decrease when u increase. The gaps between simulation results and PA and AME gradually increase. PA curve drops to zero around $u = 0.9$, however, the AME curve does not have this qualitative change. Therefore, throughout all the scenarios listed in this figure, PA does no better prediction than the AME method. The AME method always provides satisfying qualitative approximation of the simulation results, and it gives accurate predictions at the critical points.

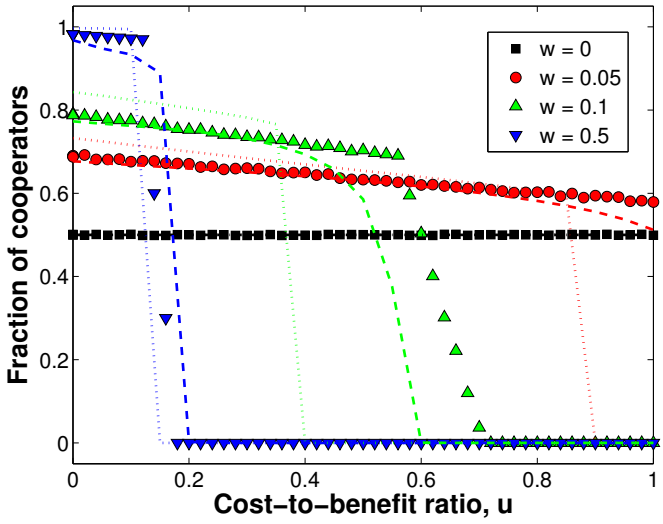

Figure 5.5: Fraction of cooperators versus cost-to-benefit ratio u with different strategy updating probability w values in stationary states. Markers are the averages of 1,000 simulations results, dotted lines are the semi-analytical results of pair approximation (PA), and the dashed lines are the semi-analytical results of approximate master equations (AMEs).

Comparing Figure 5.5 with Figure 4.8, the difference between these two models is that if DD edges are also allowed to rewire, when in the case when w is small but not zero, the final fraction of C nodes is higher. In the case when $w = 0.05$ and $w = 0.1$, in these two cases the two trajectories start at the same high when $u = 0$, and the C ratio in the second model is always no less than the first model as u increases. This is because when we allow DD to rewire, D nodes become more unfavorable. In the first model, if a DD link is formed, then it is fixed unless the state of either node changes. This effect provides less chance for a node to escape its defective partner.

Similarly, we plot the final fraction in the stationary state of cooperators C versus strategy updating probability w with a different set of cost-to-benefit ratio, u in Figure 5.6. Though not perfect, AME in this case still yields more accurate prediction than PA. Hence, the AME method improves the results PA could acquire in this figure.

5.3.3 Network Dynamics

After knowing the status in the stationary states, now we explore how the networks evolve. We know there are two things happening to the networks: nodes change their states and the structure

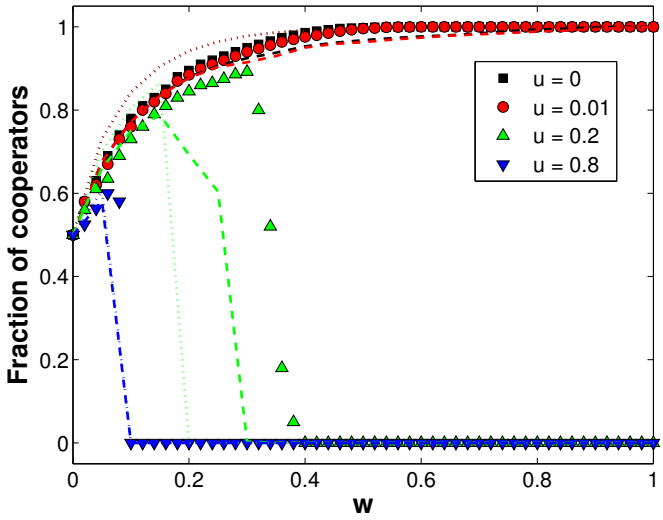

Figure 5.6: Fraction of cooperators versus strategy updating probability w with different cost-to-benefit ratio u values in stationary states. Markers are the averages of 1,000 simulations results, dotted lines are the semi-analytical results of pair approximation (PA), and the dashed lines are the semi-analytical results of approximate master equations (AMEs).

of the networks also change. To see how the networks change with time, we also investigate the evolution of five fundamental quantities of the networks: C, D, CC, CD, and DD as in the previous Chapter. And we compare the simulation results with the two semi-analytical approximations we have. We choose a set of parameters $u = 1$ and $w = 0.05$. Since the time scale of PA and AME are fixed in the differential equations, in order to keep our simulation results and semi-analytical results on the same time scale, we carry out 100 updates at each time step in the simulations. In this fashion, the three results will enjoy the same time scale as we show in Figure 5.7. To perform the experiment, we do the 50 simulations and take the averages of them at each time step.

In this figure, since the initial fraction of defectors ρ is set to be 0.5, and we follow the Erdős-Rényi $G(N, M)$ random graph model, both C and D are 0.5, CC and DD are 0.25, and CD is 0.5 initially. These are also the initial conditions of PA and parts of the initial conditions of AME. One thing worth noticing is that the total amount of nodes and edges are constant during the evolution, as both the fraction of C and D and the fraction of CC, CD, and DD should always be summed up to be 1. The networks evolve as time goes by, and it stops evolving when there are no CD and DD edges, i.e. when CD (the black markers) and DD (the magenta markers) both equal to zero. At the

time soon after $t = 200$, the networks stops evolving and all five quantities keep constant after this stopping time. The PA method in this case stops evolving before $t = 10$, and it gives the prediction that the networks are dominated by defectors and their links, which is totally off. On the other hand, the AME method stops evolving around $t = 150$, the black line goes to zero and other four lines stay as constants. And the AME method gives us a fairly good estimation in this case. Not only the AME method gives the correct order of these quantities, but during the evolution, the AME method provides qualitatively correct trajectories of how these quantities change with time. For example, the quantity of D first goes up and then goes down below the quantity of C. The AME method could capture this phenomenon. Moreover, the AME method also knows that DD edges would disappear before CD in this case. Hence comparing to PA, the AME method still works much better in the second model.

In Figure 5.8, we compare the simulation results with the AME approximation. Since we know the AME method does no worse than PA, we only focus on AMEs and simulation results comparison. We choose the same four different parameter sets as the previous Chapter here: $u = 0.2, w = 0.1$, $u = 0.2, w = 0.3$, $u = 0.5, w = 0.1$, and $u = 0.5, w = 0.3$. In the case $u = 0.2, w = 0.3$ the AME method is off, it predicts that ratio of C nodes would go to 0. However, in Figure 5.5, PA gives the same wrong results too. This is a case when there are no C nodes for the network to have future strategy updating and hence the network stops. In the other three cases, the AME method gives a fairly accurate prediction of the final levels of these quantities. Moreover, throughout the evolution, the AME method generates similar qualitatively correct curves as the simulation results. Hence, not only do we have a better idea of the final level of these important quantities, but we can also get qualitatively good evolution trajectories by plotting the AME trajectories while solving these equations.

5.3.4 Degree Distribution

Here in Figure 5.9, we also plot the degree distribution of C and D nodes separately in the stationary states and compare the simulation results with the AME approximations. In each case, since we start with the Erdős-Rényi $G(N, M)$ random graph model, the initial degree distribution is approximately Poisson when the network size N is large enough. Here we only show the degree

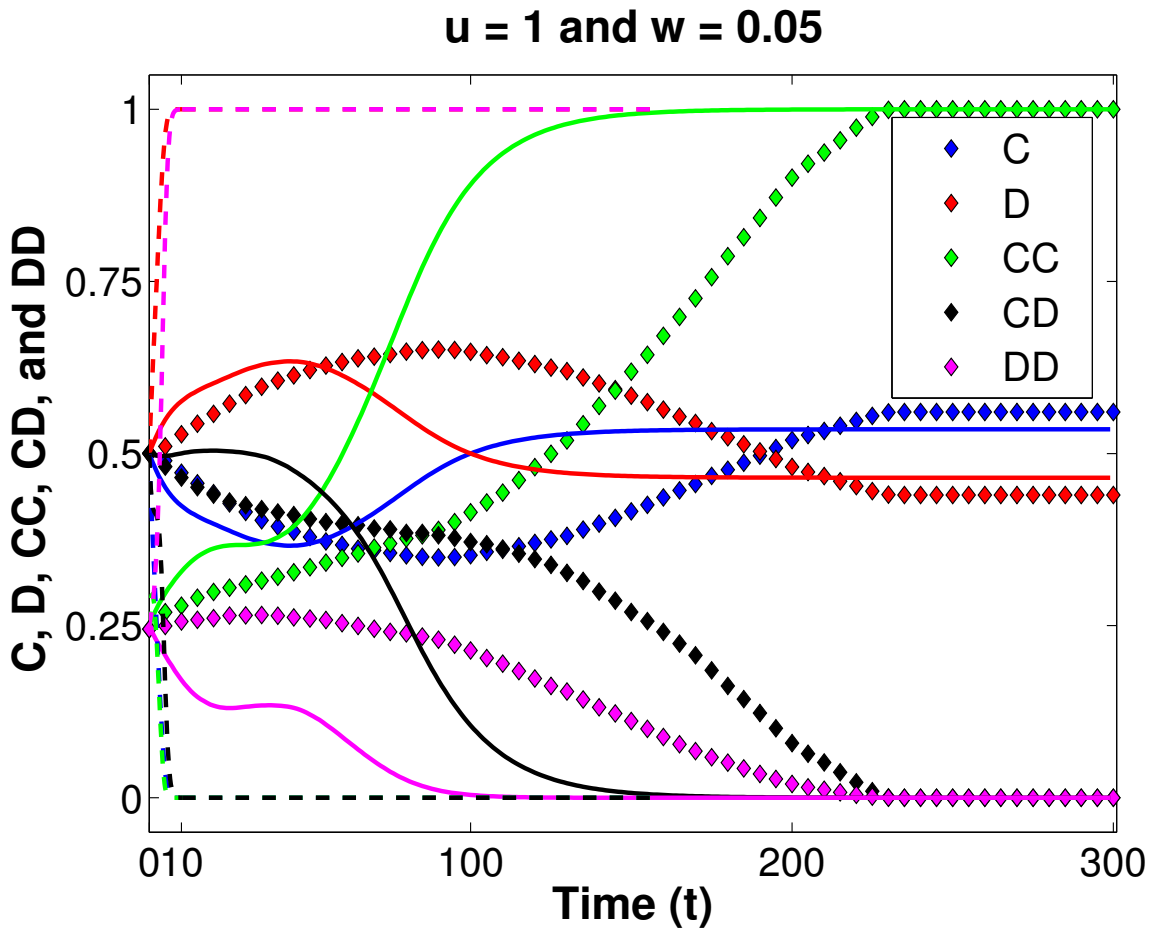

Figure 5.7: Evolution of five fundamental quantities versus time t when cost-to-benefit ratio $u = 1$ and strategy updating probability $w = 0.05$. We plot C (blue), D (red), CC (green), CD (magenta), DD (black) ratios and compare these with two semi-analytical approximations. Markers are the averages of 50 simulations results, dotted lines are the semi-analytical results of pair approximation (PA), and the dashed lines are the semi-analytical results of approximate master equations (AMEs). The dynamic stops evolving when there are no CD and DD edges, which happens around $t = 220$. PA dynamics stop around $t = 10$, and it gives bad estimations. On the other hand, the AME method provides better estimations of the simulation results.

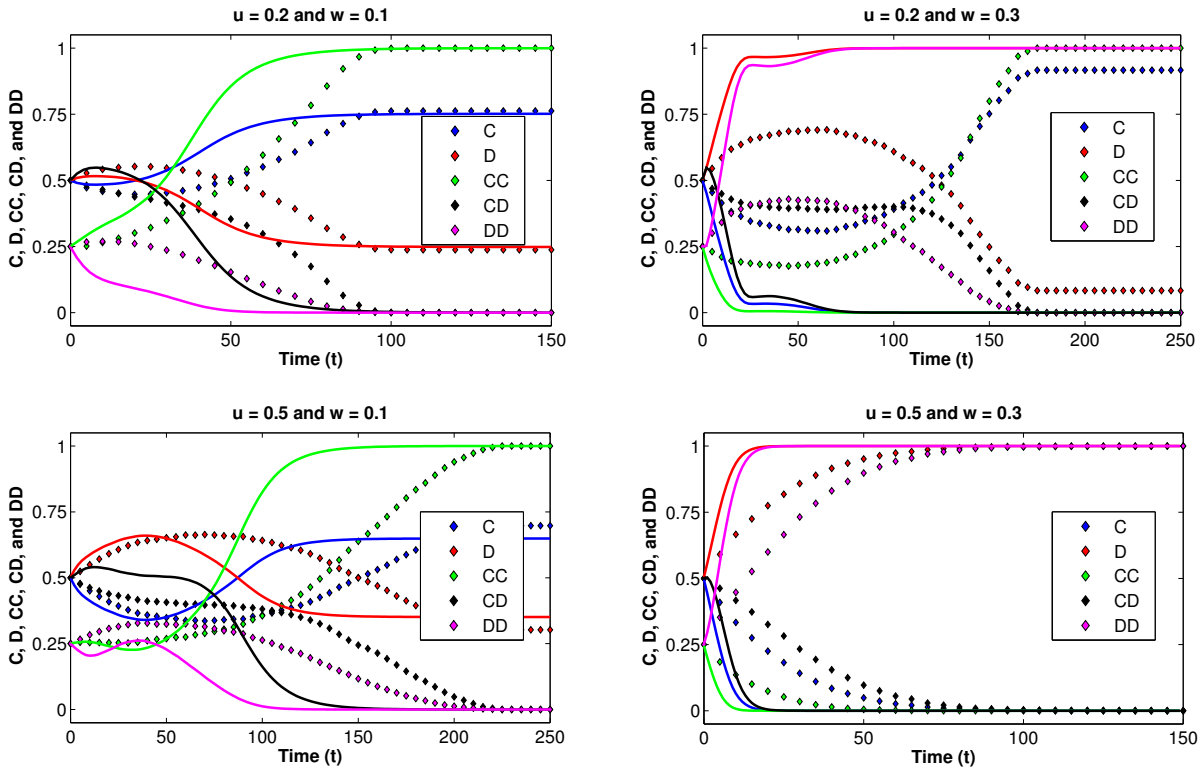

Figure 5.8: Evolution of five fundamental quantities versus time t in different parameter sets, upper left: $u = 0.2$, $w = 0.1$, upper right: $u = 0.2$, $w = 0.3$, lower left: $u = 0.5$, $w = 0.1$, and lower right: $u = 0.5$, $w = 0.3$. We plot C (blue), D (red), CC (green), CD (magenta), DD (black) ratios and compare these with our semi-analytical approximations. Markers are the averages of 50 simulations results and the lines are the semi-analytical results of approximate master equations (AMEs). The AME method provides qualitatively good estimations of the simulation results.

distributions in the stationary states. We choose the same parameter sets as in the previous figure: $u = 0.2, w = 0.1$; $u = 0.2, w = 0.3$; $u = 0.5, w = 0.1$; and $u = 0.5, w = 0.3$. Except the case $u = 0.2$ and $w = 0.3$, which AME goes off, the method yields really accurate prediction of C, D, CC, CD, and DD levels as we shown in the figure. In the case $u = 0.5, w = 0.3$, not surprisingly, since it predicts the evolution so well, the AME method also gives us a very good prediction of the final degree distribution. In the stationary state of this case, D nodes dominate the whole network and there are no C nodes.

The difference between the two models in the stationary distribution is as follows. In the case when DD could also rewire, there would be no DD links unless the whole network is full of D nodes. Hence, this makes D node in every edge extremely unfavorable, a lot of D isolated nodes are generated, and they can't change anymore. Therefore, in the case $u = 0.2, w = 0.1$, $u = 0.2, w = 0.3$, and $u = 0.5, w = 0.1$, we see the only D nodes are isolated nodes and the AME method could successfully capture this occurrence if it predicts the network evolution correctly.

5.3.5 Exploration of the Initial Fraction of Defectors, ρ

Finally, we explore the effect of the initial fraction of defectors parameter ρ in Figure 5.10 and Figure 5.11. In these two figures, we fix the parameter $w = 0.1$ in Figure 5.10 and $u = 0.2$ in Figure 5.11 and we change the other parameter u, and w, respectively, to see the final fraction of cooperators against ρ in stationary states. And we compare the simulation results (markers) with our AME approximation (lines). It is worth noting that in both figures, all the trajectories generated by simulation and approximation results would pass through the upper left and the lower right corners. This is because when $\rho = 0$, there is no D nodes in the networks, there is no discordant edge, and the networks would not evolve. The final fraction of cooperators remains 100%. The final cooperators is 0% for the similar reason in the case $\rho = 1$.

In Figure 5.10 for all u curves, the final fraction of cooperators would first gradually decrease and drop to zero suddenly at different values of ρ, and the AME method generally captures this qualitative behavior in different levels of u. Moreover, fixing $w = 0.1$, smaller u results in higher cooperative level, since the incentive of defecting is smaller when u is small. We also find out that the AME method is more accurate when u is small in this figure.

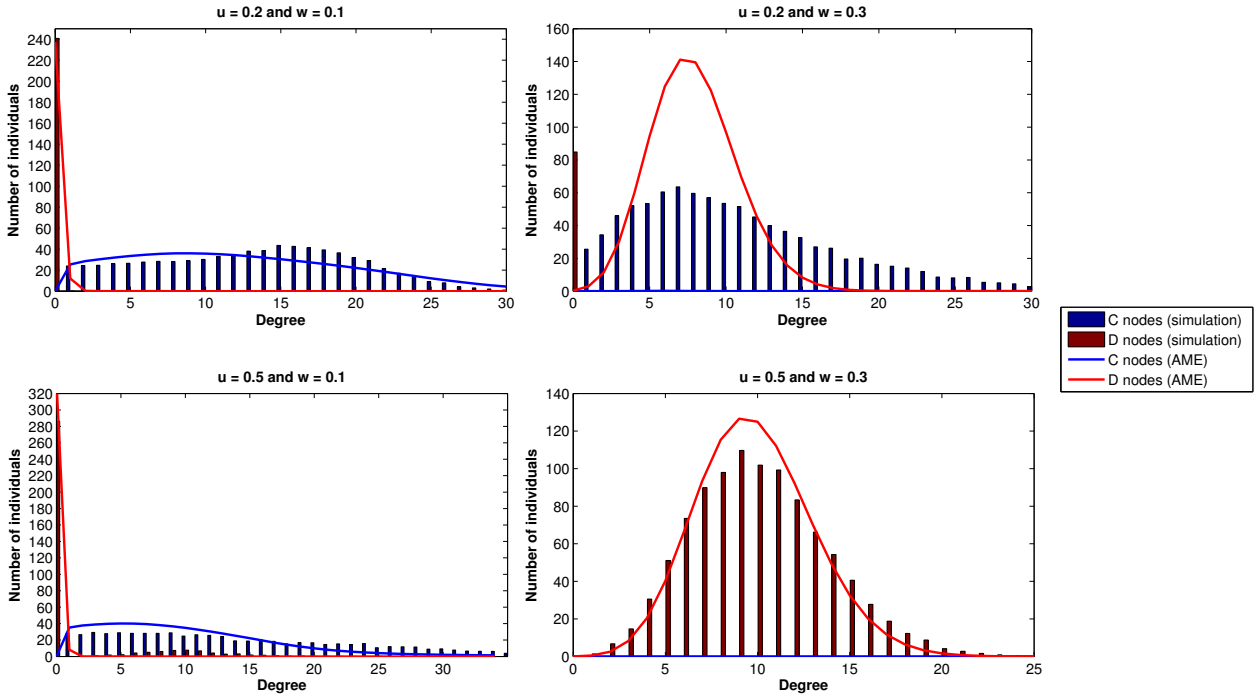

Figure 5.9: Degree distribution in the stationary states in different parameter sets, upper left: $u = 0.2$, $w = 0.1$, upper right: $u = 0.2$, $w = 0.3$, lower left: $u = 0.5$, $w = 0.1$, and lower right: $u = 0.5$, $w = 0.3$. Bars are the averages of 50 simulations results and the lines are the semi-analytical results of the approximate master equations (AMEs). AME provides qualitatively good estimations of the simulation results. Blue bars and lines are degrees of cooperative nodes, and red bars and lines are degrees of defective nodes.

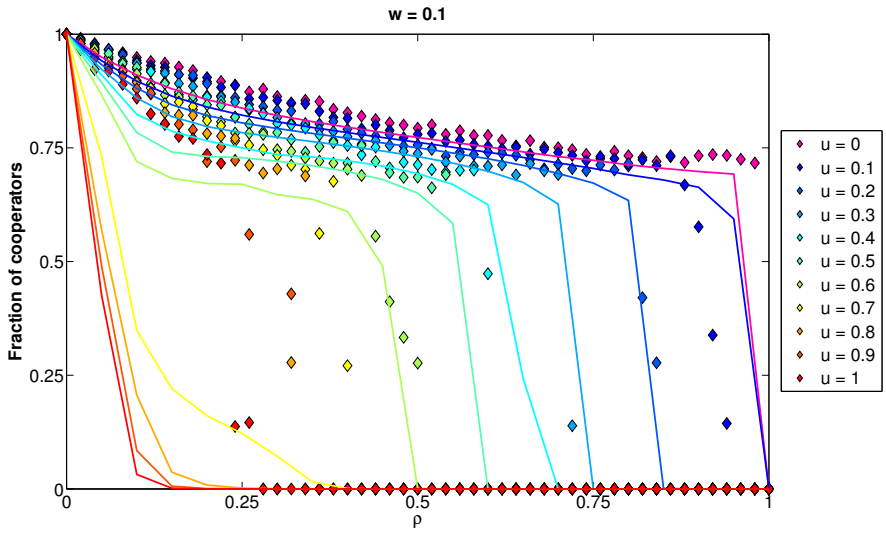

Figure 5.10: Fraction of cooperators versus the initial fraction of defectors ρ with strategy updating probability $w = 0.1$ in stationary states. Different cost-to-benefit ratio u: 0, 0.1, ..., 1 are chosen. Markers are the averages of 50 simulations results and the dashed lines are the semi-analytical results of approximate master equations (AMEs).

In Figure 5.11, fixing $u = 0.2$, the diagonal line is the case $w = 0$, there are no strategy updates happening, hence the cooperative level remains the same during the evolution. The w curves drop to zero more quickly when ρ increases, that means the strategy updating effect is more sensitive to the initial fraction of defectors ρ. When w is large, the networks count more on the strategy updating dynamics, and the final cooperative level drops to zero more quickly. As we show in this figure, the AME curves suddenly drop to zero when $w \geqslant 0.3$. Although not very accurate, the AME method still gives us qualitatively correct predictions of these scenarios. Moreover, the qualitative difference between the two models is not too much.

5.4 Conclusion

We study a slightly different dynamics as a partner switching evolutionary game model in this Chapter. We explore the overall parameter space and see the combination effect of the parameter related to partner switching and strategy updating. Also in our work, we provide the pair approximation (PA), the approximate master equations (AMEs) of the system, and get more accurate approximations of the dynamics in the stationary states. Following the previous partner

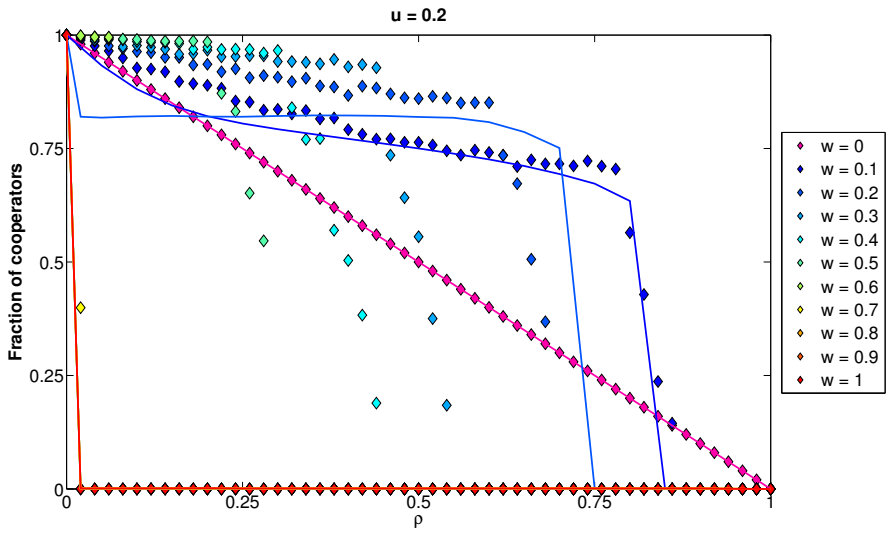

Figure 5.11: Fraction of cooperators versus the initial fraction of defectors ρ with cost-to-benefit ratio $u = 0.2$ in stationary states. Different w: 0, 0.1, ..., 1 are chosen. Markers are the averages of 50 simulations results and the dashed lines are the semi-analytical results of approximate master equations (AMEs).

switching model, we also give a holistic investigation of the effects of its parameters. We discuss how to increase the final cooperative level and improve the existing method to approximate the network dynamics. We show if we let DD edges could also rewire, this would increase the cooperation level when strategy updating probability w is small. Moreover, the final state would be either a network full of nodes with one state, or C nodes and D nodes coexist and all the D nodes are isolated. We investigate the evolution of the dynamic and see how the AMEs could approximate this. We also use the AME method to estimate the degree distributions of different parameter sets in their stationary states, which PA is not able to give this prediction. Furthermore, we explore the parameter ρ, the initial fraction of defectors and see how it affects the final cooperative level and use the AME method to estimate the dynamics.

.

CHAPTER 6

Link-based Evolutionary Games on Complex Networks

The contents of this Chapter are theoretical extensions of the previous two Chapters. However, the results here are still preliminary. We nevertheless include this Chapter in the thesis for completeness.

6.1 Model Description

We studied two partner switching models of evolutionary games on complex networks. In these settings, each individual could either play cooperatively or defect against all of his or her neighbors. However, this assumption is unrealistic compared to the availability and, indeed, the probable preferability to behave differently to different partners. In the models with node-based states considered in the previous Chapters, if a person chooses to be cooperative, then he or she needs to cooperate with all of the neighbors at the same time. On the other hand, if a person chooses to be defective, then he or she needs to defect with all of the neighbors at the same time too. This situation is contradictory to the observation we have in daily life where people form groups to collaborate and defend themselves from other groups of people. Hence, an individual in a social network should be able to cooperate with some people and defect with other people simultaneously. The previous two models simply could not offer this possibility since there are states attached to each node and the node behaves accordingly. Previous research has studied playing different strategies with different people, usually finding group formation in the society [8, 56, 102]; however, there appears to have been little such work in the setting of typical complex networks.

In this Chapter, we want to extend the previous partner switching models to a link-based model. That is, each individual could play different strategies with different neighbors based on the states of their links, without restricting a node to behave the same way across all of its links. We want this extended model to be as close as possible to our previous node-based model in order to compare and contrast the models. On an adaptive network with a game, the vertices represent players and the edges denote the pairwise partnership (game interaction) between individuals. We want to study

how players play a prisoner's dilemma (PD) game with the ability to change strategies on each individual link they have and switch partners.

We use a very similar setting to the node-based dynamics. Initially, individual strategies and graphs start from a random and statistically homogeneous state. Each of N individuals has the same expected number of interaction partners which are their neighbors on the network. The total M edges uniformly pair the nodes up at random, and each node has an equal probability to be a cooperator (C, denoted by two-dimensional unit vector $s = [1, 0]^T$) or defector (D, $s = [0, 1]^T$) associated with its end of each of its links. Note that a node here does not have its own state, instead, it has different states on its side of its edges (also known as 'stubs'). For example, say one node has 10 neighbors: 7 of its ends could be in state C and then the remaining 3 ends would be in state D.

Maintaining similarity with the models of the previous Chapters, the utility matrix is still controlled by the parameter u, and the individual still has probability $1 - w$ to switch a partner. In each time step, we first randomly pick an edge that connects a pair of players with different strategies on the two ends of their link, i.e., a CD link denoted by E_{ij} to update. With a given probability w, stub i and stub j connected by the edge E_{ij} update their strategies; otherwise, E_{ij} is rewired (with probability $1 - w$). When link E_{ij} is rewired, the player with end state C unilaterally gets rid of the partnership with its neighbor with end state D on the edge E_{ij}. Suppose node i has the end with state C, then it will randomly pick a player k from the remaining population as its new partner, and player k would play a strategy on the new stub with probability matching its own existing C and D ratio.

When one stub updates its strategy, the stub has probability ϕ given by the Fermi function to change its state. The payoff matrix is again controlled by the cost-to-benefit ratio u as before. Two chosen nodes would compare their overall utility, and the one selected probabilistically according to the Fermi function to change its stub's state selects its 'new' state with probabilities in agreement with the C and D ratios of the other node. Under this rule, it is possible that both stubs maintain their current strategies after the strategy updating process.

This link-based partner switching evolution game model would stop evolving when there is no discordant edge in the network. In the stationary state of the network, there would be no CD edges, only CC and DD edges would exist.

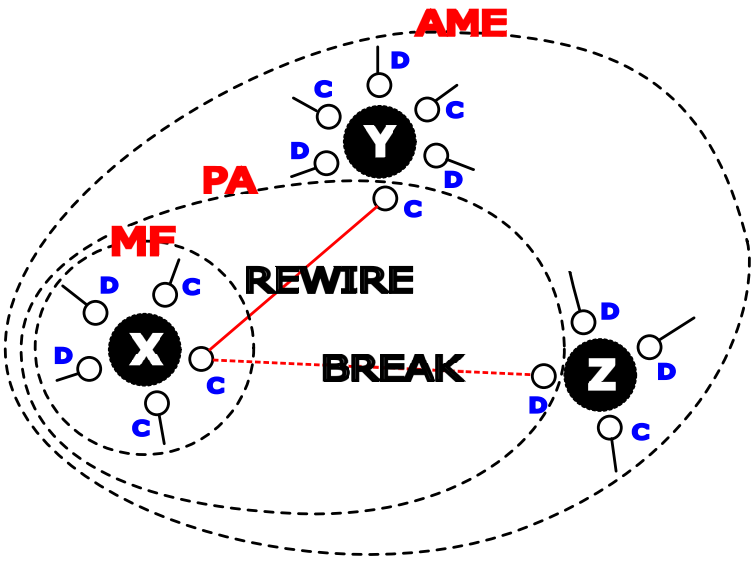

Figure 6.1: Visual depiction of the available information maintained in three different levels of analytical approximations — mean field (MF), pair approximation (PA), and approximate master equation (AME) —, in link-based dynamical evolutionary games in a network setting.

6.2 Semi-analytical Methods

Figure 6.1 depicts different levels of analytical approximation of the link based partner switching model. In the mean field (MF) approximation, one only has local information of a node. To be more specific, we use the information of a node's degree and numbers of C and D stubs to form a set of differential equations. In pair approximation (PA), one has the information of a node's degree and the pairs that node has. Lastly, in the approximate master equation (AME) method, one has the overall information of nodes and their neighbors.

6.2.1 Mean Field Approximation

Let N_{k,m_C} denote the quantity of nodes with degree k and m_C C-stubs. Then we have the following Mean Field approximation.

$$\begin{aligned}
\frac{dN_{k,m_C}}{dt} = w \cdot \Big\{ & - N_{k,m_C} \cdot m_C \cdot \frac{\frac{1}{2}N_{CD}}{N_{CC} + \frac{1}{2}N_{CD}} \cdot \phi_{D_1 \to C_1} \\
& + N_{k,m_C+1} \cdot (m_C + 1) \cdot \frac{\frac{1}{2}N_{CD}}{N_{CC} + \frac{1}{2}N_{CD}} \cdot \phi_{D_2 \to C_2} \\
& - N_{k,m_C} \cdot (k - m_C) \cdot \frac{\frac{1}{2}N_{CD}}{N_{DD} + \frac{1}{2}N_{CD}} \cdot \phi_{C_3 \to D_3} \\
& + N_{k,m_C-1} \cdot (k - m_C + 1) \cdot \frac{\frac{1}{2}N_{CD}}{N_{DD} + \frac{1}{2}N_{CD}} \cdot \phi_{C_4 \to D_4} \Big\} \\
+ (1-w) \Big\{ & \Big(N_{k+1,m_C}(k + 1 - m_C) - N_{k,m_C}(k - m_C) \Big) \cdot \frac{\frac{1}{2}N_{CD}}{N_{DD} + \frac{1}{2}N_{CD}} \\
+ \frac{N_{CD}}{N} & \Big(- N_{k,m_C} + \frac{m_C - 1}{k-1} N_{k-1,m_C-1} + \frac{k - 1 - m_C}{k-1} N_{k-1,m_C} \Big) \Big\}
\end{aligned}$$

where

$$S_C = \sum_{k=1}^{k_{\max}} \sum_{m_C=0}^{k} m_C \cdot N_{k,m_C}, \; S_D = \sum_{k=1}^{k_{\max}} \sum_{m_C=0}^{k} (k - m_C) \cdot N_{k,m_C}$$

$$N_{CC} = M \cdot \frac{S_C^2}{S_C^2 + 2S_C S_D + S_D^2}, \; N_{CD} = M \cdot \frac{2S_C S_D}{S_C^2 + 2S_C S_D + S_D^2},$$

$$N_{DD} = M \cdot \frac{S_D^2}{S_C^2 + 2S_C S_D + S_D^2}, \; N_{CC} + N_{CD} + N_{DD} = M$$

$$\begin{aligned}
\pi_{k,m_C} = & \; m_C \cdot \frac{N_{CC}}{N_{CC} + \frac{1}{2}N_{CD}} \\
& + (k - m_C) \left[\frac{N_{DD}}{N_{DD} + \frac{1}{2}N_{CD}} \cdot u + \frac{\frac{1}{2}N_{CD}}{N_{DD} + \frac{1}{2}N_{CD}} \cdot (1 + u) \right]
\end{aligned}$$

$$\bar{\pi} = \frac{total\ utility}{N} = \frac{2N_{CC} + (1+u)N_{CD} + 2uN_{DD}}{N}$$

The differential equation system above contains $2(k_{\max} + 1)^2$ differential equations, where $k_{\max}$ is the maximum degree a node can have in the network. Usually $k_{\max}$ depends on network structure and the mean degree. Here we choose $k_{\max} = 50$. We use these differential equations to estimate the evolution of networks and solve their solutions numerically, arriving at a semi-analytical approximation of the network evolution. To solve these hundreds of ODEs, the ode45 solver in

MATLAB is used and we stop when all the solutions converge.

6.2.2 Pair Approximation

Let $N_{k,m_{CC},m_{CD},m_{DC},m_{DD}}$ denote the quantity of nodes with degree k, m_{CC} CC links and so on, and S_C and S_D are numbers of C stubs and Dstubs. Note that m_{DD} is redundant.
Then we have the following pair approximation.

$$
\begin{aligned}
\frac{dN_{k,m_{CC},m_{CD},m_{DC},m_{DD}}}{dt} = w\cdot\Big\{ & N_{k,m_{CC}-1,m_{CD},m_{DC}+1,m_{DD}} \cdot (m_{DC}+1) \cdot \phi_{C_1\to D_1} \\
& + N_{k,m_{CC},m_{CD}+1,m_{DC},m_{DD}-1} \cdot (m_{CD}+1) \cdot \phi_{D_2\to C_2} \\
& - N_{k,m_{CC},m_{CD},m_{DC},m_{DD}} \cdot \Big(m_{DC}\cdot\phi_{C_3\to D_3} + m_{CD}\cdot\phi_{D_4\to C_4} \Big) \Big\} \\
+(1-w)\cdot\Big\{ & - N_{k,m_{CC},m_{CD},m_{DC},m_{DD}} \cdot \frac{S_C}{S_C+S_D} \cdot m_{CD} \\
& + N_{k,m_{CC}-1,m_{CD}+1,m_{DC},m_{DD}} \cdot \frac{S_C}{S_C+S_D} \cdot (m_{CD}+1) \\
& - N_{k,m_{CC},m_{CD},m_{DC},m_{DD}} \cdot m_{DC} \\
& + N_{k+1,m_{CC},m_{CD},m_{DC}+1,m_{DD}} \cdot (m_{DC}+1) \\
& + \frac{N_{CD}}{N}\Big[- N_{k,m_{CC},m_{CD},m_{DC},m_{DD}} + N_{k-1,m_{CC}-1,m_{CD},m_{DC},m_{DD}} \frac{m_{CC}-1+m_{CD}}{k-1} \\
& + -N_{k-1,m_{CC},m_{CD},m_{DC}-1,m_{DD}} \frac{m_{DC}-1+m_{DD}}{k-1} \Big] \Big\}
\end{aligned}
$$

The differential equation system above contains $2(k_{\max}+1)^4$ differential equations, where $k_{\max}$ is the maximum degree a node can have in the network. Usually, $k_{\max}$ depends on network structure and the mean degree. Here we choose $k_{\max}=10$. We use these differential equations to estimate the evolution of networks and solve their solutions numerically, arriving at a semi-analytical approximation of the network evolution. To solve these thousands of ODEs, the ode45 solver in MATLAB is used and we stop when all the solutions converge.

6.3 Numerical Results and Discussion

We study networks with $N = 1,000$ nodes and $M = 1,000$ edges and hence the mean degree of the network is fixed to be $\langle k \rangle = 2$. We set the imitation parameter β in the Fermi function equal to 30. Initially, we start the networks to be drawn from an Erdős-Rényi $G(N, M)$ random graph model, that is, a network is chosen uniformly at random from the collection of all graphs which have N nodes and M edges. Hence with large N, we could approximate the initial degree distribution of the networks by the Poisson distribution,

$$p_k = \frac{\langle k \rangle^k e^{-\langle k \rangle}}{k!}.$$

Moreover, we start from networks with 50% C stubs and 50 % D stubs distributed uniformly. We perform Monte Carlo simulations of the evolution of the networks. In each time step, we select and update a discordant edge. We define the unit time as 100 such updates for comparison with our semi-analytical results below. In the case when only discordant edges (i.e., CD edges) are updated, the dynamics will stop when there is no discordant edge or when it reaches our stopping time $t = 1,000$ (that is, 100,000 selections of discordant edges). We do the Monte Carlo simulations 100 times for each experiment.

The numerical simulations and the MF and PA approximations are provided in Figures 6.2 and 6.3. Note that now nodes do not have states, only edges have states. We plot the final ratio of CC to the total edges in the stationary state against the cost-to-benefit ratio u.

As we can see in the two figures, the dynamics does not depend on u value much. In order to perform a prisoner's dilemma game, we need the cost-to-benefit ratio $u \in (0, 1)$ to keep the order in the payoff matrix. However, in this region of u, fixing the value of w, the final ratio of CC links with different w levels behave almost like a constant. If we posit rational players, then their objective is to maximize the expected reward. Since the reward is aggregated linearly across edges, this means maximizing the reward on each edge separately. In steady-state, given sufficient opportunities to change strategy, it appears that the state of each stub of a node is effectively independent of the other stubs. Then what we see is the behavior is the same as if each node of degree were replaced with independent nodes of degree 1. The cost-to-benefit ratio u simply does not play a role when

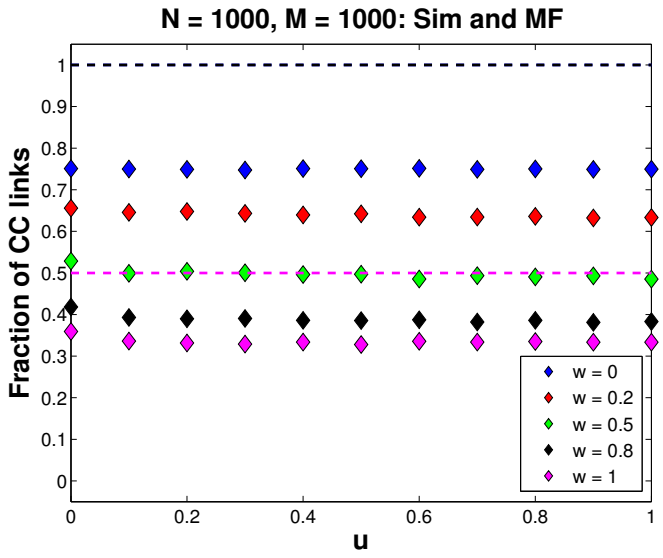

Figure 6.2: Fraction of cooperators versus cost-to-benefit ratio u with different w values in stationary states. Markers are the averages of 100 simulations results and the dashed lines are the semi-analytical results of mean field (MF) approximation (note that all 4 dashed lines for $w < 1$ combine under the black dashed line at the value 1).

the action of each stub is effectively independent.

In Figure 6.2, the MF approximation shows the dynamics is independent of the cost-to-benefit ratio u. However, it does not give us a satisfying result. It predicts for the four cases of $w < 1$, they all have the final CC level of 1. And for the case $w = 1$, it would stay on the 50 % of the CC level in the stationary state. In Figure 6.3, the PA also shows the dynamics is independent of the cost-to-benefit ratio u. However, this time, the order of the different w level is wrong, opposite to the trend observed in simulations. Both of the estimations are off, and we are not sure at this time whether our equations are not correct or there exist glitches in our codes. But since the dynamics does not depend on u, we think that perhaps we should come up with another link-based evolutionary game which has a richer behavior in the future.

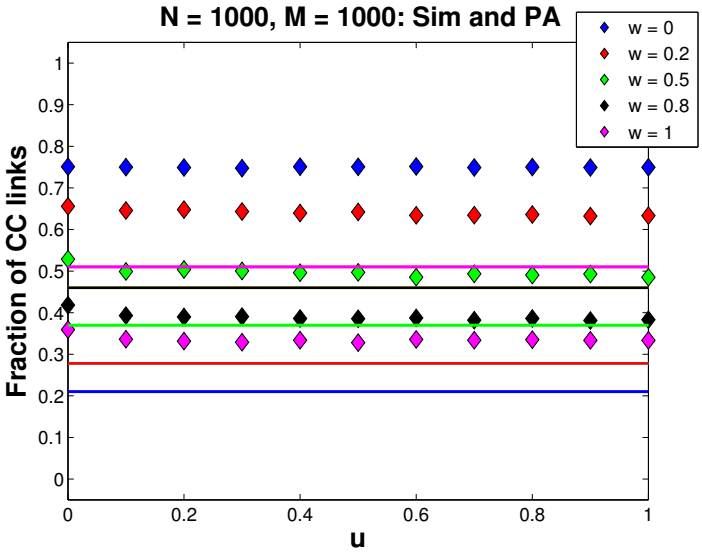

Figure 6.3: Fraction of cooperators versus cost-to-benefit ratio u with different w values in stationary states. Markers are the averages of 100 simulations results and the dashed lines are the semi-analytical results of pair approximation (PA).

CHAPTER 7

Summary

In this thesis, we have investigated three distinct models of dynamics of coevolving networks. Each of these models considers the effects of distinct interaction mechanisms for the constituent nodes. The evolution of the complex systems depends on the interaction mechanism in play. Not only the network behavior itself is interesting, but also we could use mathematical approaches to capture the fundamental phenomenon of these systems.

Clustering is one of the central properties of social networks, arising due to the ubiquitous tendency among individuals to connect to friends of a friend, and can greatly impact a coevolving network system. We study a voter model and the SIS epidemic model on a coevolving network with a certain probability to close a triangle while rewiring, leading to reinforcement of network transitivity. Under our new models, there is a probability that if a rewiring happens, a node would rewire to its neighbors' neighbor, a triangle is closed, and the local clustering increases. We show that this new mechanism we establish would indeed fundamentally affect the network dynamics, and lead to different qualitative and quantitative results. These models provide a unique opportunity to study the role of transitivity in altering the voter model and the SIS dynamics on a coevolving network.

Social networks play an important role in spreading information and forming opinions. A voter model on adaptive networks is a simplified model of a social network in which individuals have one of two opinions and their opinions and the network connections coevolve. In Chapter 2, we extend the method of approximate master equations to study our preferential attachment model and gave an accurate prediction of the stationary states of the evolution as well as study the clustering coefficients and degree distribution in the consensus states.

Coevolving networks have been introduced in the context of disease propagation on complex systems. In Chapter 3, we study disease propagation on coevolving networks and introduce a simple social network model that has a certain probability to close a triangle while rewiring. By using improved compartmental formalism method or method of approximate master equations, our

semi-analytical approximation could provide accurate predictions of disease prevalence and degree distribution of networks in their stationary states. Furthermore, in the SIS model, we studied the bifurcation diagrams and found out there exists a universal disease prevalence curve seemingly independent of initial network topologies. More complicated rewiring methods based on the degree of a node or an arbitrary distance from a node can be studied using similar semi-analytical methods.

Game theory is the study of strategic decision making and many investigations have taken place on different games played on random graphs and social networks. In Chapter 4 and 5, we bring more sophisticated mechanisms into adaptive networks. We improve the existing pair approximation by using approximate master equations, we study the model on different dynamics, and finally, explore the network structure of the stationary states. Then we extend the node-based evolutionary game model to a link-based model in Chapter 6. In this setting, each node will not have to cooperate or defect with all of his or her neighbors. This extended model gives us a more realistic scenario of the real world dynamics. We provide different level of approximation to study this model as well.

In the above models we study, the semi-analytical approximation could usually provide us satisfying results. Using approximate master equations, we can approximate in detail how the networks evolve. Although there are some limitations of the method we use, such as the tree-like assumption, it is still better than many existing approaches. We study networks with different topology and see how this could affect network dynamics, we explore the parameter spaces, investigate the dynamics of some fundamental quantities of the networks, and predict degree distributions in stationary states. With this analytical tool, we can provide a comprehensive estimation and understanding of the network dynamics.

The voter model in Chapter 2 has an assumption that the two opinions "0" and "1" are indistinguishable. Starting with the same initial fraction, the two opinions have the same probability of dominating the final consensus state, or they can together form two matching segregated consensuses. In Chapter 3, we break this symmetry between the two states, susceptible and infected individuals now have different probabilities to interchange their states, and the rewiring mechanism is also different depending on the states of nodes. Therefore, we no longer see symmetric arches in the voter model, and instead, we see endemic and disease-free states in various settings of parameters. The approximate master equations method is usually used in a situation that the transition probability is fixed or dependent on local topology. Furthermore, in Chapter 4 and 5, the game theory model

suggests a more complicated updating process. An individual needs to compare his or her utility with neighbors and changes their strategies accordingly, and thus, we need information more than ones' neighbors have. The transition probability is no longer a fixed constant, but it depends on the network topology and the specific game the model plays. To find a mathematical prediction of the system's overall behavior becomes a challenging but exciting mission.

In this thesis, we only study binary-state dynamics on coevolving networks, and surely with effort these approaches can generalize to multi-states networks. This extension will take an enormous increase in the the number of differential equations and computational costs to study the dynamics. However, we do think this field will be explored and more fascinating dynamics and complicated behaviors could also be examined in the near future.

We developed simple network dynamics models that take into account a variety of different interaction rules. Furthermore, we provide mathematical methods to study the systems and often give good approximations. However, with the growing availability of real-world network data recently, it will be more important to test and corroborate these models. Specifically, temporal network data, multilayer networks, and networks with metadata could all be very beneficial in improving our knowledge of the dynamics of opinion formation, diseases propagation, and strategy development in social networks and complex systems.

APPENDIX A

Voter Model and Social Clustering on Complex Networks

This part of the joint work was led by my coauthors, Nishant Malik and Feng Shi. For the sake of completeness, I include this in the thesis.

A.1 Evolution of Clustering in the model

Let T_G be the number of triangles and τ_G be the number of connected triplets of nodes (triads) at a given time t in the network G. Then at time t clustering will be $\mathcal{C}(t) = 3T_G/\tau_G$. Further, let us consider a triad centered at a node j is represented by the notation τ_G^j. Then the total number of triads centered at j are given by $\binom{k_j}{2}$, where k_j is the degree of node j. If during the rewiring step in the model a link is removed from a node j and rewired to a node m, then the number of triad centered at j reduces by $\binom{k_j}{2} - \binom{k_j - 1}{2}$ and triads centered at m increases by $\binom{k_m + 1}{2} - \binom{k_m}{2}$. Then the change in the number of triads in single rewiring step

$$\Delta\tau_G = \binom{k_m + 1}{2} - \binom{k_m}{2} - \binom{k_j}{2} + \binom{k_j - 1}{2} \implies \Delta\tau_G = k_m - k_j + 1.$$

Assuming that node degree is an *iid* variable, then on average the change in number of triads in time t will be $\langle\Delta\tau_G\rangle = 1$ (because $\langle k_m\rangle = \langle k_j\rangle = \langle k\rangle$). The amount rewiring at given time t is proportional to probability of rewiring α and number of discordant edges in the network l_{01}. Therefore, instantaneous rate of change of τ_G will be $\dot{\tau}_G = \alpha l_{01}\langle\Delta\tau_G\rangle$, that is

$$\dot{\tau}_G = \alpha l_{01} \tag{A.1}$$

Rewiring step also changes the number of triangles T_G in the network. Let T_G^{ij} is the number of triangles which include an edge i—j, if this edge is removed during the rewiring then T_G^{ij} triangles will be eliminated. There are two types of triads involved with edge i—j, the one centered at node i i.e., $\tau_G^i = k_i - 1$ and the other one centered at node j i.e., $\tau_G^j = k_j - 1$. Then the total number of triads involved with edge i—j are $\tau_G^i + \tau_G^j = k_i + k_j - 2$. Not all of these triads are part of triangles T_G^{ij} , as to form one triangle only two triads involving edge i—j are required. Therefore, number of triads involved in T_G^{ij} triangles must be $(k_i + k_j - 2)/2$. We know clustering coefficient is the fraction of

triads that are involved in triangles, assuming independence and uniformity $T_G^{ij} = \mathcal{C}(k_i + k_j - 2)/2$. This is the amount of triangles that will be eliminated in rewiring of i—j. Again assuming that node degree is an *iid* variable, then on average the decrease in number of triangles in time t will be $\langle \Delta T_G \rangle = -\mathcal{C}(\langle k \rangle - 1)$ (because $\langle k_m \rangle = \langle k_j \rangle = \langle k \rangle$). In the presented model there also exist a counter mechanism: rewiring to neighbor's neighbor with probability γ. If for simplicity we neglect the special rare case of 4-cycles, then this step will increase number of triangle by 1. We can combine these two mechanism into one equation and can write the instantaneous rate of change of T_G as:

$$\dot{T}_G = -\alpha l_{01} \mathcal{C}(\langle k \rangle - 1) + \alpha \gamma l_{01} \tag{A.2}$$

Using the definition $\mathcal{C}(t) = 3T_G/\tau_G$, we can write

$$\dot{\mathcal{C}} = 3\frac{\dot{T}_G \tau_G - T_G \dot{\tau}_G}{(\tau_G)^2} \tag{A.3}$$

When $\dot{\mathcal{C}} = 0$ then $\dot{T}_G \tau_G - T_G \dot{\tau}_G = 0$, therefore

$$\mathcal{C} = 3\frac{T_G}{\tau_G} = 3\frac{\dot{T}_G}{\dot{\tau}_G}.$$

Implying,

$$\mathcal{C} = 3\frac{-\alpha l_{01} \mathcal{C}(\langle k \rangle - 1) + \alpha \gamma l_{01}}{\alpha l_{01}} \tag{A.4}$$

or $\mathcal{C} = -3\mathcal{C}(\langle k \rangle - 1) + 3\gamma$, solving for $\mathcal{C}$ we get

$$\mathcal{C} = \frac{3\gamma}{3\langle k \rangle - 2}. \tag{A.5}$$

A.2 Degree Distribution

As rewiring is introduced into the model $\alpha > 0$, the structure of the network evolves. The degree distribution for $\alpha > 0$ is described by the Weibull distribution. In Fig. A.2 we have plotted the scale parameter b_1 used to fit the b_1 in Section 2.4.3. We observe bigger dispersion in the values of b_1 for small α's ($\alpha = 0.2, 0.4$). It is apparent that there are two regimes in the values of b_1, one for $\alpha < 0.6$ and $\alpha > 0.6$. In the equation above the shape parameter is a constant therefore, larger the values of

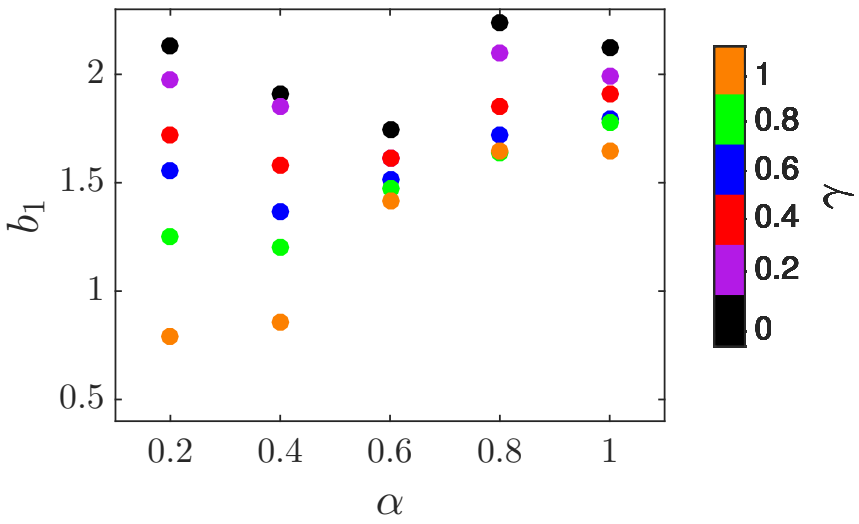

Figure A.1: Values of the parameter b_1 in Section 2.4.3

b_1 larger is the spread of the degree distribution. In other words neither the parameter α nor the parameter γ are changing the basic shape of the distribution, their combination merely stretches or contracts the spread of the degree distribution.

A.3 Transitions

The dynamics of discordant edges at time t, $l_{01}(t)$ is governed by

$$l_{01}(t) = c_1(1 - n_1(t))n_1(t) + c_2 \tag{A.6}$$

where c_1 and c_2 are constants and n_1 is the ratio of nodes holding opinion 1. c_1 and c_2 can be estimated from the simulation data by fitting Eq. A.6 to it. The simulation data used to estimate c_1 and c_2 is shown in Figure 2.6 (a). We found that $c_1/c_2 \sim \alpha^{2.1\exp(-0.75\gamma)}$ for $\alpha < \alpha_c(\gamma)$, where $\alpha_c(\gamma)$ is the solution of $\alpha^{2.1\exp(-0.75\gamma)}$. In Figure A.2 we have plotted the ratio c_1/c_2 , we observe that for $\alpha^{2.1\exp(-0.75\gamma)} < 0.5$ all the values falls on same line with slope 1. Whereas for $\alpha^{2.1\exp(-0.75\gamma)} > 0.5$ the values fall on line with slope 0. There are only very few points which show some scattering from

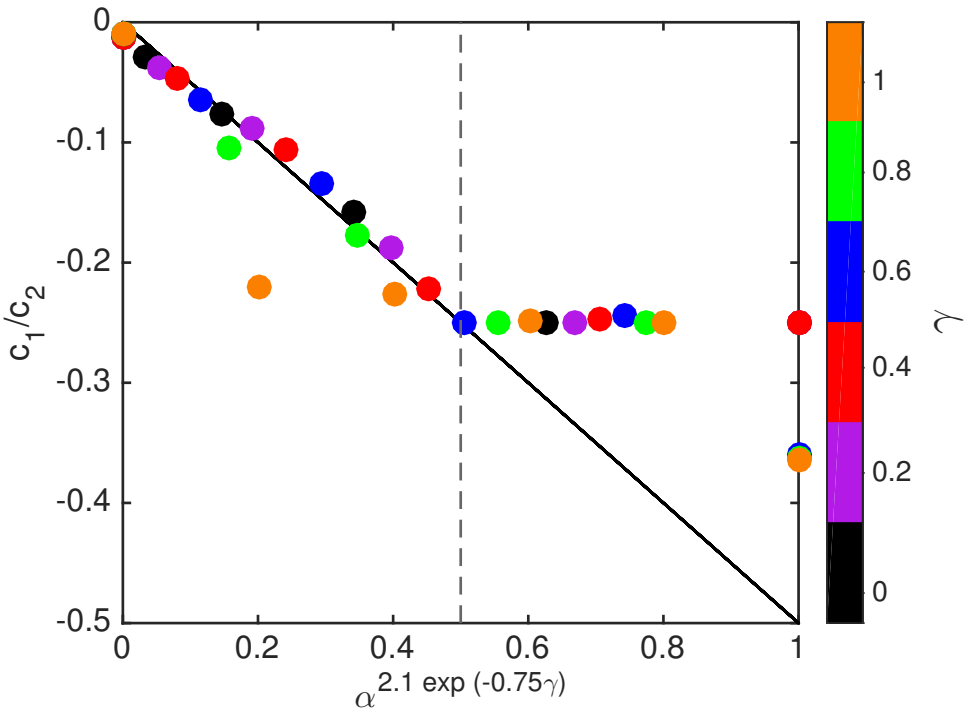

Figure A.2: In this figure we show that $c_1/c_2 \sim \alpha^{2.1\exp(-0.75\gamma)}$ for $\alpha < \alpha_c(\gamma)$, where $\alpha_c(\gamma)$ is the solution of $\alpha^{2.1\exp(-0.75\gamma)} = 0.5$. The transition point is emphasized by grey dashed line. c_1 and c_2 were obtained by fitting A.6 to the simulation data presented in Figure 2.6 (a).

this behavior, these points are due to numerical noise.

REFERENCES

[1] Guillermo Abramson and Marcelo Kuperman. Social games in a social network. *Physical Review E*, 63(3):030901, 2001.

[2] Réka Albert, István Albert, and Gary L Nakarado. Structural vulnerability of the north american power grid. *Physical review E*, 69(2):025103, 2004.

[3] Uri Alon. Biological networks: the tinkerer as an engineer. *Science*, 301(5641):1866–1867, 2003.

[4] Roy M Anderson, Robert M May, and B Anderson. *Infectious diseases of humans: dynamics and control*, volume 28. Wiley Online Library, 1992.

[5] Sinan Aral. Commentary-identifying social influence: A comment on opinion leadership and social contagion in new product diffusion. *Marketing Science*, 30(2):217–223, 2011.

[6] Sergio Arianos, E Bompard, A Carbone, and Fei Xue. Power grid vulnerability: A complex network approach. *Chaos: An Interdisciplinary Journal of Nonlinear Science*, 19(1):013119, 2009.

[7] Robert Axelrod. The evolution of cooperation: revised edition. 2006.

[8] Suryapratim Banerjee, Hideo Konishi, and Tayfun Sönmez. Core in a simple coalition formation game. *Social Choice and Welfare*, 18(1):135–153, 2001.

[9] Albert-László Barabási. The network takeover. *Nature Physics*, 8(1):14, 2011.

[10] Albert-László Barabási and Réka Albert. Emergence of scaling in random networks. *science*, 286(5439):509–512, 1999.

[11] Albert-László Barabási, Réka Albert, and Hawoong Jeong. Mean-field theory for scale-free random networks. *Physica A: Statistical Mechanics and its Applications*, 272(1):173–187, 1999.

[12] Albert-Laszlo Barabasi and Zoltan N Oltvai. Network biology: understanding the cell's functional organization. *Nature reviews genetics*, 5(2):101–113, 2004.

[13] Andrea Baronchelli, Luca Dall?Asta, Alain Barrat, and Vittorio Loreto. Topology-induced coarsening in language games. *Physical Review E*, 73(1):015102, 2006.

[14] Andrea Baronchelli, Maddalena Felici, Vittorio Loreto, Emanuele Caglioti, and Luc Steels. Sharp transition towards shared vocabularies in multi-agent systems. *Journal of Statistical Mechanics: Theory and Experiment*, 2006(06):P06014, 2006.

[15] Alain Barrat, Marc Barthelemy, and Alessandro Vespignani. *Dynamical processes on complex networks*. Cambridge University Press, 2008.

[16] Chris T Bauch and Alison P Galvani. Epidemiology. social factors in epidemiology. *Science (New York, NY)*, 342(6154):47–49, 2013.

[17] Michael GH Bell and Yasunori Iida. *Transportation network analysis*. 1997.

[18] Ginestra Bianconi. Mean field solution of the ising model on a barabási–albert network. *Physics Letters A*, 303(2):166–168, 2002.

[19] Gesa A Böhme and Thilo Gross. Fragmentation transitions in multistate voter models. *Physical Review E*, 85(6):066117, 2012.

[20] Fred Brauer, Carlos Castillo-Chavez, and Carlos Castillo-Chavez. *Mathematical models in population biology and epidemiology*, volume 1. Springer, 2001.

[21] Tom Britton, David Juher, and Joan Saldana. A network epidemic model with preventive rewiring: comparative analysis of the initial phase. *arXiv preprint arXiv:1512.00344*, 2015.

[22] Duncan S Callaway, Mark EJ Newman, Steven H Strogatz, and Duncan J Watts. Network robustness and fragility: Percolation on random graphs. *Physical review letters*, 85(25):5468, 2000.

[23] Peter J Carrington, John Scott, and Stanley Wasserman. *Models and methods in social network analysis*, volume 28. Cambridge university press, 2005.

[24] Claudio Castellano and Romualdo Pastor-Satorras. Routes to thermodynamic limit on scale-free networks. *Physical review letters*, 100(14):148701, 2008.

[25] Claudio Castellano, Daniele Vilone, and Alessandro Vespignani. Incomplete ordering of the voter model on small-world networks. *EPL (Europhysics Letters)*, 63(1):153, 2003.

[26] Kenny K Chan and Shekhar Misra. Characteristics of the opinion leader: A new dimension. *Journal of advertising*, 19(3):53–60, 1990.

[27] Yong Chen, Shao-Meng Qin, Lianchun Yu, Shengli Zhang, et al. Emergence of synchronization induced by the interplay between two prisoner?s dilemma games with volunteering in small-world networks. *Physical Review E*, 77(3):032103, 2008.

[28] Dennis Chong and James N Druckman. A theory of framing and opinion formation in competitive elite environments. *Journal of Communication*, 57(1):99–118, 2007.

[29] Peter Clifford and Aidan Sudbury. A model for spatial conflict. *Biometrika*, 60(3):581–588, 1973.

[30] Guillaume Deffuant, David Neau, Frederic Amblard, and Gérard Weisbuch. Mixing beliefs among interacting agents. *Advances in Complex Systems*, 3(01n04):87–98, 2000.

[31] Marina Diakonova, Maxi San Miguel, and Víctor M Eguíluz. Absorbing and shattered fragmentation transitions in multilayer coevolution. *Physical Review E*, 89(6):062818, 2014.

[32] James N Druckman, Erik Peterson, and Rune Slothuus. How elite partisan polarization affects public opinion formation. *American Political Science Review*, 107(01):57–79, 2013.

[33] Lee Alan Dugatkin and Michael Mesterton-Gibbons. Cooperation among unrelated individuals: reciprocal altruism, by-product mutualism and group selection in fishes. *BioSystems*, 37(1):19–30, 1996.

[34] Richard Durrett, James P Gleeson, Alun L Lloyd, Peter J Mucha, Feng Shi, David Sivakoff, Joshua ES Socolar, and Chris Varghese. Graph fission in an evolving voter model. *Proceedings of the National Academy of Sciences*, 109(10):3682–3687, 2012.

[35] Ken TD Eames and Matt J Keeling. Modeling dynamic and network heterogeneities in the spread of sexually transmitted diseases. *Proceedings of the National Academy of Sciences*, 99(20):13330–13335, 2002.

[36] David Easley and Jon Kleinberg. *Networks, crowds, and markets: Reasoning about a highly connected world*. Cambridge University Press, 2010.

[37] Holger Ebel and Stefan Bornholdt. Coevolutionary games on networks. *Physical Review E*, 66(5):056118, 2002.

[38] Holger Ebel, Jörn Davidsen, and Stefan Bornholdt. Dynamics of social networks. *Complexity*, 8(2):24–27, 2002.

[39] Paul Erdős and Alfréd Rényi. On random graphs. *Publicationes Mathematicae Debrecen*, 6:290–297, 1959.

[40] Philip Vos Fellman and Roxana Wright. Modeling terrorist networks, complex systems at the mid-range. *arXiv preprint arXiv:1405.6989*, 2014.

[41] Jeffrey A Fletcher and Martin Zwick. The evolution of altruism: Game theory in multilevel selection and inclusive fitness. *Journal of theoretical biology*, 245(1):26–36, 2007.

[42] Santo Fortunato, Vito Latora, Alessandro Pluchino, and Andrea Rapisarda. Vector opinion dynamics in a bounded confidence consensus model. *International Journal of Modern Physics C*, 16(10):1535–1551, 2005.

[43] James H Fowler and Michael Laver. A tournament of party decision rules. *Journal of Conflict Resolution*, 52(1):68–92, 2008.

[44] Feng Fu, Xiaojie Chen, Lianghuan Liu, and Long Wang. Social dilemmas in an online social network: the structure and evolution of cooperation. *Physics Letters A*, 371(1):58–64, 2007.

[45] Feng Fu, Christoph Hauert, Martin A Nowak, and Long Wang. Reputation-based partner choice promotes cooperation in social networks. *Physical Review E*, 78(2):026117, 2008.

[46] Feng Fu, Te Wu, and Long Wang. Partner switching stabilizes cooperation in coevolutionary prisoner's dilemma. *Physical Review E*, 79(3):036101, 2009.

[47] Drew Fudenberg, Martin A Nowak, Christine Taylor, and Lorens A Imhof. Evolutionary game dynamics in finite populations with strong selection and weak mutation. *Theoretical population biology*, 70(3):352–363, 2006.

[48] Sebastian Funk, Marcel Salathé, and Vincent AA Jansen. Modelling the influence of human behaviour on the spread of infectious diseases: a review. *Journal of the Royal Society Interface*, 7(50):1247–1256, 2010.

[49] Robert Gibbons. *A primer in game theory*. Harvester Wheatsheaf, 1992.

[50] Michelle Girvan and Mark EJ Newman. Community structure in social and biological networks. *Proceedings of the national academy of sciences*, 99(12):7821–7826, 2002.

[51] James P Gleeson. Bond percolation on a class of clustered random networks. *Physical Review E*, 80(3):036107, 2009.

[52] James P Gleeson. High-accuracy approximation of binary-state dynamics on networks. *Physical Review Letters*, 107(6):068701, 2011.

[53] James P Gleeson. Binary-state dynamics on complex networks: Pair approximation and beyond. *Physical Review X*, 3(2):021004, 2013.

[54] Jesús Gómez-Gardeñes, M Campillo, LM Floría, and Yamir Moreno. Dynamical organization of cooperation in complex topologies. *Physical Review Letters*, 98(10):108103, 2007.

[55] Mark Granovetter. Threshold models of collective behavior. *American journal of sociology*, pages 1420–1443, 1978.

[56] Kurt Gray, David G Rand, Eyal Ert, Kevin Lewis, Steve Hershman, and Michael I Norton. The emergence of ?us and them? in 80 lines of code modeling group genesis in homogeneous populations. *Psychological science*, page 0956797614521816, 2014.

[57] Andreas Grönlund and Petter Holme. A network-based threshold model for the spreading of fads in society and markets. *Advances in Complex Systems*, 8(02n03):261–273, 2005.

[58] Thilo Gross and Bernd Blasius. Adaptive coevolutionary networks: a review. *Journal of The Royal Society Interface*, 5(20):259–271, 2008.

[59] Thilo Gross, Carlos J Dommar D'Lima, and Bernd Blasius. Epidemic dynamics on an adaptive network. *Physical review letters*, 96(20):208701, 2006.

[60] Thilo Gross and Hiroki Sayama. *Adaptive networks*. Springer, 2009.

[61] WD Hamilton. The genetical evolution of social behaviour. i. 1964.

[62] John C Harsanyi, Reinhard Selten, et al. A general theory of equilibrium selection in games. *MIT Press Books*, 1, 1988.

[63] Christoph Hauert, Silvia De Monte, Josef Hofbauer, and Karl Sigmund. Volunteering as red queen mechanism for cooperation in public goods games. *Science*, 296(5570):1129–1132, 2002.

[64] Christoph Hauert and Michael Doebeli. Spatial structure often inhibits the evolution of cooperation in the snowdrift game. *Nature*, 428(6983):643–646, 2004.

[65] Christoph Hauert, Miranda Holmes, and Michael Doebeli. Evolutionary games and population dynamics: maintenance of cooperation in public goods games. *Proceedings of the Royal Society of London B: Biological Sciences*, 273(1600):2565–2571, 2006.

[66] Christoph Hauert, Arne Traulsen, Hannelore Brandt, Martin A Nowak, and Karl Sigmund. Via freedom to coercion: the emergence of costly punishment. *science*, 316(5833):1905–1907, 2007.

[67] Rainer Hegselmann, Ulrich Krause, et al. Opinion dynamics and bounded confidence models, analysis, and simulation. *Journal of Artificial Societies and Social Simulation*, 5(3), 2002.

[68] Jorge Hidalgo, Jacopo Grilli, Samir Suweis, Amos Maritan, and Miguel A Munoz. Cooperation, competition and the emergence of criticality in communities of adaptive systems. *arXiv preprint arXiv:1510.05941*, 2015.

[69] Josef Hofbauer and Karl Sigmund. Evolutionary game dynamics. *Bulletin of the American Mathematical Society*, 40(4):479–519, 2003.

[70] Richard A Holley and Thomas M Liggett. Ergodic theorems for weakly interacting infinite systems and the voter model. *The annals of probability*, pages 643–663, 1975.

[71] Petter Holme and Mark EJ Newman. Nonequilibrium phase transition in the coevolution of networks and opinions. *Physical Review E*, 74(5):056108, 2006.

[72] Petter Holme, Ala Trusina, Beom Jun Kim, and Petter Minnhagen. Prisoners? dilemma in real-world acquaintance networks: Spikes and quasiequilibria induced by the interplay between structure and dynamics. *Physical Review E*, 68(3):030901, 2003.

[73] Lars Hufnagel, Dirk Brockmann, and Theo Geisel. Forecast and control of epidemics in a globalized world. *Proceedings of the National Academy of Sciences of the United States of America*, 101(42):15124–15129, 2004.

[74] Gerardo Iñiguez, János Kertész, Kimmo K Kaski, and Raphael Angl Barrio. Opinion and community formation in coevolving networks. *Physical Review E*, 80(6):066119, 2009.

[75] Raghuram Iyengar, Christophe Van den Bulte, and Thomas W Valente. Opinion leadership and social contagion in new product diffusion. *Marketing Science*, 30(2):195–212, 2011.

[76] Matthew O Jackson et al. *Social and economic networks*, volume 3. Princeton university press Princeton, 2008.

[77] Matthew O Jackson and Alison Watts. On the formation of interaction networks in social coordination games. *Games and Economic Behavior*, 41(2):265–291, 2002.

[78] Björn H Junker and Falk Schreiber. *Analysis of biological networks*, volume 2. John Wiley & Sons, 2011.

[79] Krzysztof Kacperski et al. Opinion formation model with strong leader and external impact: a mean field approach. *Physica A: Statistical Mechanics and its Applications*, 269(2):511–526, 1999.

[80] Matt J Keeling and Ken TD Eames. Networks and epidemic models. *Journal of the Royal Society Interface*, 2(4):295–307, 2005.

[81] Matt J Keeling and Pejman Rohani. *Modeling infectious diseases in humans and animals*. Princeton University Press, 2008.

[82] Benjamin Kerr, Margaret A Riley, Marcus W Feldman, and Brendan JM Bohannan. Local dispersal promotes biodiversity in a real-life game of rock–paper–scissors. *Nature*, 418(6894):171–174, 2002.

[83] Timothy Killingback and Michael Doebeli. Spatial evolutionary game theory: Hawks and doves revisited. *Proceedings of the Royal Society of London B: Biological Sciences*, 263(1374):1135–1144, 1996.

[84] Beom Jun Kim, Ala Trusina, Petter Holme, Petter Minnhagen, Jean S Chung, and MY Choi. Dynamic instabilities induced by asymmetric influence: prisoners? dilemma game in small-world networks. *Physical Review E*, 66(2):021907, 2002.

[85] Simon Kirby. Natural language from artificial life. *Artificial life*, 8(2):185–215, 2002.

[86] Mirjam Kretzschmar. Sexual network structure and sexually transmitted disease prevention: a modeling perspective. *Sexually transmitted diseases*, 27(10):627–635, 2000.

[87] Marcelo Kuperman and Guillermo Abramson. Small world effect in an epidemiological model. *Physical Review Letters*, 86(13):2909, 2001.

[88] Simon A Levin and R Durrett. From individuals to epidemics. *Philosophical Transactions of the Royal Society of London B: Biological Sciences*, 351(1347):1615–1621, 1996.

[89] Erez Lieberman, Christoph Hauert, and Martin A Nowak. Evolutionary dynamics on graphs. *Nature*, 433(7023):312–316, 2005.

[90] Jennifer Lindquist, Junling Ma, P Van den Driessche, and Frederick H Willeboordse. Effective degree network disease models. *Journal of mathematical biology*, 62(2):143–164, 2011.

[91] Dunia López-Pintado. Diffusion in complex social networks. *Games and Economic Behavior*, 62(2):573–590, 2008.

[92] Jan Lorenz. Continuous opinion dynamics under bounded confidence: A survey. *International Journal of Modern Physics C*, 18(12):1819–1838, 2007.

[93] Jan Lorenz. Heterogeneous bounds of confidence: meet, discuss and find consensus! *Complexity*, 15(4):43–52, 2010.

[94] Sergi Lozano, Alex Arenas, and Angel Sánchez. Mesoscopic structure conditions the emergence of cooperation on social networks. *PLoS one*, 3(4):e1892, 2008.

[95] Qiming Lu, Gyorgy Korniss, and Boleslaw K Szymanski. The naming game in social networks: community formation and consensus engineering. *Journal of Economic Interaction and Coordination*, 4(2):221–235, 2009.

[96] Nishant Malik and Peter J Mucha. Role of social environment and social clustering in spread of opinions in coevolving networks. *Chaos: An Interdisciplinary Journal of Nonlinear Science*, 23(4):043123, 2013.

[97] Vincent Marceau, Pierre-André Noël, Laurent Hébert-Dufresne, Antoine Allard, and Louis J Dubé. Adaptive networks: Coevolution of disease and topology. *Physical Review E*, 82(3):036116, 2010.

[98] Naoki Masuda. Evolution of cooperation driven by zealots. *Scientific reports*, 2, 2012.

[99] Sergey Melnik, Adam Hackett, Mason A Porter, Peter J Mucha, and James P Gleeson. The unreasonable effectiveness of tree-based theory for networks with clustering. *Physical Review E*, 83(3):036112, 2011.

[100] Jean-François Mertens. *Repeated games*. Springer, 1989.

[101] Lauren Meyers. Contact network epidemiology: Bond percolation applied to infectious disease prediction and control. *Bulletin of the American Mathematical Society*, 44(1):63–86, 2007.

[102] Igal Milchtaich and Eyal Winter. Stability and segregation in group formation. *Games and Economic Behavior*, 38(2):318–346, 2002.

[103] Joel C Miller. Percolation and epidemics in random clustered networks. *Physical Review E*, 80(2):020901, 2009.

[104] John H Miller. The coevolution of automata in the repeated prisoner's dilemma. *Journal of Economic Behavior & Organization*, 29(1):87–112, 1996.

[105] Ron Milo, Shai Shen-Orr, Shalev Itzkovitz, Nadav Kashtan, Dmitri Chklovskii, and Uri Alon. Network motifs: simple building blocks of complex networks. *Science*, 298(5594):824–827, 2002.

[106] Joshua Mitteldorf and David Sloan Wilson. Population viscosity and the evolution of altruism. *Journal of Theoretical Biology*, 204(4):481–496, 2000.

[107] Cristopher Moore and Mark EJ Newman. Epidemics and percolation in small-world networks. *Physical Review E*, 61(5):5678, 2000.

[108] Roger B Myerson. Game theory: analysis of conflict. *Harvard University*, 1991.

[109] Richard Nadeau, Edouard Cloutier, and J-H Guay. New evidence about the existence of a bandwagon effect in the opinion formation process. *International Political Science Review*, 14(2):203–213, 1993.

[110] Mark Newman. *Networks: an introduction*. OUP Oxford, 2010.

[111] Mark Newman, Albert-Laszlo Barabasi, and Duncan J Watts. *The structure and dynamics of networks*. Princeton University Press, 2006.

[112] Mark EJ Newman. Spread of epidemic disease on networks. *Physical review E*, 66(1):016128, 2002.

[113] Mark EJ Newman. Modularity and community structure in networks. *Proceedings of the national academy of sciences*, 103(23):8577–8582, 2006.

[114] Mark EJ Newman. Random graphs with clustering. *Physical review letters*, 103(5):058701, 2009.

[115] Mark EJ Newman, Christopher Moore, and Duncan J Watts. Mean-field solution of the small-world network model. *Physical Review Letters*, 84(14):3201, 2000.

[116] Vudtiwat Ngampruetikorn and Greg J Stephens. Bias, belief and consensus: Collective opinion formation on fluctuating networks. *arXiv preprint arXiv:1512.09074*, 2015.

[117] Noam Nisan, Tim Roughgarden, Eva Tardos, and Vijay V Vazirani. *Algorithmic game theory*, volume 1. Cambridge University Press Cambridge, 2007.

[118] Martin A Nowak and Robert M May. Evolutionary games and spatial chaos. *Nature*, 359(6398):826–829, 1992.

[119] Martin A Nowak and Robert M May. The spatial dilemmas of evolution. *International Journal of bifurcation and chaos*, 3(01):35–78, 1993.

[120] Martin A Nowak and Karl Sigmund. The dynamics of indirect reciprocity. *Journal of theoretical Biology*, 194(4):561–574, 1998.

[121] Martin A Nowak and Karl Sigmund. Evolution of indirect reciprocity. *Nature*, 437(7063):1291–1298, 2005.

[122] Jorge M Pacheco, Arne Traulsen, Hisashi Ohtsuki, and Martin A Nowak. Repeated games and direct reciprocity under active linking. *Journal of Theoretical Biology*, 250(4):723–731, 2008.

[123] Matjaž Perc, Attila Szolnoki, and György Szabó. Restricted connections among distinguished players support cooperation. *Physical Review E*, 78(6):066101, 2008.

[124] Flávio L Pinheiro, Francisco C Santos, and Jorge M Pacheco. Linking individual and collective behavior in adaptive social networks. *Physical Review Letters*, 116(12):128702, 2016.

[125] Mason A Porter and James P Gleeson. Dynamical systems on networks: a tutorial. *arXiv preprint arXiv:1403.7663*, 2014.

[126] Andreas Pusch, Sebastian Weber, and Markus Porto. Impact of topology on the dynamical organization of cooperation in the prisoner?s dilemma game. *Physical Review E*, 77(3):036120, 2008.

[127] Jie Ren, Wen-Xu Wang, and Feng Qi. Randomness enhances cooperation: a resonance-type phenomenon in evolutionary games. *Physical Review E*, 75(4):045101, 2007.

[128] Carlos P Roca, José A Cuesta, and Angel Sánchez. Promotion of cooperation on networks? the myopic best response case. *The European Physical Journal B*, 71(4):587–595, 2009.

[129] Francisco C Santos, Jorge M Pacheco, and Tom Lenaerts. Cooperation prevails when individuals adjust their social ties. *PLoS Comput Biol*, 2(10):e140, 2006.

[130] Francisco C Santos, JF Rodrigues, and Jorge M Pacheco. Epidemic spreading and cooperation dynamics on homogeneous small-world networks. *Physical Review E*, 72(5):056128, 2005.

[131] Francisco C Santos, Marta D Santos, and Jorge M Pacheco. Social diversity promotes the emergence of cooperation in public goods games. *Nature*, 454(7201):213–216, 2008.

[132] Hiroki Sayama, Irene Pestov, Jeffrey Schmidt, Benjamin James Bush, Chun Wong, Junichi Yamanoi, and Thilo Gross. Modeling complex systems with adaptive networks. *Computers & Mathematics with Applications*, 65(10):1645–1664, 2013.

[133] Casey M Schneider-Mizell and Leonard M Sander. A generalized voter model on complex networks. *Journal of Statistical Physics*, 136(1):59–71, 2009.

[134] Leah B Shaw and Ira B Schwartz. Fluctuating epidemics on adaptive networks. *Physical Review E*, 77(6):066101, 2008.

[135] Feng Shi, Peter J Mucha, and Richard Durrett. Multiopinion coevolving voter model with infinitely many phase transitions. *Physical Review E*, 88(6):062818, 2013.

[136] John Maynard Smith. *Evolution and the Theory of Games*. Cambridge university press, 1982.

[137] Vishal Sood and Sidney Redner. Voter model on heterogeneous graphs. *Physical review letters*, 94(17):178701, 2005.

[138] Krzysztof Suchecki, Víctor M Eguíluz, and Maxi San Miguel. Voter model dynamics in complex networks: Role of dimensionality, disorder, and degree distribution. *Physical Review E*, 72(3):036132, 2005.

[139] Eric Sun, Itamar Rosenn, Cameron Marlow, and Thomas M Lento. Gesundheit! modeling contagion through facebook news feed. In *ICWSM*, 2009.

[140] György Szabó and Csaba Tőke. Evolutionary prisoner?s dilemma game on a square lattice. *Physical Review E*, 58(1):69, 1998.

[141] Attila Szolnoki, Matjaž Perc, György Szabó, and Hans-Ulrich Stark. Impact of aging on the evolution of cooperation in the spatial prisoner?s dilemma game. *Physical Review E*, 80(2):021901, 2009.

[142] Michael Taylor, Péter L Simon, Darren M Green, Thomas House, and Istvan Z Kiss. From markovian to pairwise epidemic models and the performance of moment closure approximations. *Journal of mathematical biology*, 64(6):1021–1042, 2012.

[143] Marc Timme, Fred Wolf, and Theo Geisel. Coexistence of regular and irregular dynamics in complex networks of pulse-coupled oscillators. *Physical review letters*, 89(25):258701, 2002.

[144] Arne Traulsen, Martin A Nowak, and Jorge M Pacheco. Stochastic payoff evaluation increases the temperature of selection. *Journal of theoretical biology*, 244(2):349–356, 2007.

[145] Arne Traulsen, Torsten Röhl, and Heinz Georg Schuster. Stochastic gain in population dynamics. *Physical review letters*, 93(2):028701, 2004.

[146] Federico Vazquez et al. Analytical solution of the voter model on uncorrelated networks. *New Journal of Physics*, 10(6):063011, 2008.

[147] Gunjan Verma, Ananthram Swami, and Kevin Chan. The impact of competing zealots on opinion dynamics. *Physica A: Statistical Mechanics and its Applications*, 395:310–331, 2014.

[148] Jeromos Vukov, György Szabó, and Attila Szolnoki. Cooperation in the noisy case: Prisoner?s dilemma game on two types of regular random graphs. *Physical Review E*, 73(6):067103, 2006.

[149] Zhen Wang, Lin Wang, Attila Szolnoki, and Matjaž Perc. Evolutionary games on multilayer networks: a colloquium. *The European Physical Journal B*, 88(5):1–15, 2015.

[150] Helen Ward. Prevention strategies for sexually transmitted infections: importance of sexual network structure and epidemic phase. *Sexually transmitted infections*, 83(suppl 1):i43–i49, 2007.

[151] Stanley Wasserman and Katherine Faust. *Social network analysis: Methods and applications*, volume 8. Cambridge university press, 1994.

[152] Duncan J Watts. A simple model of global cascades on random networks. *Proceedings of the National Academy of Sciences*, 99(9):5766–5771, 2002.

[153] Duncan J Watts and Peter Sheridan Dodds. Influentials, networks, and public opinion formation. *Journal of consumer research*, 34(4):441–458, 2007.

[154] Duncan J Watts and Steven H Strogatz. Collective dynamics of ?small-world?networks. *nature*, 393(6684):440–442, 1998.

[155] Jörgen W Weibull. *Evolutionary game theory*. MIT press, 1997.

[156] Han-Xin Yang, Wen-Xu Wang, Zhi-Xi Wu, Ying-Cheng Lai, and Bing-Hong Wang. Diversity-optimized cooperation on complex networks. *Physical Review E*, 79(5):056107, 2009.

[157] Damián H Zanette and Sebastián Risau-Gusmán. Infection spreading in a population with evolving contacts. *Journal of biological physics*, 34(1-2):135–148, 2008.

[158] Weituo Zhang, Chjan C Lim, Gyorgy Korniss, and Boleslaw K Szymanski. Opinion dynamics and influencing on random geometric graphs. *Scientific reports*, 4, 2014.

[159] Jie Zhou, Gaoxi Xiao, and Guanrong Chen. Link-based formalism for time evolution of adaptive networks. *Physical Review E*, 88(3):032808, 2013.